

1977

Determination of the rate of photoresist polymer breakdown by an oxygen plasma

Paul Robert Saunders
Lehigh University

Follow this and additional works at: <https://preserve.lehigh.edu/etd>

 Part of the [Chemical Engineering Commons](#)

Recommended Citation

Saunders, Paul Robert, "Determination of the rate of photoresist polymer breakdown by an oxygen plasma" (1977). *Theses and Dissertations*. 5121.
<https://preserve.lehigh.edu/etd/5121>

This Thesis is brought to you for free and open access by Lehigh Preserve. It has been accepted for inclusion in Theses and Dissertations by an authorized administrator of Lehigh Preserve. For more information, please contact preserve@lehigh.edu.

DETERMINATION OF THE RATE OF PHOTORESIST
POLYMER BREAKDOWN BY AN OXYGEN PLASMA

DETERMINATION OF THE RATE OF PHOTORESIST POLYMER
BREAKDOWN BY AN OXYGEN PLASMA

by

Paul Robert Saunders

A Thesis

Presented to the Department of Chemical Engineering

of Lehigh University in partial fulfilment

of the requirements for the degree of

Master of Science

in

Chemical Engineering

Lehigh University

1977

(5-1977)

This thesis is accepted and approved in partial fulfillment of the requirements for the degree of Master of Science.

AJ McHugh
Dr. A. J. McHugh

Dr. L. A. Wenzel
Chairman,
Chemical Engineering Dept.

ACKNOWLEDGEMENTS

I would like to thank Thomas Briggs of Western Electric for helpful suggestions on Infrared Spectroscopy. A special acknowledgement goes to Charles Pearce of W.E. Co. for his patience during the six months that I monopolized his spectrometer. For their continued aide in the use of the various computer systems required for this project, I thank Dr. Paul Langer, Bell Laboratories, and the entire Bell Laboratories Computer group working for William Furjanic for kindness above and beyond the call of duty. As guiding light to bring this divergent project to completion and for his helpful discussions on polymer degradation theory, I would like to thank Dr. Anthony McHugh. Also of great help were the suggestions of Glen Offord of W.E. Co. on effective circuit design, and Robert Heinz of the W. E. Research Center for laser alignment of the gas cell used in this experiment. For his fine suggestions on improving this text, I thank Dr. Gilbert Mowery of Bell Laboratories.

TABLES and FIGURES - Main Text

Table	1	Reduced Data from Run #1	33a
Table	2	Reduced Data from Run #2	33b
Table	3	Reduced Data from Run #3	33c
Table	4	Reduced Data from Run #4	33d
Figure	5	Plot of Pressure vs. Time for all Runs	33e
Figure	6	Plot of Temperature vs. Time for all Runs	33f
Figure	7	Plot of Absorbance vs. Time for all Runs	33g
Figure	8	Plot of CO ₂ Wt. Loss/Min. vs. Time for all Runs ..	33h
Figure	9	Plot of Total CO ₂ Loss vs. Time for all Runs	33i
Table	10	Reduced Data from Run #5	33j
Table	11	Reduced Data from Run #9	33k
Table	12	Data from the Weight Loss Experiment	33l
Figure	12a	Plot of Wt. Loss of Polymer vs. Time	33m
Figure	12b	Plot of Temperature vs. Time (Wt. Loss Exp.)	33n
Figure	12c	Plot of Pressure vs. Time (Wt. Loss Exp.)	33o
Table	13	Data from the Variable Polymer Load Experiment ...	33p
Figure	14	Plot of Weight Loss / Wafer vs. Polymer Load	33q
Figure	15	Plot of Removal Rate vs. % O ₂ in the Feed Gas	33r
Figure	16	Raw Data from Run #6	33s
Figure	17	Raw Data from Run #7	33t
Figure	18	Raw Data from Run #8	33u
Figure	19	Computer Program - Calculations Block Diagram	34a
Figure	20	Computer Program - Plotting Block Diagram	34b
Table	21	Carbon Mass Balance Comparison	35a

Figure 22a	Plot of $\ln (\text{Rate})$ vs. $1/T(^{\circ}\text{K})$	36a
Figure 22b	Enlargement of Fig. 22a	36b
Table 23	Values for E_{act} , A in all Experimental Runs	38
Table 24	Values for N , h , T_{∞} , T_0 , in all Experimental Runs.	43
Figure 25	Plot of $\ln (T_{\infty} - T)$ vs. Time	43a

TABLES and FIGURES - Appendices

Table AP I-1	Oxygen - Carbon Dioxide Pressure Conversion	A-6a
Table AP I-2	Oxygen - Water Vapor Pressure Conversion	A-6b
Table AP I-3	Hastings Nomograph for Various Gases	A-6c
Table AP I-4	Chart of Correlating Pressure Measurements	A-6d
Figure AP II-1	Thermocouple Temp. vs. Time (800 watts)	A-8a
Table AP II-2	Chart of Correlating Temperature Measurements	A-8b
Figure AP II-3	Hot Chuck vs. Chemical Temp. Calibration	A-8c
Figure AP II-4	Pyrometer Emissivity Calibration	A-8d
Figure AP II-5	Calibration of Hot Chuck to Reactor Thermocouple..	A-8e
Figure AP II-6	Plot of Exhaust Gas Temperature vs. Pressure	A-8f
Figure AP III-1	Overall Equipment Diagram	A-8g
Figure AP III-2	Common Mode Rejection Circuit Diagram	A-8h
Table AP IV-1	Tylan Chart of Gas Factors (Flow)	A-9a
Table AP IV-2	CO ₂ Flow Controller Calibration	A-10
Table AP IV-3	O ₂ Flow Controller Calibration	A-11
Figure AP IV-4	Flow vs. Pressure Calibration	A-11a
Table AP IV-5	Flow vs. Pressure for CO ₂ , H ₂ O, and O ₂	A-11b
Figure AP IV-6	Plot of the Data from Table AP IV-5	A-11c
Table AP IV-7	Oxygen Flow vs. Pressure Data	A-11d
Table AP V-1a	Transmittance Calibration Data #1	A-17a
Table AP V-1b	Transmittance Calibration Data #2	A-17b
Figure AP V-2	Plot of Absorbance vs. CO ₂ Concentration	A-17c
Figure AP V-3	Plot of Transmittance vs. Time for Product Run #4.	A-17d
Table AP VII-1	Raw Data for Run #1 (800 watts)	A-45a

Table AP VII-2 Raw Data for Run #2 (200 watts)	A-45b
Table AP VII-3 Raw Data for Run #3 (400 watts)	A-45c
Table AP VII-4 Raw Data for Run #4 (600 watts)	A-45d
Table AP VII-5 Raw Data for Run #5 (800 watts)	A-45e
Table AP VII-6 Raw Data for Run #9 (800 watts)	A-45f

TABLE OF CONTENTS

Certificate Page	ii
Acknowledgments	iii
List of tables and figures - Main text.....	iv
List of tables and figures - Appendices.....	v
Abstract.....	1
Introduction and Problem Statement.....	3
Theory - Review of the Literature.....	6
Theory - Descriptive Equations.....	12
Objective of the Research.....	16
Experimental Equipment Description.....	15
Experimental Procedure.....	22
Results.....	30
Discussion of Results.....	34
Conclusions.....	46
References	48
Bibliography	53
Appendix I - Pressure Measurement and Calibration.....	A-1
Appendix IA - Pressure Iteration Technique	A-3
Appendix II - Temperature Measurement and Calibration...	A-7
Appendix III - Equipment Diagrams.....	A-8f
Appendix IV - Flow Measurement and Calibration.....	A-9
Appendix IVA - Principle of the Flow Controller.....	A-12
Appendix V - Absorbance Measurement and Calibration.....	A-14
Appendix VI - Computer Solution - Program.....	A-18
Appendix VII - Raw Data Compilations.....	A-45a
Appendix VIII - Sources of Error	A-46
Vita	A-47

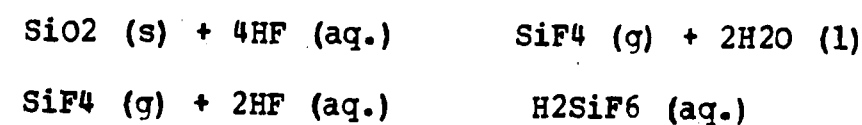
ABSTRACT

The rate of breakdown of cyclic polyisoprene photoresist has been determined for a range of temperatures between 100-220 °C, two oxygen gas feed rates, three compositions of the feed gas, and three power levels. Calculations based on these data indicate a linear increase in the heat transfer coefficient to the silicon substrate with increasing power, $h = 0.00070 - 0.0019 \text{ cal./cm}^2 \text{ -min.-}^\circ\text{C}$, while this coefficient is nearly constant versus oxygen feed rate (i.e. pressure). On the other hand, the activation energy for the polymer degradation process appears to be essentially constant versus power in the 600-800 watt rf power region. However, activation energy undergoes a significant decrease as oxygen feed rate (i.e. pressure) decreases indicating that the rate limiting step for the polymer decomposition is evaporation of chain fragments from the polymer surface. Further confirmation of this conclusion is provided by calculation of the theoretical evaporation energy for the polymer (i.e. isoprene monomer fragments). This polymer evaporation energy is calculated as 5.5 Kcal./gmmole. while the measured activation energy for the degradation process is 2.5-5.5 Kcal./gmmole. A large increase in the activation energy of the process to 14 Kcal./gmmole. was observed at lower rf power levels (400 watts). This increase indicates that a change in the nature of the degradation process oc-

curs in low power oxygen plasmas. This data base on oxygen plasma decomposition of cyclic polyisoprene will be examined even more extensively in the future for further conclusions.

INTRODUCTION AND PROBLEM STATEMENT

In the generation of a diffusion barrier, usually silicon dioxide, for group III-A and V-A dopants, the semiconductor industry uses various photosensitive polymers to create a patterned acid etch barrier for the silicon dioxide. Currently two common photosensitive polymers (photoresists or simply resists) are a cyclized polyisoprene negative-working resist and a novalak (phenol- formaldehyde) resin positive-working resist. The designation negative or positive working is determined by whether the polymer becomes more soluble (positive-working) or less soluble (negative-working) in their respective developing solutions after exposure to ultraviolet light. Developing refers to the process of dissolving the most soluble areas of the polymer, thereby leaving the silicon dioxide surface exposed in the required regions. The developing solution for the polyisoprene resist is xylene while the novalak resin is developed in an aqueous alkali solution. The regions covered by the polymer will act as a barrier to the hydrofluoric acid used to etch the exposed silicon dioxide areas. The reactions which occur in the etching operation are as follows:



Following the etching of the patterned SiO₂ diffusion barrier, the residual resist layer protecting the non-etched areas of the SiO₂ must be removed. The present work concerns this operation following the etching step, namely the oxygen plasma removal of the polymer prior to diffusion. Among the methods of negative photoresist removal in current use are J-100 phenolic stripping solution (produced by Indust-Ri-Chem Laboratory), LSI non-phenolic stripping solution (produced by Inland Chemical), sulfuric acid-hydrogen peroxide Caros acid stripping solution, oxygen plasma resist removal, and ozone gas breakdown of the polymer. The first three methods comprise the bulk of industrial usage in microelectronics production, while oxygen plasma usage is a steadily increasing alternative to these major wet chemical methods. The two major methods of positive resist removal are dissolution in acetone, ethyl cellosolve (2ethoxyethanol), or another suitable solvent. Oxygen plasma has not been commercially used for positive resist removal due to the slow observed removal rate. However, positive resist will be included in this study in an attempt to discover the cause of the observed slow rate of removal.

The oxygen plasma removal method which will be examined in this paper consists of exposing the photosensitive polymer (negative or positive) silicon wafer to an oxygen gas activated by a radio frequency field so that the gas becomes a plasma of oxygen ions and electrons. The removal

occurs under nearly constant pressure vacuum conditions during the course of the photoresist breakdown. Although this plasma procedure is being used commercially, little is known of the plasma-polymer reaction kinetics and mechanisms. The process appears to be oxidation of the nitrogen, carbon, hydrogen, and oxygen in the polymers to form volatile gases such as CO, CO₂, (NO)_x, NO₂, H₂O, OH-, O₂, and O₃. The nitrogen molecules are reaction products only of the novalak resin polymers (positive resists) which contain nitrogen and oxygen groups. The cyclic polyisoprene polymers (negative resists) yield exclusively carbon and hydrogen containing reaction products; any ozone present is generated by the action of the rf field on the oxygen gas reactant.

The scope of this paper will be to determine the reaction rate and possibly the kinetics for the breakdown of the two types of polymers; of major interest will be cyclic polyisoprene and novalak resin (phenol-formaldehyde) photoresists.

THEORY-REVIEW OF THE LITERATURE

In the study of heterogeneous chemical reactions, the usual analysis entails the determination of whether diffusion or chemical reaction is the controlling step in the overall rate. When reaction rate is controlling, the study would include an analysis of the temperature dependence of the rate which usually takes the form of an Arrhenius type equation,

$$dC/dt = \text{Rate} = A \cdot \exp(-E/RT) * f(C) \quad (1)$$

Using this equation, mass balances, and kinetic data (e.g. C vs. t, and Rate vs. T), the value of unknowns E and A can be calculated for a specific reaction. From this complete knowledge of eqn. (1), the reactor design can be made. However, researchers report that reaction processes in a radio frequency plasma do not rigorously fit this method of analysis [1].

The number of oxygen ion species in the plasma has been examined by several researchers [2-11]. Hollahan and Carlson note the presence of: O^+ , $(O_2)^+$, O^- , $(O_2)^-$, $O(3P)$, $O_2(1\Delta_g)$, and electrons [12]. The positive ions and free electrons are formed by dissociation due to the oscillating radio frequency field, whereas the negative ions and metastable species are products of electron-neutral ion collisions. The oxidation reaction has been attributed mainly to the metastable species (i.e. $O(3P)$ and $O_2(1\Delta_g)$) because of their

long lifetimes compared to the charged ion species [12,7,4]. Additionally, to complicate the analysis, Hansen et. al. have found experimentally that electron bombardment of polymers increases the rate of decomposition by the metastable ions [2]. Since electrons are also an active specie in a plasma, Hansen's finding indicates that many species participate in the polymer oxidation reaction in addition to the two metastable oxygen species. Therefore, all the species in an oxygen plasma have a role in the reaction, since even non-reacting ions affect the velocities of the active species.

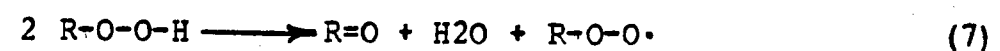
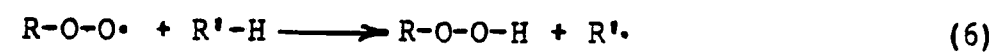
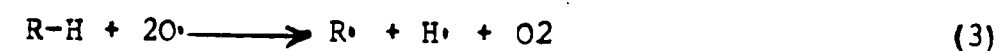
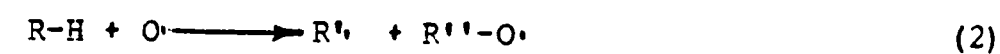
Activation of polymer surfaces by electron and ion bombardment has been an area of extensive research over the last two decades [12-18]. One major purpose of this work was to analyze the reasons for the improvement of adhesive bonding and printability on polymer surfaces treated in either a neutral ion or oxygen plasma. Some of this research investigated oxygen plasmas to achieve both improved surface properties and bulk electrical characteristics [18-21]. The work with plasma treated polymer surfaces led to speculation on whether the surface contained large numbers of free radicals which then degraded to form hydroxy and peroxy compounds on exposure to air [4,12-15]. These peroxy compounds then might react to form a denser surface layer by cross-linking than existed in the bulk polymer, thereby improving the chemical resistance and bondability of the polymer.

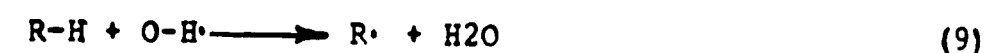
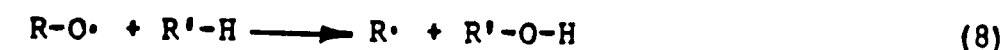
Since the Arrhenius form of the rate equation is not applicable to a plasma reaction, other mathematical descriptions of the reaction must be examined. The Boltzman equation which uses a Maxwellian distribution of charged specie energies might be used to describe the non-reacting plasma [22]. However, even for non-reacting gas plasmas the Boltzman equation would be so complex that lengthy computer solutions would be required. This solution would then be limited to a non-reacting, "equilibrium" region of the plasma away from the reactor walls. Another mathematical description that might be attempted would be to apply quantum mechanics to the plasma reactions. An extensive discussion of this method is presented by Venugopalan [23]. Hollahan and Bell have also presented an excellent summary of the possible mathematical descriptions of a plasma [24]. Although some insight into plasma processes can be obtained from these descriptions, they are far too limited to provide an understanding of the complex interactions of plasma reactions.

With a mathematical description of the oxygen plasma reactions being currently incomplete, chemical engineering kinetic data must be taken and analyzed to describe the plasma reaction process in terms of engineering concepts (i.e. boundary layers, film coefficients). Also, the overall rate of polymer removal can be experimentally determined. This removal rate can then be studied as a function of power

level, pressure(O₂ flow), and O₂ concentration in a neutral gas. During these analyses of removal rate, the temperature of the silicon wafers should be monitored so that the heating effect of the ion energy transfer can be described. Also, if the polymer phase reactions rather than the plasma reactions are rate controlling in this process, then an Arrhenius type of analysis may be performed on these polymer reactions. Whether plasma or polymer reactions control the process, meaningful determinations can be made of the concentration, temperature, pressure, and wafer loading effects on the reaction rate.

A very good overview of the recent developments in plasma polymerization and plasma polymer interactions was completed by Havens et. al. [33]. However, in order to obtain the specific background information on oxygen plasma-polymer reactions, the review in Hollahan and Bell's book is recommended [25]. This more detailed review was written by Martin Hudis. Hudis lists the following polymer oxidation reactions as characteristic in an oxygen plasma [26],





The most important findings cited in this review are those of Hansen et. al. whose work with eight polymers in an oxygen plasma revealed that the major mechanism of polymer degradation was ablation. Hansen found that for these eight polymers, the weight loss was a linear function of the time of exposure to the plasma and that the slope of this line was determined by the polymer structure. Hudis states,

"Ablation appears to be an exclusive property of oxygen containing plasmas. Ablation also causes changes in surface morphology. Small molecular weight degradation products which are covalently bonded to the surface migrate around the surface, producing small bumps which have been detected using a scanning electron microscopy (sic)." [27]

The present research will attempt to determine if the degradation mechanism of cyclic polyisoprene and novalak resin resists is by chemical reaction, ablation, or a combination of these two processes.

Also of interest is the formation of multi-ringed compounds, such as naphthalene, from both linear and cyclic olefins during plasma reactions. This work is cited in an article by Harald Suhr in Hollahan and Bell [28]. It is possible that some of the reactions at the polymer surface are ring formations or ring de-saturations. Hydrogen abstraction which would create ring de-saturation in cyclic-polyisoprene is referred to in the literature as a common

plasma reaction because of the low dissociation energy associated with this process [18,30,29].

THEORY-DESCRIPTIVE EQUATIONS

Since the system being used in this study operates in a transient mode during most of the reaction, the descriptive equations which must be used are those for a semi-batch reactor. The material balance for each component is [31],

$$(\dot{v} \cdot C_i)_f - (\dot{v} \cdot C_i)_e + V_r \cdot R = V_t \cdot (dC_i / dt) \quad (11)$$

where R = reaction rate, gmmoles/liter-minute, of component i

\dot{v} = volumetric flow rate, liters/minute

V = volume (reactor, r, or total, t)

f, e = subscripts designating feed or exit points

C_i = concentration in gmmoles/liter of component i

t = time

In eqn. (11), the first term accounts for the molar rate of component (i) entering the reactor, the second accounts for (i) leaving the reactor, the third accounts for (i) formed by reaction, and the term on the right hand side accounts for the overall rate of change in concentration of (i) in the system with time. From the same source, the energy balance equation for the reactor is [32],

$$-\Delta H \cdot R \cdot V_r \cdot dt + (\dot{v} \cdot C_t)_f \cdot CP_f \cdot (T_o - T) = N_t \cdot CP \cdot dT + U \cdot AR \cdot (T - T_s) \cdot dt \quad (12)$$

where ΔH = heat of reaction, kcal/gmmole
CP = heat capacity of the feed or reaction mixture, kcal/gmmole-°K

T = temperature, $^{\circ}\text{K}$

N = total gmmoles of reaction mixture

AR = area for heat transfer to the surroundings

U = overall heat transfer coefficient, $\text{kcal/cm}^2\text{-hr-}^{\circ}\text{K}$

In equation (12), the first term accounts for the heat of reaction, the second for heating the feed, and on the right hand side of the equation, the first term accounts for heating of the reaction mixture, and the second for heat loss to the surroundings.

In order to simplify solution of equations (11) and (12), several independent relationships were established. First, since the vacuum pump operates as a positive displacement pump down to about 0.01 torr, a linear or quadratic function should exist between volumetric flow rate and pressure. This relationship may be empirically determined, and it then becomes an additional equation eliminating one unknown variable. A slight complication arises in determining this relationship, however, because the thermal conductivity type of pressure gauge used is composition dependent due to the differing thermal conductivities of the reaction gases. Therefore, an iteration procedure described in Appendix I was required to determine the actual total pressure in the concentration measuring cell.

Once the total pressure has been determined, the volumetric flow rate leaving the system can be calculated

using the flow-pressure relationship described above. Since the exit concentration of the product gases will be monitored with time and no product gases enter the system with the oxygen feed, the first two terms in eqn. (11) will be known. Only two terms remain unknown in eqn. (11), the reaction rate and the change of concentration with time in the whole system, dC_i/dt . However, since no reaction occurs outside the reactor, then the exhaust gas measuring apparatus can be included in the system for calculation purposes. Now the appropriate smooth function can be fitted to the exhaust gas concentration-time data and analytically differentiated to give, dC_i/dt . Thus with these relationships established empirically, a direct calculation of the plasma reaction rate can be made.

The scope of the present work does not include a full thermal study of the plasma reactor system. Therefore, no solution of eqn. (12) will be examined.

OBJECTIVE OF THE RESEARCH

The purpose of this study is to provide an understanding of those properties of an oxidizing plasma which are of interest to the chemical engineer in the description of polymer degradation. The experimental work will seek to determine the rates of breakdown of cyclic polyisoprene and novalak resin resist in this plasma. Variables affecting the rate to be examined are: radio frequency (rf) power, total pressure, $f(O_2)$ flow rate, oxygen concentration in a neutral gas, and initial polymer load (number of coated wafers) in the reactor.

Since polymer degradation in an oxygen plasma has been termed "ablative" rather than reactive, this research will attempt to determine which mode is applicable to cyclic polyisoprene and novalak resin resists. whichever mode is applicable, this work seeks to utilize the results of the experiments to improve the reactor and process design not only for oxygen plasma degradation of polymers, but also similar plasma processes in the semiconductor industry.

EQUIPMENT DESCRIPTION

Background

Since the overriding consideration in this study is that the reaction occurs in a vacuum, the optimum equipment for the study of the reaction products is a sampling residual gas analyzer (RGA, or mass spectrometer). This analyzer would not only permit examination of the products, but also the long-lived intermediates in the reaction. High cost and lack of availability eliminated use of the optimum equipment (most plasma research is performed with some variant of the mass spectrometer). The alternatives to the RGA with the exception of emission spectroscopy all take a step back from the reaction intermediates themselves to the reaction products: CO₂, H₂O, and CO. The exploration of workable analytical techniques for examining the concentration of these reaction products versus time involved a literature search of CO₂, H₂O, and CO detection techniques. Among the techniques available are sonic velocity of the exhaust gas, conductance of a solution in which the CO₂ is absorbed, gaseous ionization, sound and ultrasound attenuation, and infrared spectroscopy. Since the infrared spectrometer alone could monitor all of the expected reaction products including the N-O family of gases from the breakdown of the novalak resin resist, it was chosen as the detection instrument for studying the exhaust gases.

Reactor

The apparatus (see Appendix III for diagrams) used for this study was a production model International Plasma Corporation photoresist stripper, model no. 2100. The radio frequency (rf) oscillation of 13.56 megahertz is capacitively coupled and has a maximum forward power of 1000 watts. Balance controls permit adjustment of the rf circuit to maintain minimum reflected power when varying loads are present in the reaction chamber. Cycle times, gas supplies, and power levels were set up on the IPC PM-508 controller. The reactor has two quartz reaction chambers (6" inches diameter by 13" inches long). Oxygen flows into the bottom of the reaction chamber and exhaust gases are drawn out the top by vacuum, supplied by a 17 cfm Welch oil-diffusion pump. During all of the experiments, the wafer diameter was parallel to the reactor diameter.

Pressure Gauges

Reaction chamber pressure was measured with a Hastings-Raydist model DV-4DM thermocouple gauge installed in the exhaust line downstream from the chamber. Since the gauge was factory calibrated for 0-20 mm Hg (torr) of air, the conversion tables and nomograph to read the correct pressure of a different gas (e.g. O₂, CO₂, H₂O) are reproduced in Appendix I Tables AP I-1, 2, and 3. The meter for the vacuum gauge was readable near experimental conditions as 7.0 ± 0.1 torr. Since the meter has a log scale, readable precision was better below 7 torr and somewhat worse above it.

Due to the remote location of the 17 CFM pump under the experimental conditions of this study, the minimum pressure (no O₂ flow) obtainable was 0.6 torr. The experimental pressure of 3.0 torr was obtained with an oxygen flow of 55 cc/minute. Under normal production conditions, the pump is typically connected closer to the reaction chamber exhaust and can attain a pressure as low as 0.1 torr.

Flow Controllers

Initially, calibrated Brooks rotameters were used for oxygen and carbon dioxide flow measurement during the setup of the experimental apparatus. However, since the gas density around the float was variable in the vacuum flow system, the only way to obtain absolute flow rates with the rotameters was to continually solve the Stokes terminal velocity equation. A new means of flow measurement was obviously needed. Therefore, two Tylan Corp. model FCS-100 mass flow controllers were obtained. Each controller was factory calibrated for a flow of 0-200 cc/minute of hydrogen at STP (the appropriate conversion factors for other gases is contained in Appendix IV). The readable precision of the controller was ± 0.5 cc/minute over the entire 0-200 range. The principle of operation of the controller is differential thermal conductivity (see Appendix IV-A). One controller was used for oxygen flow while the other was used for CO₂ flow during the calibration runs. The oxygen and carbon dioxide were supplied to the controller at 5 psig.

Temperature-Thermocouples and Pyrometer

Silicon wafer temperature measurements were made using two devices, a thermocouple or an infrared pyrometer. The thermocouple was a Simpson model 388-3L iron-constantan type with plexiglas protection of the metal leads. A Hewlett-Packard digital voltmeter was used to read the thermocouple signal with the high frequency rf pickup appropriately attenuated by the common mode rejection circuit shown in Fig. AP III-2. This thermocouple was inserted into the reaction chamber through an epoxy-sealed tee on a special quartz adapter for the exhaust line. The junction bead of the thermocouple was protected from the rf field by the aluminum oxide binder (Insa-Lute adhesive cement no. 1, Sauerreisen Cement Co.) which was used to attach it to the silicon wafer. An observation developed from the measurements with this thermocouple. When the wafer-thermocouple probe was placed parallel to the reactor diameter (i.e. perpendicular to the rf electrodes), no rf interference (pickup) occurred in the measurement. However, when the probe was perpendicular to the reactor diameter, a +2.3 millivolt jump in the thermocouple signal occurred whenever the rf power was turned on at 800 watts. This rf pickup is demonstrated by the large gap in the two curves of thermocouple data appearing on Fig. AP II-1. A second identical thermocouple also was inserted through the adapter into the exhaust line to obtain exhaust gas temperatures.

Although some data were taken with the thermocouples, the majority of the silicon wafer temperature data were taken with an IR Industries model TD-7B infrared pyrometer. It operates by measuring the intensity of the infrared radiation being emitted by an object in the 1.75-2.7 micron region of the spectrum. No significant loss of infrared radiation is caused by the quartz window on the reactor. In comparing the pyrometer readings with the earlier thermocouple temperature measurements, it was noted that the thermocouple values were identical to the pyrometer temperatures.

Gas Concentration-Infrared Spectrometer

Measurement of the exhaust gas concentrations of H₂O, CO₂, and CO was made by passing the exhaust through a Beckman model 22557 variable pathlength (0.01 to 10 meter) cell which was placed in the sample beam of a Perkin-Elmer model 457 double beam infrared spectrometer. Since both a separate Nernst glower and a mirror were used in the optical path of the sample beam, a diagram of this instruments layout is included in Fig. AP III-1. A preliminary examination of the exhaust gas to identify the components, revealed that only CO₂ and H₂O were present. Therefore, the spectrometer wavelength was able to be fixed at the major CO₂ absorption peak at 2349 cm⁻¹ (4.3 microns) for the polyisoprene exhaust gas measurements. The Nernst glower for the sample beam was supplied power by a 6.3 Volt, 10 Amp filament transformer controlled by a 115 VAC variac. The transformer delivered

approximately 4V at 10 A to the glower. In order to minimize the effects of changes in the atmospheric CO₂ concentration on the transmittance readings, the entire spectrometer and gas cell were enclosed in a plexiglas box purged with nitrogen.

PROCEDURE - CALIBRATIONS

Temperature

In order to obtain close to absolute temperature calibration for these experiments, the melting points of pure chemicals were used. A detailed description of the calibration technique is given in Appendix II. The pertinent relationships derived from the calibration are:

For the thermocouples,

$$T \text{ hot chuck } (^{\circ}\text{C}) = 1.065 * T \text{ thermocouple } (^{\circ}\text{C}) \quad (13)$$

$$T \text{ actual } (^{\circ}\text{C}) = 1.005 * T \text{ hot chuck } + 7.0165 \quad (14)$$

$$T \text{ actual } (^{\circ}\text{C}) = 1.07 * T \text{ thermocouple } + 7.0165 \quad (15)$$

For the infrared pyrometer,

$$T \text{ hot chuck } (^{\circ}\text{C}) = 0.9922 * T \text{ pyrometer } (^{\circ}\text{C}) + 0.1318 \quad (16)$$

combining equation (14) and (16),

$$T \text{ actual } (^{\circ}\text{C}) = 0.997 * T \text{ pyrometer } + 7.149 \quad (17)$$

Pressure

Using the closest pressure measurement technique to absolute for the 3 torr region of this experiment, the two thermocouple pressure gauges were calibrated to a McLeod gauge by the technique described in Appendix I. From this calibration work, several important relationships were developed for oxygen pressure in the system:

$$P \text{ gas cell (torr)} = 0.4969 * P \text{ exhaust gauge (torr)} + .0027 \quad (18)$$

$$P \text{ reactor (torr)} = 0.5960 * P \text{ exhaust gauge (torr)} - .0856$$

(19)

Although these relationships apply only to oxygen, they are very important for deriving the actual total pressure for the multicomponent mixture of oxygen, carbon dioxide, and water created in the experiment. A complete description of the iteration technique used to obtain the total pressure is contained in Appendix I-A.

Flow

Absolute gas flow calibration can be done by displacing a measured volume of liquid in an interval of time long enough to reduce the error to a small amount. The gas should be insoluble and unreactive in this liquid, therefore, mercury is often used. The calibration of the two mass flow controllers used in this experiment is described in Appendix IV. Although the controllers were claimed to be factory calibrated, the readings from them were approximately 45% low. The relationships developed are,

$$\dot{V} \text{ O}_2 \text{ (cc/min.)} = 1.38 * \dot{V} \text{ reading (cc/min.)} * [1.0] \quad (20)$$

$$\dot{V} \text{ carbon dioxide} = 1.48 * \dot{V} \text{ reading} * [0.74] \quad (21)$$

The numbers in the square brackets are the correction factors from the manufacturer's literature, Table AP IV-1, to account for the different properties of the two gases.

Another important flow relationship needed for the solution of the system equations (see Descriptive Equations) was flow vs. pressure for the IR gas cell. Since at the low pressures involved in the experiment, the gases should all behave as ideal gases, oxygen was chosen for the actual measurement used in the experimental calculations. However, as a precaution pressure vs. flow data were also taken for CO₂ and H₂O. These raw data were reduced using the calibration equations for flow and pressure previously developed. A plot of the oxygen data appears on Fig. AP IV-4 while all of the data are charted on Table AP IV-5 and plotted on Fig. AP IV-6. For easy use in the calculations, a quadratic equation was fitted to the oxygen data, (Table AP IV-7)

$$\dot{V} \text{ (cc/min.)} = -7.993 + 5.329 * \text{Pir cell} + 4.789 * \text{Pir cell}^2$$

(21-A)

where Pir cell = actual gas cell pressure, torr.

Absorbance-Transmittance

In quantitative infrared analysis, large sections of many books are dedicated to equipment calibration due to the low energies being measured. Many factors can lead to inaccuracies because of the numerous operating components in both the experimental and measuring system. Gases may be adsorbed on the measuring cell walls and mirrors, mirrors may be dirty and scatter the infrared signal, mirrors may be misaligned, amplifiers and electronic components may fail

causing signal drift. However, many of these problems can be avoided through careful rechecking of baselines and full scale deflection points during the course of the experimental work. In Appendix V, the details of the calibration measurements are discussed.

The relationship between carbon dioxide concentration and absorbance obtained from these quantitative infrared measurements was,

$$C_{CO_2} \text{ (gmmoles/liter)} = (8.022E-4) * A_{gas} - (2.139E-5) \quad (22)$$

where A_{gas} = per cent absorbance of the gas

PROCEDURE - PRELIMINARY EXPERIMENTS

Temperature Measurements

Initially, the cause of the wafer temperature rise was unknown. However, since the lightly doped (1×10^{15} atoms/cc) silicon used will not couple to the rf field, rf heating of the wafers cannot occur. Therefore, the activated ions and electrons must transfer energy to the wafers to cause the temperature rise. Since this is the mechanism of energy transfer, the most direct measurement technique would be a surface temperature method because the polymer removal is a surface reaction in conjunction with surface heating of both the polymer and substrate silicon. Thermistors, thermocouples, and infrared pyrometers might be used for the

measurement. However, since rf is present, thermistors cannot be used because the carbon sensor would couple with the rf field, absorbing energy and giving a false reading. However, thermocouples could be used if the metallic junction could be shielded from the rf. To test the use of thermocouples, one was attached to a silicon wafer as described earlier, and temperature vs. time was measured at an rf power of 800 watts (each reaction chamber was loaded with 50 wafers to simulate normal operation). The data from this experiment are plotted on Fig. AP II-1. The exponential equation which describes these curves is the solution to the heat transfer problem of an object with negligible surface resistance to heat transfer being suddenly immersed in an ambient of higher temperature. This finding is completely consistent with ion-electron bombardment as the mechanism for energy transfer to the wafer. The equation is shown below [39],

$$(T_{\text{gas}} - T) / (T_{\text{gas}} - T(0)) = \exp(-N \cdot t) \quad (23)$$

where T = temperature of the gas ambient or the wafer, °K

$N = (AR \cdot h / \rho \cdot CP \cdot V)$ silicon wafers, a constant

AR = surface area of the wafer, cm^2

V = volume of the wafer, cm^3

CP = heat capacity of the silicon, calories/gram-°K

h = heat transfer coefficient to the silicon,
cal./ cm^2 -min.-°K

$T(0)$ = wafer initial temperature, °K

The constants for this equation are listed in Table 24. A second thermocouple was used to measure exhaust gas temperature downstream from the reactor. This thermocouple was monitored as the pressure in the reactor was varied and provided a plot of steady-state exhaust temperature vs. pressure, Fig. APII-6. The higher exhaust temperature at lower pressure is caused by expansion of the plasma into the exhaust line which increases the energy transfer from the longer lived excited species to the thermocouple junction. Of course, the expansion of the plasma is due to the reduced collision frequency or longer mean free path at low pressures.

This thermocouple system survived about twenty trial reaction runs after which the fiberglass covering on the leads finally disintegrated. The exposed metal coupled directly to the rf field, glowed red hot, and conducted heat to the junction, ending the feasibility of thermocouple temperature measurement for the set of primary experimental runs.

In order to obtain long term reproducibility in the wafer temperature measurement, an infrared pyrometer was obtained. The temperature scale on this pyrometer began at 110 °C. Therefore, the initial heating of the wafer could not be monitored using this instrument. However, since the equation

for the temperature rise is known, eqn.(23), it was used to estimate this initial temperature rise region by calculating the eqn.(23) constants from the actual data obtained above 110°C.

Concentration Measurement

Using the spectrometer system previously described, a full infrared spectrum was run on the exhaust gases at a pathlength of 6.4 meters. Since the characteristic CO bands between 4.5 and 4.9 microns were absent, the CO gas concentration was eliminated from experimental consideration. The implication of this finding is that either the 800 watt plasma is energetic enough to completely oxidize all reaction products or that the nature of the reaction precludes formation of CO.

Continuing the check on variables affecting the CO₂ concentration measurement, the possibility of H₂O vapor absorption interfering with the CO₂ absorption at 2349 cm⁻¹ was examined. Since data had already been taken on IR transmittance vs. time for three different groups of product wafers, Fig. AP V-3, a calculation was performed to estimate the total grammoles of CO₂ which had been produced. From this estimate the CO₂ concentration corresponding to the minimum transmittance (72.5%) was calculated and found to be 1.345×10^{-4} gmmoles/liter. After the absorbance-transmittance calibration was complete, the concentration corresponding to 72.5% transmittance (14% absorbance) was found to be 1.0×10^{-4}

gmmoles/liter. The close agreement of these values indicates that there was no H₂O interference with the CO₂ concentration measurement. As a final precaution, water vapor was drawn through the gas cell while the transmittance was monitored. No absorption was observed.

One significant problem with constructing the calibration curve appeared when the data were plotted. When a least square straight line was fitted to the data, the zero concentration point intercepted the absorbance axis at +2.3% rather than 0%. No experimental or theoretical explanation of this offset was apparent, although many possible explanations can be found in the literature on infrared quantitative analysis. The present research will treat this offset value as zero CO₂ concentration.

RESULTS

Background to the Primary Experiments

In order to determine the removal rate of photoresist from silicon wafers, the information needed was the total weight loss of photoresist for the time exposed to the plasma. Also, to define when the weight was lost during the cycle, a plot of CO₂ concentration in the exhaust gas vs. time was required. Since the integral of the CO₂ concentration with time should correspond directly to the measured total weight loss, these data act as an internal check on the consistency between these two measurements. The weight loss was obtained simply by weighing the silicon wafers coated with photoresist both before and after each plasma run. Measurement of the CO₂ concentration was made with the Perkin-Elmer spectrometer system and required simultaneous reading of the transmittance and the total pressure of the reaction chambers. Ten 3" diameter wafers coated on each side with resist were placed in each of the reaction chambers. The quartz rack holding the wafers had a wafer to wafer spacing of 0.25 inches. The silicon wafers were oxidized on one side to simulate normal product. To weigh the wafers, they were stacked on the pan of the Mettler balance described earlier. An additional parameter, the wafer temperature, was monitored as a measure of the energy input to the resist surface. In order to prevent inaccuracies in the

relationship between carbon dioxide formation and polymer weight loss, most of the solvents in the resist were driven off by vacuum and baking treatments (160°C) before the experiments began.

Primary Experiments

The experiments to determine overall removal rates of the resists required measurement of: weight loss vs. rf power and time, pressure (pressure is controlled by the oxygen feed rate), initial polymer load (number of coated wafers), and the per cent oxygen in the feed. In the first category of experiments, four runs of 25-44 minutes duration were made at 200, 400, 600, and 800 watts rf power. Longer times were used for the 200, and 400 watt runs in order to remove enough resist to reduce the error in the weight loss and CO₂ concentration measurements. Ten coated wafers were placed in each chamber and the oxygen feed rate was held at 55 cc/minute. Data from these runs are charted on Tables 1-4 and plotted on Figs. 5-9. For the second set of experiments two runs were made at 800 watts and a 27 cc/minute oxygen feed rate. Data on the time variance of absorbance, pressure, and temperature at this new oxygen feed rate are charted on Tables 10 and 11 and plotted on Figs. 5-9. During the third experiment, the power was held constant at 800 watts and the feed rate at 27 cc/minute, while the time was varied for each run. The weight loss, wafer temperature, and total pressure were monitored for run times of 1, 2, 3,

4, 5, 7, 8, 10, 12, 16, 18, and 24 minutes. The chart of weight loss vs. time data is Table 12 and Figs. 12a, 12b, 12c. The next experiment measured the weight loss from 2, 6, and 10 coated wafers per chamber while time, power, and feed rate were held constant at 20 minutes, 800 watts, and 55 cc/minute, respectively. Table 13 presents the details of these data and weight loss vs. load is plotted in Fig. 14. In addition to using pure oxygen as the reaction gas for the negative resist removal measurements, several measurements were taken of polymer removal rates for 0, 12.5, and 22 % oxygen in nitrogen which acts as a neutral gas. The experiments were performed at 800 watts of power and weight loss, wafer temperature, and pressure were monitored. A plot of the weight loss data is presented in Figure 15. The small positive removal rate observed in the pure nitrogen run was caused by a small amount of air leakage into the system.

Positive Resist

The attempt to perform these same five primary experiments with positive resist failed. Although three runs were made in which all parameters were monitored, a rapid pressure rise developed about eight minutes into each run. This effect brought the run to a halt, since the high pressures could not be measured precisely and the plasma could barely be maintained. Consequently, novalak resin resist stripping was dropped from this project. It was suspected initially that a byproduct of novalak breakdown was reacting with the

silicone rubber reactor seals causing an air leak. However, the seals suffered no damage because this supposed air leak was absent during subsequent negative resist runs and vacuum testing. Therefore, an explanation based on the novalak reaction itself was sought. One possible cause of enhanced reaction of positive resist is the breakdown of the naphthoquinone diazide sensitizer to ketene releasing nitrogen followed by the rapid breakdown of the ketene releasing carbon dioxide. In addition, the oxygen content of both the novalak resin ($C_{71}H_{79}O_9$) and the sensitizer ($C_{23}H_{14}O_7S$) is very high compared to the nearly pure hydrocarbon structure of the polyisoprene. Therefore, this positive resist structure should breakdown more rapidly than the polyisoprene, yielding a larger pressure rise.

" Fluorocarbon polymers have the smallest ablation rate. Hydrogen polymers have a larger ablation rate and hydrocarbon polymers containing oxygen have the largest ablation rate." [34]

This general observation by Hudis runs contrary to the observed slow removal rate of positive resist and the data in D'Allelio and Parker's book which attest to the excellent resistance to removal of the novalak resin family of polymers. [35] Recent attempts to recreate this pressure rise effect have failed, leaving the phenomenon even more perplexing. The scant data gathered from these three runs is presented in Tables 16-18 for completeness.

TABLE 1

RUN NUMBER 1
 NO. DATA POINTS 25
 NUMBER OF WAFERS 20
 POWER LEVEL RF WATTS 800.0000
 O₂ FEED RATE 55.199966 CC/MINUTE
 BASELINE TRANSMITTANCE 0.8650

THE DATA ON THIS PAGE WAS REDUCED USING THE CALIBRATION RELATIONS DEVELOPED EARLIER IN THIS PROGRAM
 FLOW NORMALIZATION FACTOR WAS, 1.30996

THE MEASURED WT. LOSS IS 0.1689 GRAMS THE CO₂ LOSS CALCULATED FROM TRANSMITTANCE DATA IS 0.5464 GRAMS

TIME (MINUTES)	ABSORBANCE	TRANSMIT- TANCE	RXN-RATE GRAMMOLES/ LITER-MIN.	IR CELL PRESSURE (TORR)	CO ₂ MOLE FFACTION	CO ₂ LOSS GRAMS PER MINUTE	TOTAL CO ₂ LOSS (GRAMS)	WAFER TEMPERATURE (DEGREES C)	D(O ₂)/DT GRAMMOLES/ LITER-MIN.
0.1000E+01	0.2853E-01	0.9364E+00	0.1965E-05	0.3219E+01	0.8276E-02	0.6956E-03	0.6956E-03	0.0	0.1982E-04
0.2000E+01	0.4492E-01	0.9017E+00	0.1328E-04	0.3164E+01	0.8663E-01	0.6709E-02	0.7405E-02	0.0	0.2547E-04
0.3000E+01	0.4771E-01	0.8960E+00	0.1554E-04	0.3245E+01	0.9737E-01	0.7932E-02	0.1534E-01	0.1208E+03	0.2168E-04
0.4000E+01	0.5222E-01	0.8867E+00	0.1877E-04	0.3259E+01	0.1177E+00	0.9671E-02	0.2501E-01	0.1268E+03	0.2174E-04
0.5000E+01	0.5620E-01	0.8786E+00	0.2165E-04	0.3271E+01	0.1356E+00	0.1122E-01	0.3623E-01	0.1348E+03	0.2179E-04
0.6000E+01	0.5907E-01	0.8728E+00	0.2351E-04	0.3248E+01	0.1498E+00	0.1222E-01	0.4845E-01	0.1478E+03	0.2355E-04
0.7000E+01	0.6778E-01	0.8555E+00	0.3010E-04	0.3293E+01	0.1875E+00	0.1572E-01	0.6417E-01	0.1567E+03	0.2262E-04
0.8000E+01	0.7369E-01	0.8439E+00	0.3462E-04	0.3321E+01	0.2126E+00	0.1813E-01	0.8230E-01	0.1667E+03	0.2215E-04
0.9000E+01	0.7968E-01	0.8324E+00	0.3940E-04	0.3360E+01	0.2369E+00	0.2067E-01	0.1030E+00	0.1737E+03	0.2114E-04
0.1000E+02	0.8576E-01	0.8208E+00	0.4341E-04	0.3325E+01	0.2669E+00	0.2280E-01	0.1258E+00	0.1807E+03	0.2405E-04
0.1100E+02	0.9192E-01	0.8092E+00	0.4808E-04	0.3338E+01	0.2935E+00	0.2528E-01	0.1510E+00	0.1966E+03	0.2440E-04
0.1200E+02	0.9192E-01	0.8092E+00	0.4873E-04	0.3387E+01	0.2893E+00	0.2563E-01	0.1767E+00	0.2006E+03	0.2188E-04
0.1300E+02	0.9192E-01	0.8092E+00	0.4871E-04	0.3387E+01	0.2893E+00	0.2563E-01	0.2023E+00	0.2046E+03	0.2190E-04
0.1400E+02	0.9192E-01	0.8092E+00	0.4869E-04	0.3387E+01	0.2893E+00	0.2563E-01	0.2280E+00	0.2066E+03	0.2191E-04
0.1500E+02	0.9503E-01	0.8035E+00	0.5144E-04	0.3417E+01	0.3004E+00	0.2709E-01	0.2550E+00	0.2106E+03	0.2084E-04
0.1600E+02	0.9503E-01	0.8035E+00	0.5142E-04	0.3417E+01	0.3004E+00	0.2709E-01	0.2821E+00	0.2126E+03	0.2085E-04
0.1700E+02	0.1013E+00	0.7919E+00	0.5572E-04	0.3391E+01	0.3306E+00	0.2937E-01	0.3115E+00	0.2146E+03	0.2333E-04
0.1800E+02	0.1013E+00	0.7919E+00	0.5571E-04	0.3391E+01	0.3306E+00	0.2937E-01	0.3409E+00	0.2166E+03	0.2333E-04
0.1900E+02	0.1013E+00	0.7919E+00	0.5570E-04	0.3391E+01	0.3306E+00	0.2937E-01	0.3702E+00	0.2186E+03	0.2334E-04
0.2000E+02	0.1013E+00	0.7919E+00	0.5569E-04	0.3391E+01	0.3306E+00	0.2937E-01	0.3996E+00	0.2205E+03	0.2335E-04
0.2100E+02	0.1013E+00	0.7919E+00	0.5568E-04	0.3391E+01	0.3306E+00	0.2937E-01	0.4290E+00	0.2215E+03	0.2336E-04
0.2200E+02	0.1013E+00	0.7919E+00	0.5568E-04	0.3391E+01	0.3306E+00	0.2937E-01	0.4583E+00	0.2225E+03	0.2336E-04
0.2300E+02	0.1013E+00	0.7919E+00	0.5567E-04	0.3391E+01	0.3306E+00	0.2937E-01	0.4877E+00	0.2235E+03	0.2337E-04
0.2400E+02	0.1013E+00	0.7919E+00	0.5566E-04	0.3391E+01	0.3306E+00	0.2937E-01	0.5171E+00	0.2245E+03	0.2337E-04
0.2500E+02	0.1013E+00	0.7919E+00	0.5566E-04	0.3391E+01	0.3306E+00	0.2937E-01	0.5464E+00	0.2255E+03	0.2337E-04

ABSORBANCE FOR RUN NO. 1 THE COEFFICIENT VALUES ARE A=0.9352E-01 R=0.1163E+00 Y0=0.9583E-01

PRESSURE IR CELL FOR RUN NO. 1 THE COEFFICIENT VALUES ARE A=0.7848E+00 R=0.1133E+00 Y0=0.3183E+01

TEMPERATURE FOR RUN NO. 1 THE COEFFICIENT VALUES ARE A=0.1725E+03 R=0.1057E+00 Y0=0.6960E+02

BEST QUADRATIC FIT OF THE TOTAL CO₂ LOSS (GRAMS) WITH TIME GIVES COEFFS. A=-.1712E-01 R=0.9501E-02 C=0.5472E-03

TABLE 2

RUN NUMBER 2
 NO. DATA POINTS 20
 NUMBER OF WATERS 20
 PUMP LEVEL IN WATTS 200.0000
 O₂ FEED RATE 55.199966 CC/MINUTE
 BASELINE TRANSMITTANCE 0.8950

THE DATA ON THIS PAGE WAS REDUCED USING THE CALIBRATION RELATIONS DEVELOPED EARLIER IN THIS PROGRAM
 FLOW NORMALIZATION FACTOR WAS 1.00000

THE MEASURED WT. LOSS IS 0.0525 GRAMS THE CO₂ LOSS CALCULATED FROM TRANSMITTANCE DATA IS 0.0 GRAMS

TIME (MINUTES)	ABSORBANCE	TRANSMIT- TANCE	RXN-RATE GRAMMOLES/ LITER-MIN.	IR CELL PRESSURE (TORR)	CO ₂ MOLE FRACTION	CO ₂ LOSS GRAMS PER MINUTE	TOTAL CO ₂ LOSS (GRAMS)	WAFER TEMPERATURE (DEGREES C)	D(CO ₂)/DT GRAMMOLES/ LITER-MIN.
0.1000E+01	0.7340E-02	0.9832E+00	0.1198E-06	0.3028E+01	0.0	0.0	0.0	0.0	0.5985E-05
0.2000E+01	0.1230E-01	0.9721E+00	0.1097E-06	0.3227E+01	0.0	0.0	0.0	0.0	-1.7606E-05
0.3000E+01	0.1230E-01	0.9721E+00	0.9861E-07	0.3326E+01	0.0	0.0	0.0	0.0	-1.1467E-04
0.4000E+01	0.1230E-01	0.9721E+00	0.8946E-07	0.3376E+01	0.0	0.0	0.0	0.0	-1.827E-04
0.5000E+01	0.1481E-01	0.9665E+00	0.8115E-07	0.3401E+01	0.0	0.0	0.0	0.0	-2.008E-04
0.6000E+01	0.1481E-01	0.9665E+00	0.7362E-07	0.3401E+01	0.0	0.0	0.0	0.0	-2.008E-04
0.8000E+01	0.1732E-01	0.9609E+00	0.6059E-07	0.3401E+01	0.0	0.0	0.0	0.0	-2.007E-04
0.1000E+02	0.1986E-01	0.9553E+00	0.4987E-07	0.3401E+01	0.0	0.0	0.0	0.0	-2.006E-04
0.1200E+02	0.1986E-01	0.9553E+00	0.4104E-07	0.3401E+01	0.0	0.0	0.0	0.0	-2.006E-04
0.1400E+02	0.2240E-01	0.9497E+00	0.3378E-07	0.3401E+01	0.0	0.0	0.0	0.0	-2.005E-04
0.1600E+02	0.2240E-01	0.9497E+00	0.2780E-07	0.3401E+01	0.0	0.0	0.0	0.0	-2.005E-04
0.1800E+02	0.2394E-01	0.9464E+00	0.2298E-07	0.3401E+01	0.0	0.0	0.0	0.0	-2.004E-04
0.2000E+02	0.2394E-01	0.9464E+00	0.1983E-07	0.3401E+01	0.0	0.0	0.0	0.0	-2.004E-04
0.2400E+02	0.2497E-01	0.9441E+00	0.1275E-07	0.3401E+01	0.0	0.0	0.0	0.0	-2.003E-04
0.2800E+02	0.2497E-01	0.9441E+00	0.8638E-08	0.3401E+01	0.0	0.0	0.0	0.0	-2.003E-04
0.3200E+02	0.2651E-01	0.9408E+00	0.5851E-08	0.3401E+01	0.0	0.0	0.0	0.0	-2.002E-04
0.3600E+02	0.2651E-01	0.9408E+00	0.3963E-08	0.3401E+01	0.0	0.0	0.0	0.0	-2.002E-04
0.4000E+02	0.2651E-01	0.9408E+00	0.2684E-08	0.3401E+01	0.0	0.0	0.0	0.0	-2.002E-04
0.4200E+02	0.2651E-01	0.9408E+00	0.2209E-08	0.3401E+01	0.0	0.0	0.0	0.0	-2.002E-04
0.4400E+02	0.2651E-01	0.9408E+00	0.1818E-08	0.3401E+01	0.0	0.0	0.0	0.0	-2.002E-04

ABSORBANCE
 FOR RUN NO. 2 THE COEFFICIENT VALUES ARE A=0.2028E-01 B=0.9740E-01 Y0=0.0000E-02

PRESSURE IN CELL
 FOR RUN NO. 2 THE COEFFICIENT VALUES ARE A=0.3832E+00 B=0.4036E+00 Y0=0.3034E+01

TEMPERATURE
 FOR RUN NO. 2 THE COEFFICIENT VALUES ARE A=0.4000E+02 B=0.0000E-01 Y0=0.7000E+02

BEST QUADRATIC FIT OF THE TOTAL CO₂ LOSS (GRAMS) WITH TIME GIVES COEFS. A=0.0 B=0.0 C=0.0

TABLE 3

RUN NUMBER 3
 NO. DATA POINTS 22
 NUMBER OF WAFERS 20
 POWER LEVEL RF WATTS 400.0000
 O₂ FEED RATE 55.199966 CC/MINUTE
 BASELINE TRANSMITTANCE 0.9100

THE DATA ON THIS PAGE WAS REDUCED USING THE CALIBRATION RELATIONS DEVELOPED EARLIER IN THIS PROGRAM
 FLOW NORMALIZATION FACTOR WAS, 0.97836

THE MEASURED WT. LOSS IS 0.0883 GRAMS THE CO₂ LOSS CALCULATED FROM TRANSMITTANCE DATA IS 0.2857 GRAMS

TIME (MINUTES)	ABSORBANCE	TRANSMIT- TANCE	RXN-RATE GRAMMOLES/ LITER-MIN.	IR CELL PRESSURE (TORR)	CO ₂ MOLE FRACTION	CO ₂ LOSS GRAMS PER MINUTE	TOTAL CO ₂ LOSS (GRAMS)	WAFER TEMPERATURE (DEGREES C)	D(021/01) GRAMMOLES/ LITER-MIN.
0.1000E+01	0.1456E-01	0.9670E+00	0.1863E-06	0.3078E+01	0.0	0.0	0.0	0.0	0.2896E-06
0.2000E+01	0.1952E-01	0.9560E+00	0.1723E-06	0.3277E+01	0.0	0.0	0.0	0.0	-1.379E-04
0.3000E+01	0.2203E-01	0.9505E+00	0.1595E-06	0.3376E+01	0.0	0.0	0.0	0.0	-2.110E-04
0.4000E+01	0.2454E-01	0.9451E+00	0.1475E-06	0.3425E+01	0.0	0.0	0.0	0.0	-2.748E-04
0.5000E+01	0.2708E-01	0.9396E+00	0.5391E-06	0.3385E+01	0.1793E-02	0.2126E-03	0.2126E-03	0.0	-2.167E-04
0.6000E+01	0.2962E-01	0.9341E+00	0.3155E-05	0.3492E+01	0.1269E-01	0.1599E-02	0.1812E-02	0.0	-2.920E-04
0.7000E+01	0.3218E-01	0.9286E+00	0.5786E-05	0.3499E+01	0.2333E-01	0.2993E-02	0.4805E-02	0.0	-2.911E-04
0.8000E+01	0.3218E-01	0.9286E+00	0.5854E-05	0.3549E+01	0.2333E-01	0.3034E-02	0.7839E-02	0.0	-3.293E-04
0.9000E+01	0.3218E-01	0.9286E+00	0.5769E-05	0.3499E+01	0.2366E-01	0.2993E-02	0.1083E-01	0.0	-2.904E-04
0.1000E+02	0.3476E-01	0.9231E+00	0.8330E-05	0.3463E+01	0.3508E-01	0.3349E-02	0.1518E-01	0.0	-2.577E-04
0.1200E+02	0.3632E-01	0.9198E+00	0.9587E-05	0.3350E+01	0.4324E-01	0.5020E-02	0.2522E-01	0.1144E+03	-1.642E-04
0.1400E+02	0.3632E-01	0.9198E+00	0.9576E-05	0.3350E+01	0.4324E-01	0.5020E-02	0.3526E-01	0.1188E+03	-1.691E-04
0.1600E+02	0.3735E-01	0.9176E+00	0.1058E-04	0.3345E+01	0.4776E-01	0.5554E-02	0.4637E-01	0.1244E+03	-1.674E-04
0.1800E+02	0.4523E-01	0.9011E+00	0.1813E-04	0.3310E+01	0.8417E-01	0.9549E-02	0.6547E-01	0.1288E+03	-1.202E-04
0.2000E+02	0.4523E-01	0.9011E+00	0.1813E-04	0.3310E+01	0.8417E-01	0.9549E-02	0.8457E-01	0.1318E+03	-1.202E-04
0.2200E+02	0.4682E-01	0.8978E+00	0.1962E-04	0.3301E+01	0.9167E-01	0.1034E-01	0.1052E+00	0.1338E+03	-1.109E-04
0.2400E+02	0.4788E-01	0.8956E+00	0.2091E-04	0.3343E+01	0.9527E-01	0.1102E-01	0.1273E+00	0.1348E+03	-1.340E-04
0.2600E+02	0.5056E-01	0.8901E+00	0.2340E-04	0.3324E+01	0.1079E+00	0.1234E-01	0.1520E+00	0.1368E+03	-1.182E-04
0.2800E+02	0.5056E-01	0.8901E+00	0.2340E-04	0.3324E+01	0.1079E+00	0.1234E-01	0.1766E+00	0.1368E+03	-1.181E-04
0.3000E+02	0.5325E-01	0.8846E+00	0.2583E-04	0.3299E+01	0.1210E+00	0.1363E-01	0.2039E+00	0.1408E+03	-9.380E-05
0.3200E+02	0.5325E-01	0.8846E+00	0.2583E-04	0.3299E+01	0.1210E+00	0.1363E-01	0.2312E+00	0.1398E+03	-9.378E-05
0.3600E+02	0.5325E-01	0.8846E+00	0.2583E-04	0.3299E+01	0.1210E+00	0.1363E-01	0.2857E+00	0.1408E+03	-9.374E-05

ABSORBANCE
 FOR RUN NO. 3 THE COEFFICIENT VALUES ARE A=0.3876E-01 B=0.776E-01 Y0=0.150E-01

PRESSURE IR CELL
 FOR RUN NO. 3 THE COEFFICIENT VALUES ARE A=0.4198E+00 B=0.2355E+00 Y0=0.3084E+01

TEMPERATURE
 FOR RUN NO. 3 THE COEFFICIENT VALUES ARE A=0.8072E+02 B=0.7700E-01 Y0=0.6700E+02

BEST QUADRATIC FIT OF THE TOTAL CO₂ LOSS (GRAMS) WITH TIME GIVES COEFFS. A=-1.715E-02 B=-.6205E-03 C=0.452E-03

10-10-68
10-11-68
10-12-68
10-13-68
10-14-68
10-15-68
10-16-68
10-17-68
10-18-68
10-19-68
10-20-68
10-21-68
10-22-68
10-23-68
10-24-68
10-25-68
10-26-68
10-27-68
10-28-68
10-29-68
10-30-68
10-31-68

1. The first step is to identify the problem or question that needs to be answered. This involves understanding the context and the specific requirements of the task.

100

100

100

TABLE 4

RUN NUMBER 4
NO. DATA POINTS 18
NUMBER OF WAFERS 20
POWER LEVEL RF WATTS 600.0000
O2 FEED RATE 55.199966 CC/MINUTE
BASELINE TRANSMITTANCE 0.9250

THE DATA ON THIS PAGE WAS REDUCED USING THE CALIBRATION RELATIONS DEVELOPED EARLIER IN THIS PROGRAM
FLOW NORMALIZATION FACTOR WAS, 0.97168

THE MEASURED WT. LOSS IS 0.0949 GRAMS THE CO₂ LOSS CALCULATED FROM TRANSMITTANCE DATA IS 0.3232 GRAMS

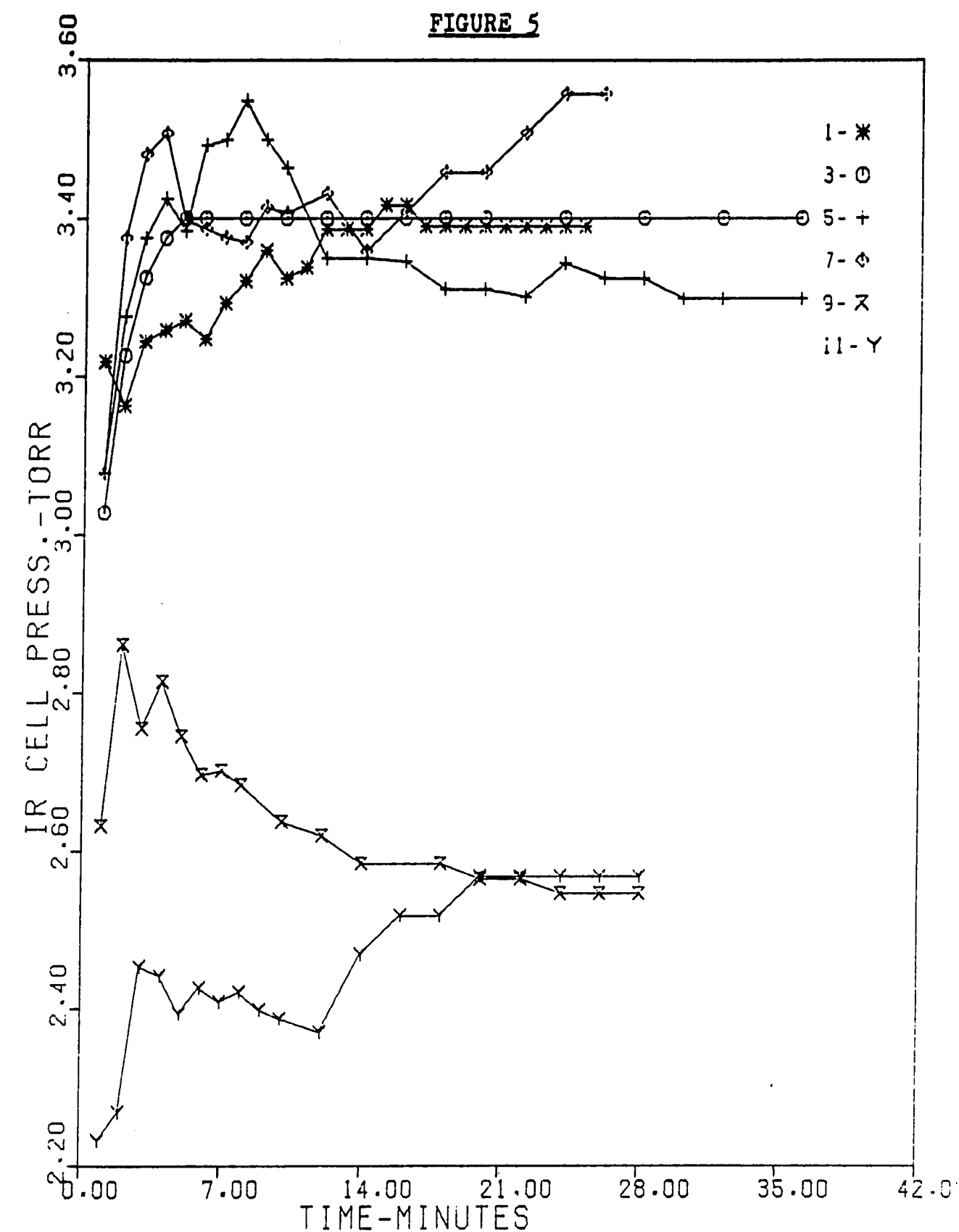
TIME (MINUTES)	ABSORBANCE	TRANSMIT- TANCE	RXN-RATE GRAMMOLES/ LITER-MIN.	IR CELL PRESSURE (TORR)	CO2 MOLE FRACTION	CO2 LOSS GRAMS PER MINUTE	TOTAL CO2 LOSS (GRAMS)	WAFER TEMPERATURE (DEGREES C)	D(02)/DT GRAMMOLES/ LITER-MIN.
0.1000E+01	0.1920E-01	0.9568E+00	0.3198E-06	0.3078E+01	0.0	0.0	0.0	0.0	-5517E-06
0.2000E+01	0.2667E-01	0.9405E+00	0.2847E-06	0.3376E+01	0.0	0.0	0.0	0.0	-2208E-04
0.3000E+01	0.2913E-01	0.9351E+00	0.2782E-05	0.3481E+01	0.1059E-01	0.1335E-02	0.1335E-02	0.0	-2944E-04
0.4000E+01	0.3418E-01	0.9243E+00	0.8013E-05	0.3507E+01	0.3213E-01	0.4112E-02	0.5447E-02	0.0	-3032E-04
0.5000E+01	0.3672E-01	0.9189E+00	0.1032E-04	0.3398E+01	0.4442E-01	0.5341E-02	0.1079E-01	0.0	-2135E-04
0.6000E+01	0.3929E-01	0.9135E+00	0.1283E-04	0.3387E+01	0.5592E-01	0.6682E-02	0.1747E-01	0.1148E+03	-1944E-04
0.7000E+01	0.4186E-01	0.9081E+00	0.1535E-04	0.3376E+01	0.6757E-01	0.8023E-02	0.2549E-01	0.1218E+03	-1853E-04
0.8000E+01	0.4342E-01	0.9049E+00	0.1686E-04	0.3370E+01	0.7461E-01	0.8827E-02	0.3432E-01	0.1288E+03	-1770E-04
0.9000E+01	0.4446E-01	0.9027E+00	0.1811E-04	0.3415E+01	0.7821E-01	0.9495E-02	0.4381E-01	0.1378E+03	-2076E-04
0.1000E+02	0.5233E-01	0.8865E+00	0.2600E-04	0.3407E+01	0.1131E+00	0.1367E-01	0.5748E-01	0.1388E+03	-1836E-04
0.1200E+02	0.5498E-01	0.8811E+00	0.2886E-04	0.3431E+01	0.1239E+00	0.1519E-01	0.7886E-01	0.1476E+03	-1954E-04
0.1400E+02	0.5766E-01	0.8757E+00	0.3090E-04	0.3358E+01	0.1385E+00	0.1628E-01	0.1204E+00	0.1557E+03	-1353E-04
0.1600E+02	0.5766E-01	0.8757E+00	0.3133E-04	0.3408E+01	0.1365E+00	0.1651E-01	0.1534E+00	0.1597E+03	-1716E-04
0.1800E+02	0.5766E-01	0.8757E+00	0.3176E-04	0.3458E+01	0.1346E+00	0.1674E-01	0.1869E+00	0.1637E+03	-2084E-04
0.2000E+02	0.5766E-01	0.8757E+00	0.3175E-04	0.3458E+01	0.1346E+00	0.1674E-01	0.2204E+00	0.1687E+03	-2083E-04
0.2200E+02	0.5766E-01	0.8757E+00	0.3218E-04	0.3507E+01	0.1327E+00	0.1698E-01	0.2544E+00	0.1727E+03	-2456E-04
0.2400E+02	0.5766E-01	0.8757E+00	0.3261E-04	0.3557E+01	0.1308E+00	0.1721E-01	0.2888E+00	0.1757E+03	-2834E-04
0.2600E+02	0.5766E-01	0.8757E+00	0.3261E-04	0.3557E+01	0.1308E+00	0.1721E-01	0.3232E+00	0.1777E+03	-2834E-04

ABSORBANCE
FOR RUN NO. 4 THE COEFFICIENT VALUES ARE $A=0.4624E-01$ $B=0.1162E+00$ $Y_0=0.1539E-01$

PRESSURE IN CELL
 FOR RUN NO. 4 THE COEFFICIENT VALUES ARE $A=0.7059E+00$ $H=0.1285E+00$ $Y_0=0.3084E+01$

TEMPERATURE
FOR RUN NO. 4 THE COEFFICIENT VALUES ARE $A=0.1307E+03$ $R=0.7069E-01$ $Y_0=0.7057E+02$

BEST QUADRATIC FIT OF THE TOTAL CO₂ LOSS (GRAMS) WITH TIME GIVES COEFS. A=-.1145E-01 B=0.3730E-02 C=0.3711E-03



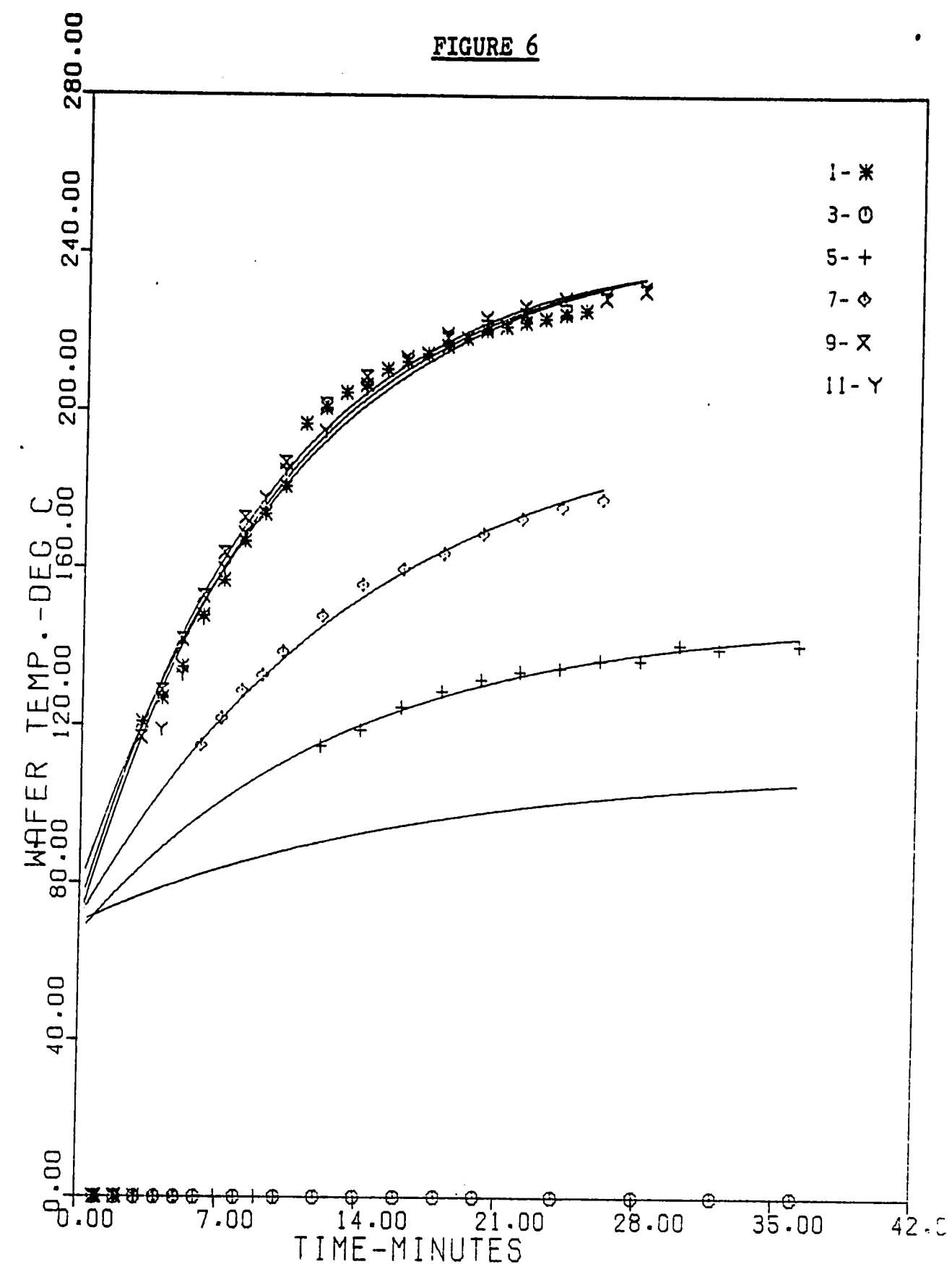
THE SYMBOL NUMBERS ON THE GRAPH CORRESPOND TO RUN NUMBERS AS FOLLOWS:
 SYMBOL 1-RUN 1. SYMBOL 3-RUN 2. SYMBOL 5-RUN 3. SYMBOL 7-RUN 4. SYMBOL 9-RUN 5. SYMBOL 11-RUN 6

RUN 1-800 WATTS. RUN 2-200 WATTS. RUN 3-400 WATTS. RUN 4-600 WATTS---02 55 CC/MIN

RUN 5-800 WATTS. RUN 9-800 WATTS-----02 28-30 FEED RATE

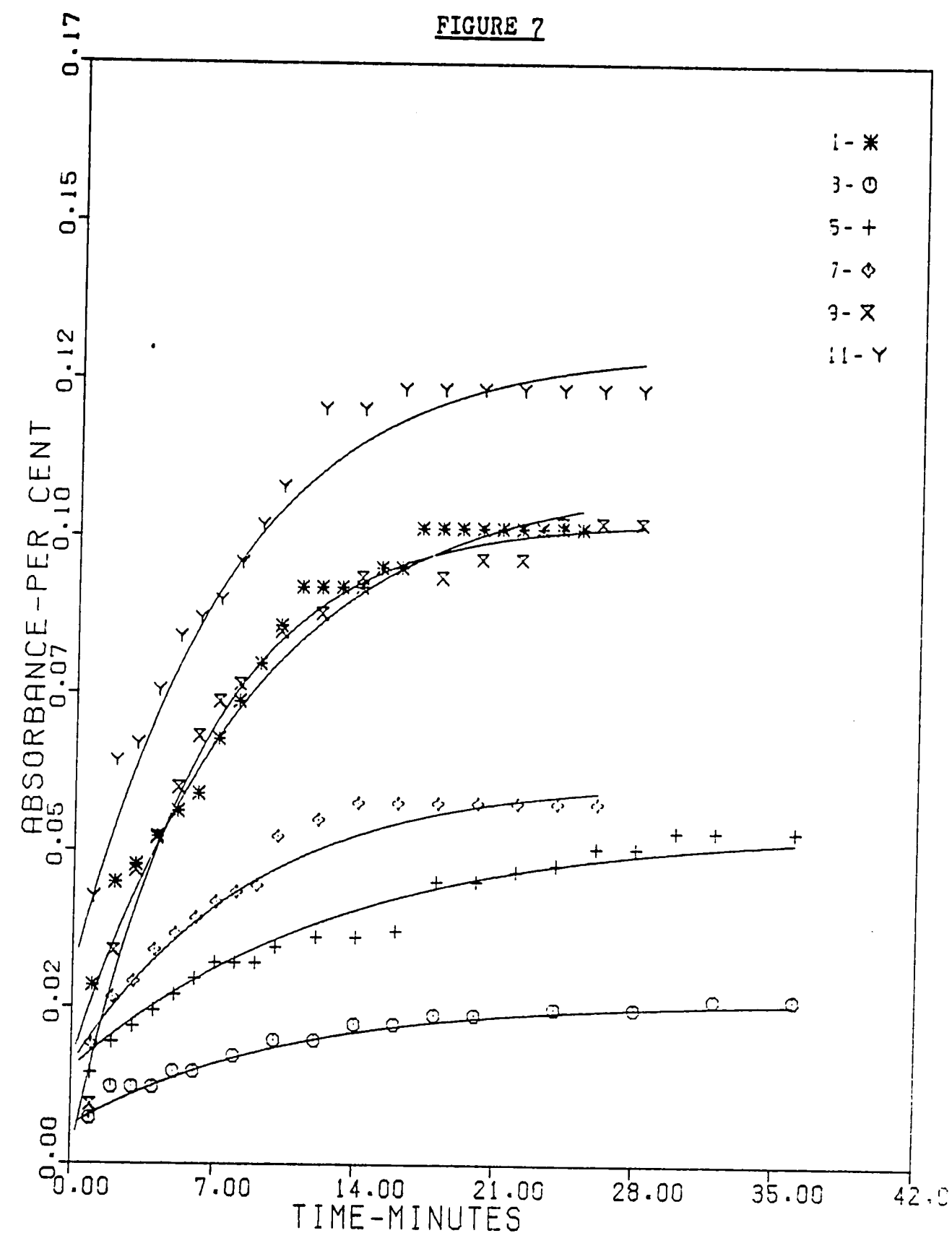
-33e-

FIGURE 6

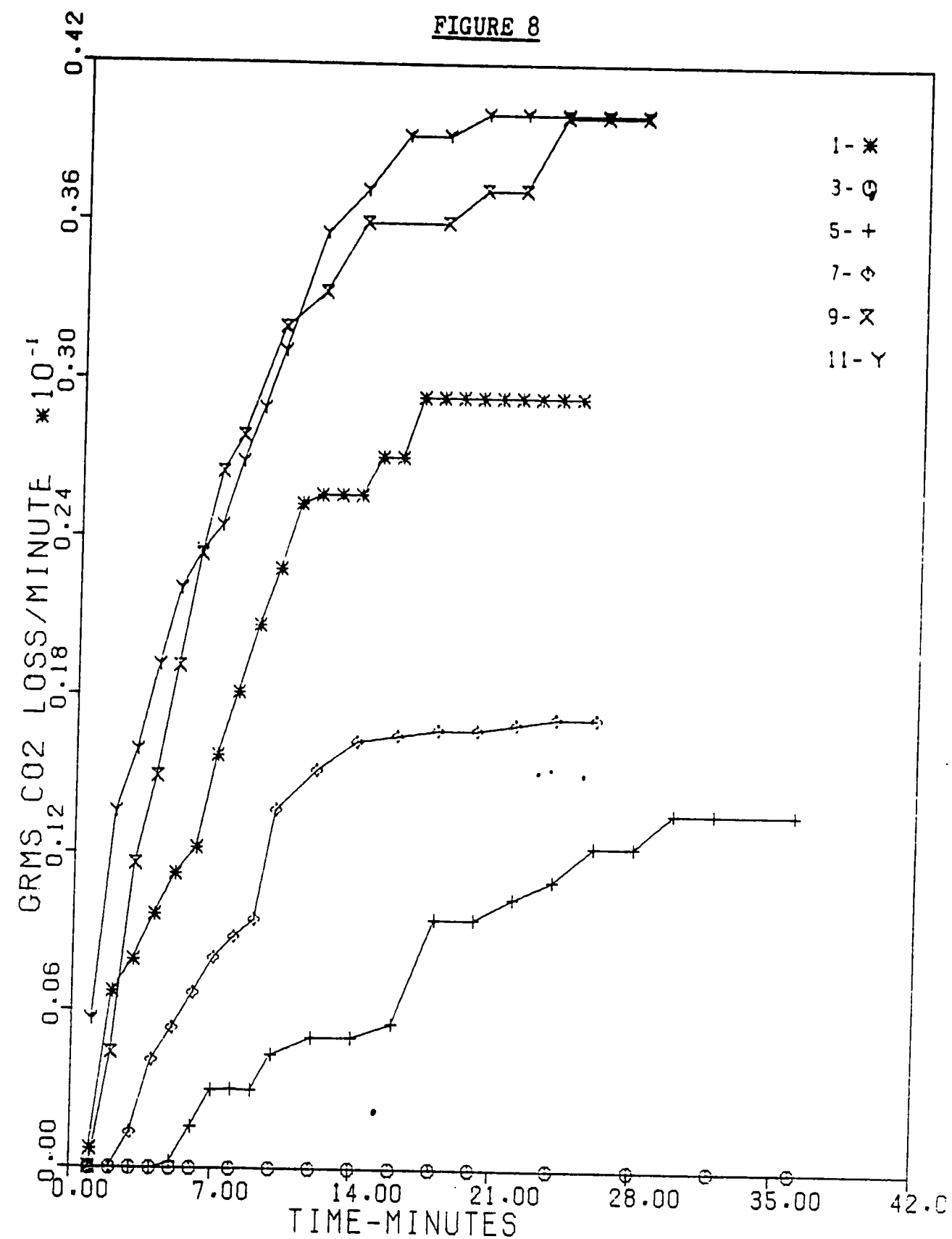


THE SYMBOL NUMBERS ON THE GRAPH CORRESPOND TO RUN NUMBERS AS FOLLOWS:
 SYMBOL 1-RUN1. SYM. 3-RUN2. SYM. 5-RUN3. SYM. 7-RUN4. SYM. 9-RUN5. SYM. 11-RUN6

THE LINE WITH NO DATA IS ESTIMATED CURVE (RUN2). TEMP. RUN2 < 100.0
 WAFER TEMPERATURE WAS MEASURED WITH AN IR PYROMETER.
 TEMP. DATA BELOW 100 DEG C IS CALCULATED FROM A FIT OF DATA ABOVE 100 DEG C TO
 $Y = A * (1 - \exp(-B * \text{TIME})) + Y_0$. WHERE A, B, Y0 ARE CONSTANTS

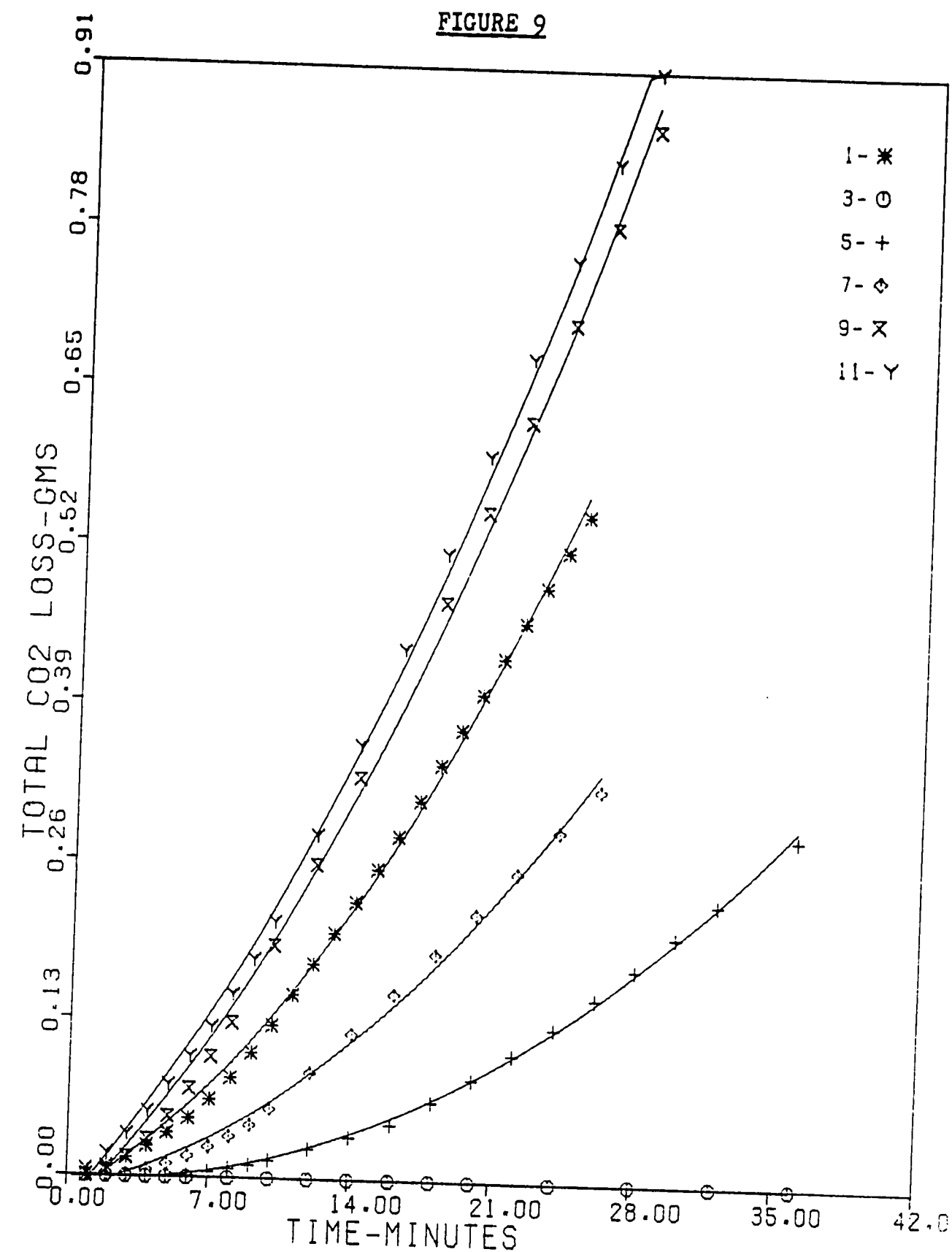


THE SYMBOL NUMBERS ON THE GRAPH CORRESPOND TO RUN NUMBERS AS FOLLOWS:
 SYMBOL 1-RUN 1. SYM. 3-RUN 2. SYM. 5-RUN 3. SYM. 7-RUN 4. SYM. 9-RUN 5. SYM. 11-RUN 6
 THE LINES ON THIS PLOT WERE CALCULATED FROM A RELATIONSHIP OF THE FORM
 $Y = A * (1 - \exp(-B * \text{TIME})) - Y_0$ WHERE A, B, Y₀ ARE CONSTANTS



THE SYMBOL NUMBERS ON THE GRAPH CORRESPOND TO RUN NUMBERS AS FOLLOWS.
 SYMBOL 1-RUN 1. SYMBOL 3-RUN 2. SYMBOL 5-RUN 3. SYMBOL 7-RUN 4. SYMBOL 9-RUN 5. SYMBOL 11-RUN 6

- 33h -



THE SYMBOL NUMBERS ON THE GRAPH CORRESPOND TO RUN NUMBERS AS FOLLOWS:
 SYMBOL 1-RUN 1, SYM. 3-RUN 2, SYM. 5-RUN 3, SYM. 7-RUN 4, SYM. 9-RUN 5, SYM. 11-RUN 6
 THE LINES ON THIS PLOT WERE CALCULATED FROM THE RELATIONSHIP $Y=A+B \cdot X+C \cdot X^2$
 WHERE A, B, AND C ARE CONSTANTS

RECEIVED
FEB 11 1964
U.S. AIR FORCE
RESEARCH AND
DEVELOPMENT
COMMAND
WALLINGFORD
MASSACHUSETTS
01901

TABLE 10

RUN NUMBER 5
NO. DATA POINTS 17
NUMBER OF WAFERS 20
POWER LEVEL RF WATTS 800.0000
O2 FLOW RATE 30.359970 CC/MINUTE
BASELINE TRANSMITTANCE 0.9300

THE DATA ON THIS PAGE WAS REDUCED USING THE CALIBRATION RELATIONS DEVELOPED EARLIER IN THIS PROGRAM
FLOW NORMALIZATION FACTOR WAS, 0.72761

THE MEASURED WT. LOSS IS 0.2668 GRAMS THE CO2 LOSS CALCULATED FROM TRANSMITTANCE DATA IS 0.8632 GRAMS

TIME (MINUTES)	ABSORBANCE	TRANSMIT- TANCE	RXN-RATE GRAMMOLES/ LITER-MIN.	IR CELL PRESSURE (TORR)	CO2 MOLE FRACTION	CO2 LOSS GRAMS PER MINUTE	TOTAL CO2 LOSS (GRAMS)	WAFER TEMPERATURE (DEGREES C)	D(CO2)/DT GRAMMOLES/ LITER-MIN.
0.1000E+01	0.9442E-02	0.9785E+00	0.9711E-06	0.2632E+01	0.0	0.0	0.0	0.0	-4.646E-04
0.2000E+01	0.3398E-01	0.9247E+00	0.9111E-05	0.2861E+01	0.3839E-01	0.4377E-02	0.4377E-02	0.0	-6.376E-04
0.3000E+01	0.4680E-01	0.8978E+00	0.2264E-04	0.2755E+01	0.1097E+00	0.1159E-01	0.1597E-01	0.1168E+03	-5.142E-04
0.4000E+01	0.5203E-01	0.8871E+00	0.2886E-04	0.2814E+01	0.1353E+00	0.1493E-01	0.3089E-01	0.1288E+03	-5.497E-04
0.5000E+01	0.6000E-01	0.8710E+00	0.3671E-04	0.2745E+01	0.1823E+00	0.1912E-01	0.5001E-01	0.1418E+03	-4.714E-04
0.6000E+01	0.6812E-01	0.8548E+00	0.4463E-04	0.2696E+01	0.2308E+00	0.2334E-01	0.7335E-01	0.1527E+03	-4.117E-04
0.7000E+01	0.7361E-01	0.8441E+00	0.5053E-04	0.2701E+01	0.2609E+00	0.2649E-01	0.9984E-01	0.1637E+03	-4.019E-04
0.8000E+01	0.7639E-01	0.8387E+00	0.5306E-04	0.2683E+01	0.2783E+00	0.2786E-01	0.1277E+00	0.1727E+03	-3.802E-04
0.1000E+02	0.8487E-01	0.8226E+00	0.6081E-04	0.2637E+01	0.3312E+00	0.3199E-01	0.1917E+00	0.1866E+03	-3.253E-04
0.1200E+02	0.8767E-01	0.8172E+00	0.6327E-04	0.2619E+01	0.3498E+00	0.3332E-01	0.2583E+00	0.2016E+03	-3.026E-04
0.1400E+02	0.9342E-01	0.8065E+00	0.6820E-04	0.2584E+01	0.3879E+00	0.3595E-01	0.3302E+00	0.2086E+03	-2.626E-04
0.1800E+02	0.9342E-01	0.8065E+00	0.6815E-04	0.2584E+01	0.3879E+00	0.3595E-01	0.4740E+00	0.2186E+03	-2.421E-04
0.2000E+02	0.9633E-01	0.8011E+00	0.7053E-04	0.2564E+01	0.4079E+00	0.3722E-01	0.5485E+00	0.2215E+03	-2.409E-04
0.2200E+02	0.9633E-01	0.8011E+00	0.7052E-04	0.2564E+01	0.4079E+00	0.3722E-01	0.6229E+00	0.2245E+03	-2.408E-04
0.2400E+02	0.1022E+00	0.7903E+00	0.7586E-04	0.2546E+01	0.4454E+00	0.4004E-01	0.7030E+00	0.2255E+03	-2.138E-04
0.2600E+02	0.1022E+00	0.7903E+00	0.7586E-04	0.2546E+01	0.4454E+00	0.4004E-01	0.7831E+00	0.2285E+03	-2.137E-04
0.2800E+02	0.1022E+00	0.7903E+00	0.7586E-04	0.2546E+01	0.4454E+00	0.4004E-01	0.8632E+00	0.2305E+03	-2.137E-04

ABSORBANCE
FOR RUN NO. 5 THE COEFFICIENT VALUES ARE A=0.1025E+00 B=0.1675E+00 Y0=0.0000E-02

PRESSURE IR CELL
FOR RUN NO. 5 THE COEFFICIENT VALUES ARE A=0.4048E+00 B=0.3414E+00 Y0=0.7637E+01

TEMPERATURE
FOR RUN NO. 5 THE COEFFICIENT VALUES ARE A=0.1695E+03 B=0.1071E+00 Y0=0.7268E+02

BEST QUADRATIC FIT OF THE TOTAL CO2 LOSS (GRAMS) WITH TIME GIVES COEFFS. A=-.3251E-01 B=0.1720E-01 C=0.5533E-03

TABLE 11

RUN NUMBER 9
 NO. DATA POINTS 19
 NUMBER OF WAFERS 20
 POWER LEVEL RF WATTS 800.0000
 O₂ FEED RATE 27.599976 CC/MINUTE
 BASELINE TRANSMITTANCE 0.9100

THE DATA ON THIS PAGE WAS REDUCED USING THE CALIBRATION RELATIONS DEVELOPED EARLIER IN THIS PROGRAM
 FLOW NORMALIZATION FACTOR WAS, 0.93794

THE MEASURED WT. LOSS IS 0.2829 GRAMS THE CO₂ LOSS CALCULATED FROM TRANSMITTANCE DATA IS 0.9153 GRAMS

TIME (MINUTES)	ABSORBANCE	TRANSMIT- TANCE	RXN-RATE GRAMMOLES/ LITER-MIN.	IR CELL PRESSURE (TORR)	CO ₂ MOLE FRACTION	CO ₂ LOSS GRAMS PER MINUTE	TOTAL CO ₂ LOSS (GRAMS)	WAFER TEMPERATURE (DEGREES C)	D(CO ₂)/DT GRAMMOLES/ LITER-MIN.
0.1000E+01	0.4259E-01	0.9066E+00	0.1152E-04	0.2232E+01	0.1071E+00	0.5661E-02	0.5661E-02	0.0	-0.2053E-05
0.2000E+01	0.6417E-01	0.8626E+00	0.2642E-04	0.2268E+01	0.2483E+00	0.1359E-01	0.1925E-01	0.0	-0.5394E-06
0.3000E+01	0.6695E-01	0.8571E+00	0.3075E-04	0.2453E+01	0.2466E+00	0.1592E-01	0.3516E-01	0.0	-0.1015E-04
0.4000E+01	0.7538E-01	0.8407E+00	0.3679E-04	0.2441E+01	0.2996E+00	0.1915E-01	0.5431E-01	0.1188E+03	-0.7982E-05
0.5000E+01	0.8398E-01	0.8242E+00	0.4221E-04	0.2393E+01	0.3596E+00	0.2204E-01	0.7635E-01	0.1328E+03	-0.3819E-05
0.6000E+01	0.8689E-01	0.8187E+00	0.4492E-04	0.2426E+01	0.3728E+00	0.2351E-01	0.9986E-01	0.1468E+03	-0.5058E-05
0.7000E+01	0.8981E-01	0.8132E+00	0.4665E-04	0.2408E+01	0.3938E+00	0.2445E-01	0.1243E+00	0.1597E+03	-0.3550E-05
0.8000E+01	0.9572E-01	0.8022E+00	0.5123E-04	0.2420E+01	0.4284E+00	0.2689E-01	0.1512E+00	0.1687E+03	-0.3191E-05
0.9000E+01	0.1017E+00	0.7912E+00	0.5505E-04	0.2398E+01	0.4699E+00	0.2892E-01	0.1801E+00	0.1777E+03	-0.4519E-04
0.1000E+02	0.1078E+00	0.7802E+00	0.5914E-04	0.2387E+01	0.5104E+00	0.3111E-01	0.2112E+00	0.1846E+03	0.6800E-06
0.1200E+02	0.1202E+00	0.7582E+00	0.6757E-04	0.2370E+01	0.5927E+00	0.3558E-01	0.2824E+00	0.1946E+03	-0.6976E-06
0.1400E+02	0.1202E+00	0.7582E+00	0.7061E-04	0.2469E+01	0.5689E+00	0.3721E-01	0.3568E+00	0.2056E+03	-0.3145E-05
0.1600E+02	0.1234E+00	0.7527E+00	0.7453E-04	0.2518E+01	0.5765E+00	0.3930E-01	0.4354E+00	0.2136E+03	-0.6299E-05
0.1800E+02	0.1234E+00	0.7527E+00	0.7451E-04	0.2518E+01	0.5765E+00	0.3930E-01	0.5140E+00	0.2196E+03	-0.6279E-05
0.2000E+02	0.1234E+00	0.7527E+00	0.7605E-04	0.2568E+01	0.5654E+00	0.4012E-01	0.5943E+00	0.2235E+03	-0.7570E-05
0.2200E+02	0.1234E+00	0.7527E+00	0.7604E-04	0.2568E+01	0.5654E+00	0.4012E-01	0.6745E+00	0.2265E+03	-0.7508E-05
0.2400E+02	0.1234E+00	0.7527E+00	0.7603E-04	0.2568E+01	0.5654E+00	0.4012E-01	0.7548E+00	0.2285E+03	-0.7500E-05
0.2600E+02	0.1234E+00	0.7527E+00	0.7602E-04	0.2568E+01	0.5654E+00	0.4012E-01	0.8350E+00	0.2295E+03	-0.7493E-05
0.2800E+02	0.1234E+00	0.7527E+00	0.7601E-04	0.2568E+01	0.5654E+00	0.4012E-01	0.9153E+00	0.2315E+03	-0.7488E-05

ABSORBANCE FOR RUN NO. 9 THE COEFFICIENT VALUES ARE A=0.9977E-01 R=0.1363E+00 Y0=0.3080E-01

PRESSURE IR CELL FOR RUN NO. 9 THE COEFFICIENT VALUES ARE A=0.8064E+00 R=0.1364E+00 Y0=0.2334E+01

TEMPERATURE FOR RUN NO. 9 THE COEFFICIENT VALUES ARE A=0.1669E+03 R=0.9508E-01 Y0=0.7840E+02

BEST QUADRATIC FIT OF THE TOTAL CO₂ LOSS (GRAMS) WITH TIME GIVES COEFIS. A=-0.2465E-01 B=0.1932E-01 C=0.5782E-03

TABLE 12

All of the temperature and pressure data on this table are uncalibrated.

<u>Wt. Loss</u> <u>(grams)</u>	<u>Wt. Loss Rate</u> <u>(grams/min.)</u>	<u>Temperature</u> <u>(Deg. C)</u>	<u>Pressure</u> <u>(torr)</u>	<u>Time</u> <u>(min.)</u>
0.0048	0.0048	---	5.2	1
0.0092	0.0046	---	5.2	2
0.0142	0.0047	---	5.2	3
0.0212	0.0053	109	5.2	4
0.0291	0.0058	120	5.2	5
0.0483	0.0069	148	5.3	7
0.0552	0.0069	162	5.6	8
0.0674	0.0068	180	6.0	10
0.0954	0.0080	190	6.2	12
0.1463	0.0091	205	6.5	16
0.1800	0.0100	210	6.5	18
0.2605	0.0110	216	6.5	24

FIGURE 12a

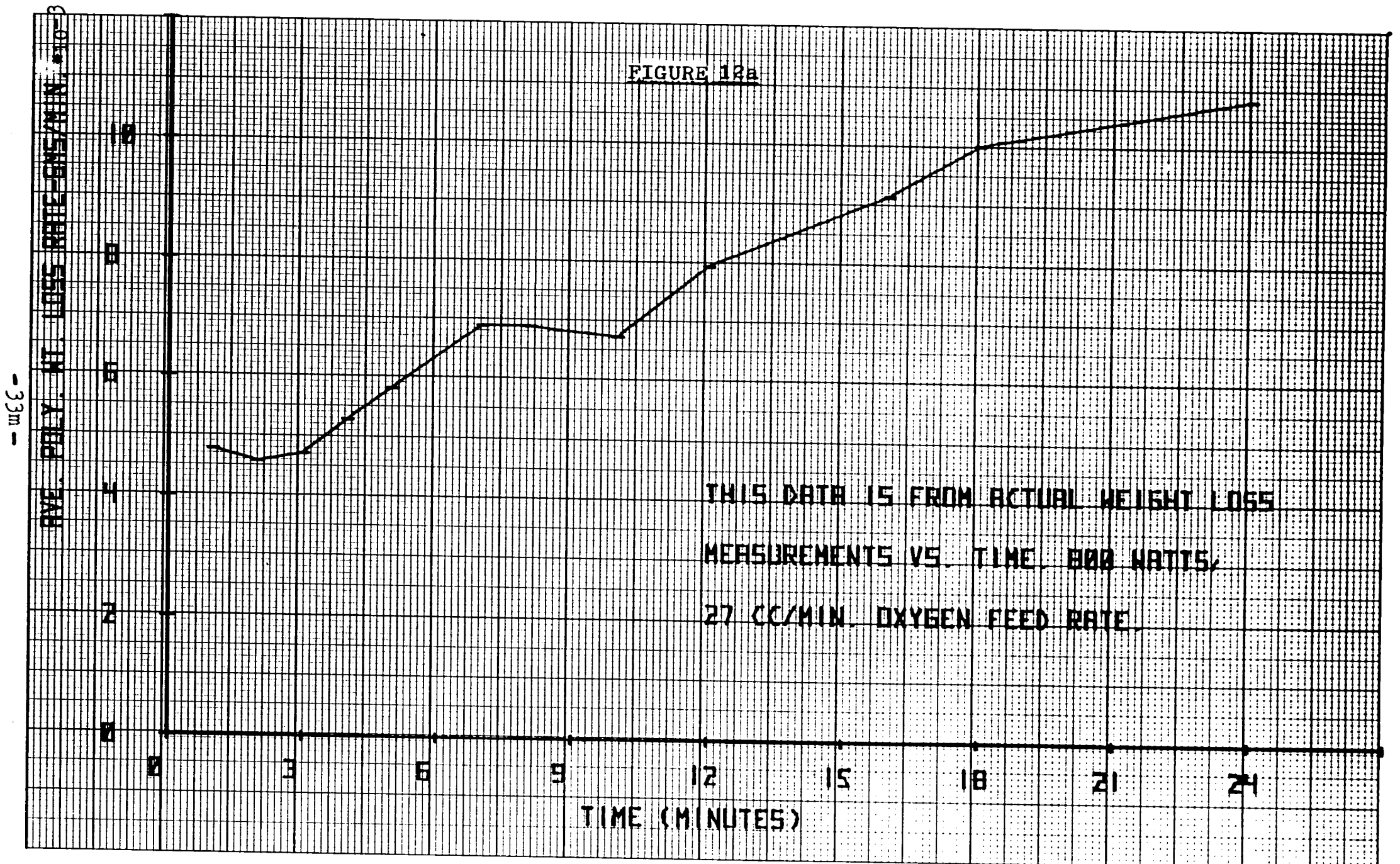


FIGURE 12b

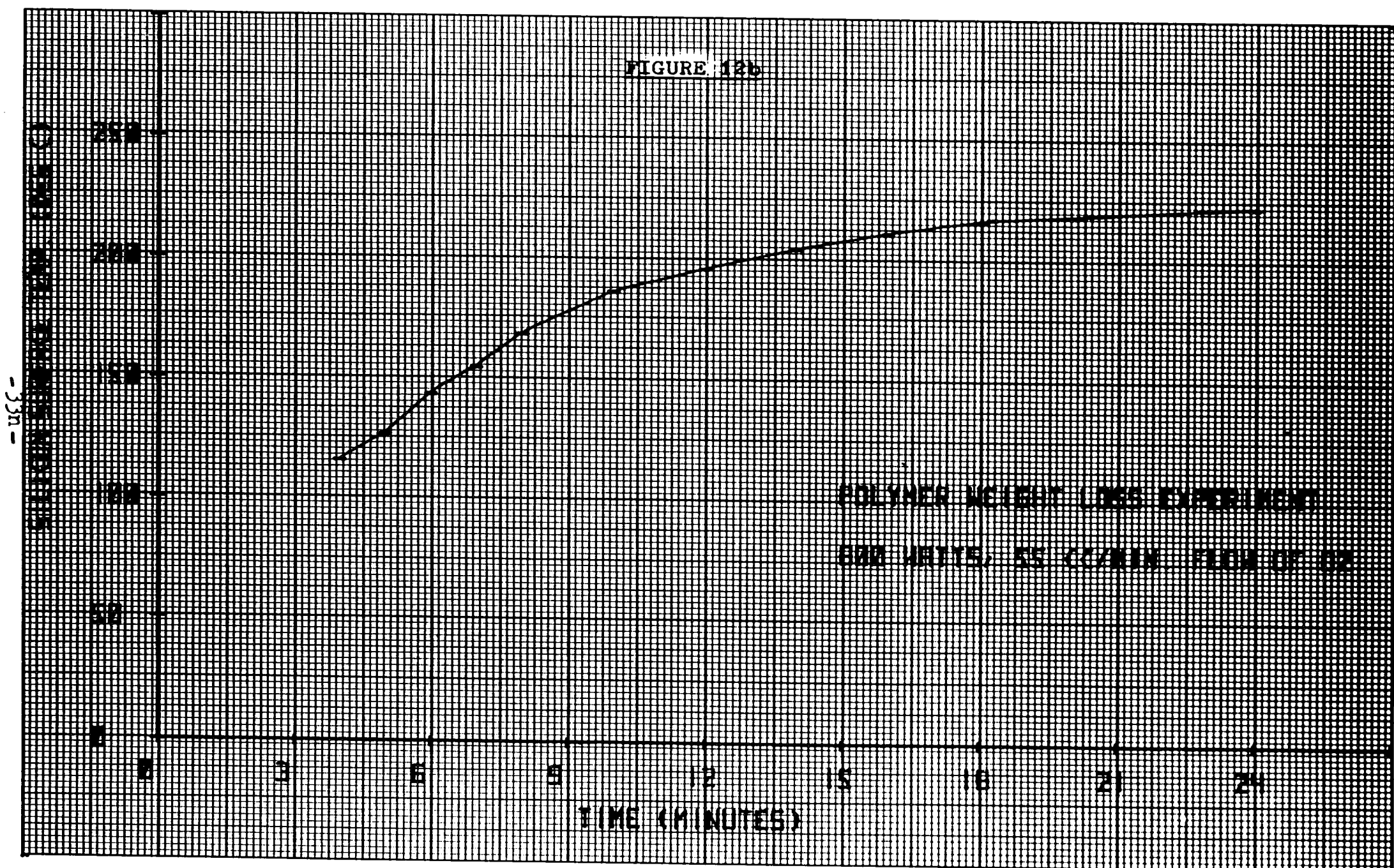


FIGURE 12e

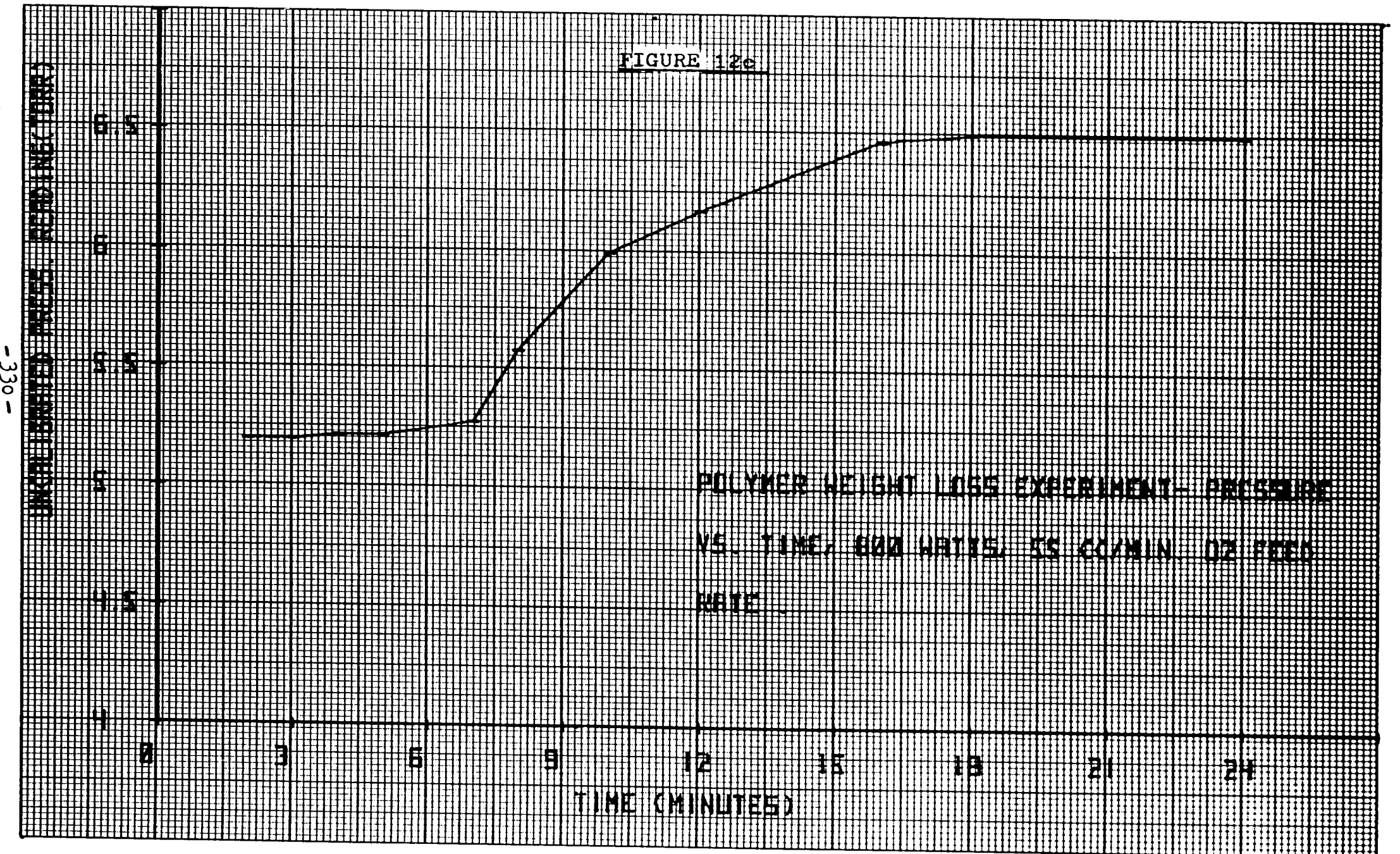


TABLE 13

All of the temperature and pressure data on this table are uncalibrated.

No wafers/chamber		2 wafers/chamber		6 wafers/chamber		10 wafers/chamber		Time (min.)
Temp. (= .5) (Deg. C)	Press. (torr)	Temp. (= .5) (Deg. C)	Press. (torr)	Temp. (= .5) (Deg. C)	Press. (torr)	Temp. (= .5) (Deg. C)	Press. (torr)	
---	6.0	---	5.9	---	5.9	---	6.0	1
---	6.0	---	6.1	---	6.1	---	6.3	2
---	6.0	---	6.3	---	6.2	---	6.5	3
---	6.0	---	6.4	---	6.3	---	6.7	4
---	6.0	110	6.5	108	6.5	110	6.8	5
108	6.0	120	6.6	120	6.6	120	6.9	6
114	6.0	130	6.7	130	6.7+	129	6.9	7
120	6.0	140	6.7	139	6.9	138	7.0	8
126	6.0	---	---	---	---	---	---	9
132	6.0	153	6.8	154	6.9+	150	7.0	10
140	6.0	162	6.9	164	7.0	164	7.1	12
148	5.9	170	6.9	172	7.0	174	7.1	14
154	5.9	175	6.9	177	7.0	180	7.2	16
159	5.9	End= 16.4min.		182	7.0	186	7.2	18
164	5.9			186	7.0	192	7.2	20

Resist Wt. Loss =
in Grams

0.0429

0.1085

0.1421

Ave. Wt. Loss Rate =
in Grams/minute

0.00262

0.00542

0.00710

Wt. Loss Rate/wafer =
in gms./min.-wafer

0.00131

0.00090

0.00071

FIGURE 14

WEIGHT LOSS EXPERIMENT--
LOSS RATE IS IN (GMS / MIN.)
800 WATTS, 55 CC/MIN O₂ FEED RATE

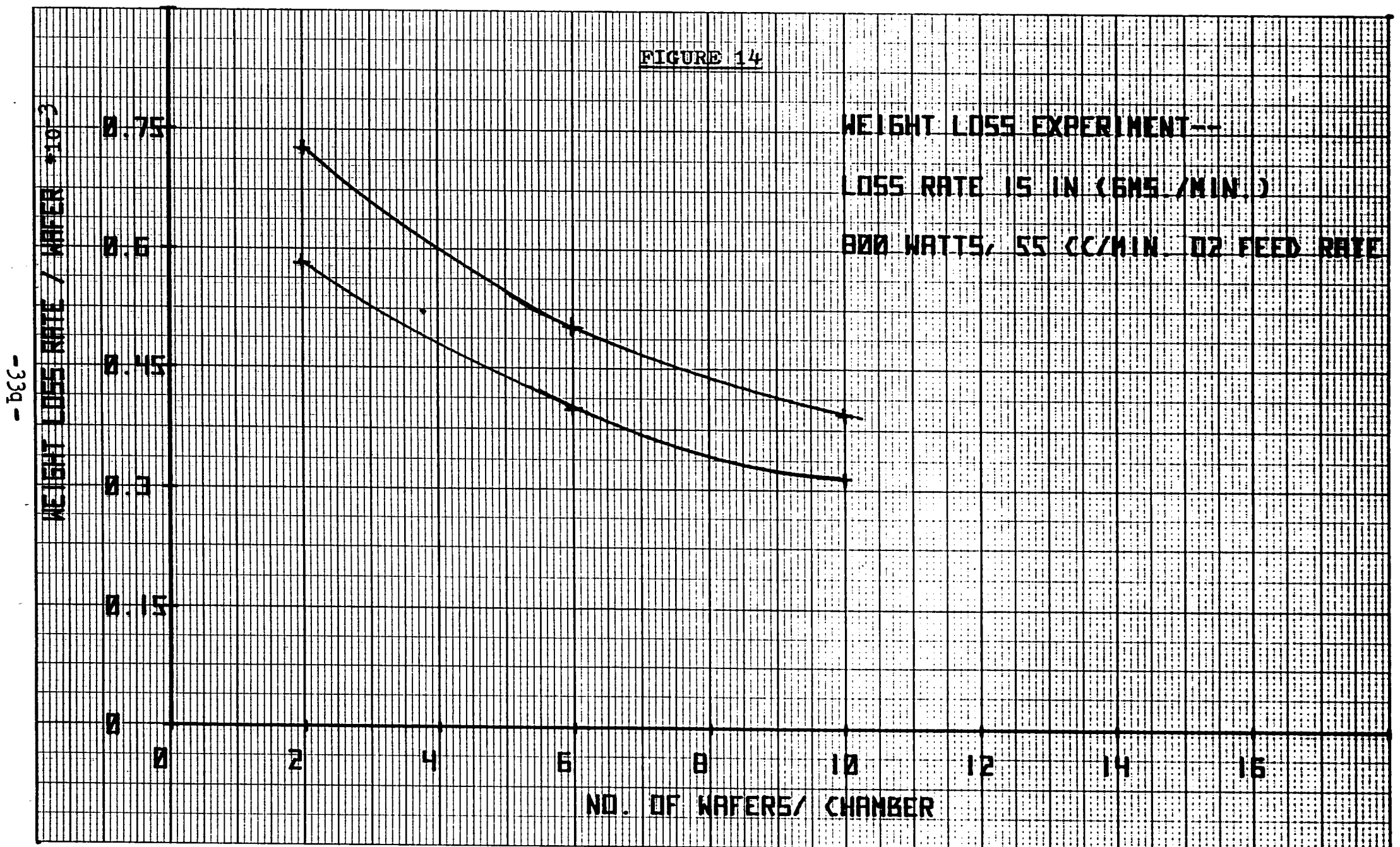
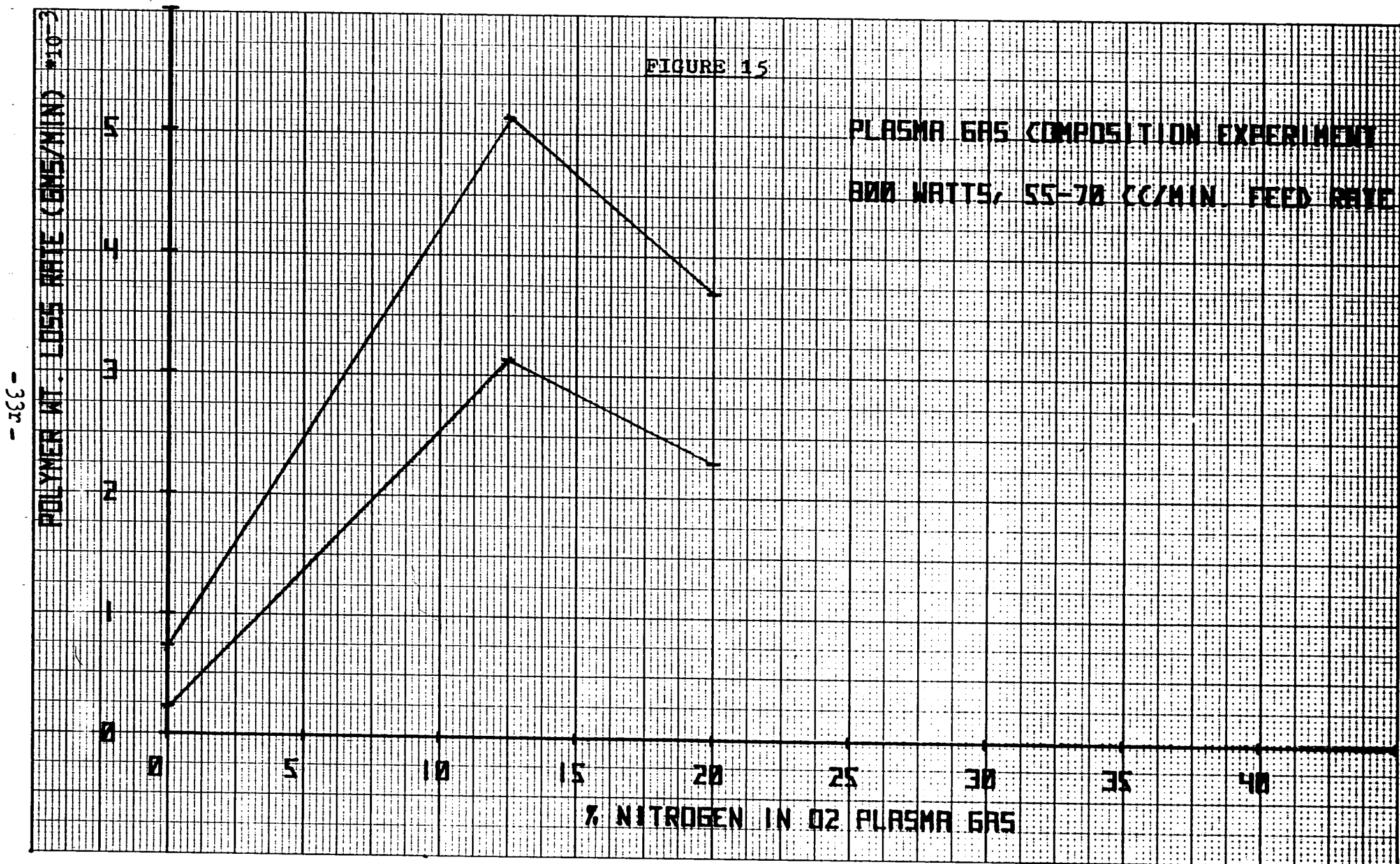


FIGURE 15

PLASMA GAS COMPOSITION EXPERIMENT
800 WATTS, 55-70 CC/MIN. FEED RATE



ED-111E
SERIAL

TABLE 16

RUN NUMBER 6
NO. DATA POINTS 10
NUMBER OF WAFERS 20
POWER LEVEL RF WATTS 800.0000
O₂ FEED RATE 20.000000 CC/MINUTE
BASELINE TRANSMITTANCE 0.9300

TIME (MINUTES)	RELATIVE TRANSMITTANCE	REACTOR PRESSURE METER (TORR)	PYROMETER METER (DEG. CELSIUS)
1.0000	0.8850	5.5000	0.0
2.0000	0.8650	5.8000	0.0
3.0000	0.8500	5.9000	0.0
4.0000	0.8300	5.9000	0.0
5.0000	0.8000	6.0000	118.0000
6.0000	0.7850	6.1000	135.0000
7.0000	0.7800	6.3000	145.0000
8.0000	0.7600	8.5000	150.0000
10.0000	0.7500	10.0000	156.0000
12.0000	0.7400	10.0000	170.0000
			188.0000

RUN NUMBER 7
 NO. DATA POINTS 8
 NUMBER OF WAFERS 20
 POWER LEVEL RF WATTS 800.0000
 O₂ FEED RATE 20.000000 CC/MINUTE
 BASELINE TRANSMITTANCE 0.9200

TABLE 12

TIME (MINUTES)	RELATIVE TRANSMITTANCE	REACTOR PRESSURE METER (TORR)	PYROMETER METER (DEG. CELSIUS)
1.0000	0.8700	5.4000	0.0
2.0000	0.8400	5.6000	0.0
3.0000	0.8400	5.5000	110.0000
4.0000	0.8200	5.5000	125.0000
5.0000	0.8000	5.5000	138.0000
6.0000	0.7900	5.5000	152.0000
7.0000	0.7650	5.6000	162.0000
8.0000	0.7300	5.8000	172.0000

TABLE 18

RUN NUMBER 8
NO. DATA POINTS 11
NUMBER OF WAFERS 20
POWER LEVEL RF WATTS 800.0000
O2 FEED RATE 20.000000 CC/MINUTE
BASELINE TRANSMITTANCE 0.9100

TIME (MINUTES)	RELATIVE TRANSMITTANCE	REACTOR PRESSURE METER (TORR)	PYROMETER METER (DEG. CELSIUS)
1.0000	0.8350	4.6000	0.0
2.0000	0.8150	4.7500	0.0
3.0000	0.7950	4.9000	110.0000
4.0000	0.7800	5.0000	128.0000
5.0000	0.7750	5.0000	138.0000
6.0000	0.7550	5.1000	154.0000
7.0000	0.7450	5.2000	166.0000
8.0000	0.7350	5.3000	177.0000
9.0000	0.7150	5.6000	184.0000
10.0000	0.7050	5.8000	190.0000
12.0000	0.6850	7.5000	206.0000

DISCUSSION OF RESULTS

The purpose of this research was to determine the effect of several variables on the rate of breakdown of cyclic polyisoprene and novalak resin photoresists in an oxygen plasma. Most of the experiments with negative resist were very successful with a significant addition to the data base on the process of oxygen plasma removal. However, positive resist (novalak resin) was dropped from the project when the experiments could not be adequately controlled to obtain useful information.

Computer Solution

In order to solve the myriad relationships necessary to correlate the data into useful information, it was necessary to construct the computer program which comprises Appendix VI. A two part block diagram is used to describe this program's computations in overview. The first part, Table 19, breaks out the major sections of the calibration and experiment calculations including reference to equations in the text. While the second part, Table 20, details the plotting performed. Since the program is fundamentally algebraic and the method of carrying out the analytical solution is presented in a previous section of this paper (see Theory - Descriptive Equations), only the data and new relationships discovered in data analysis will be discussed.

FIGURE 19

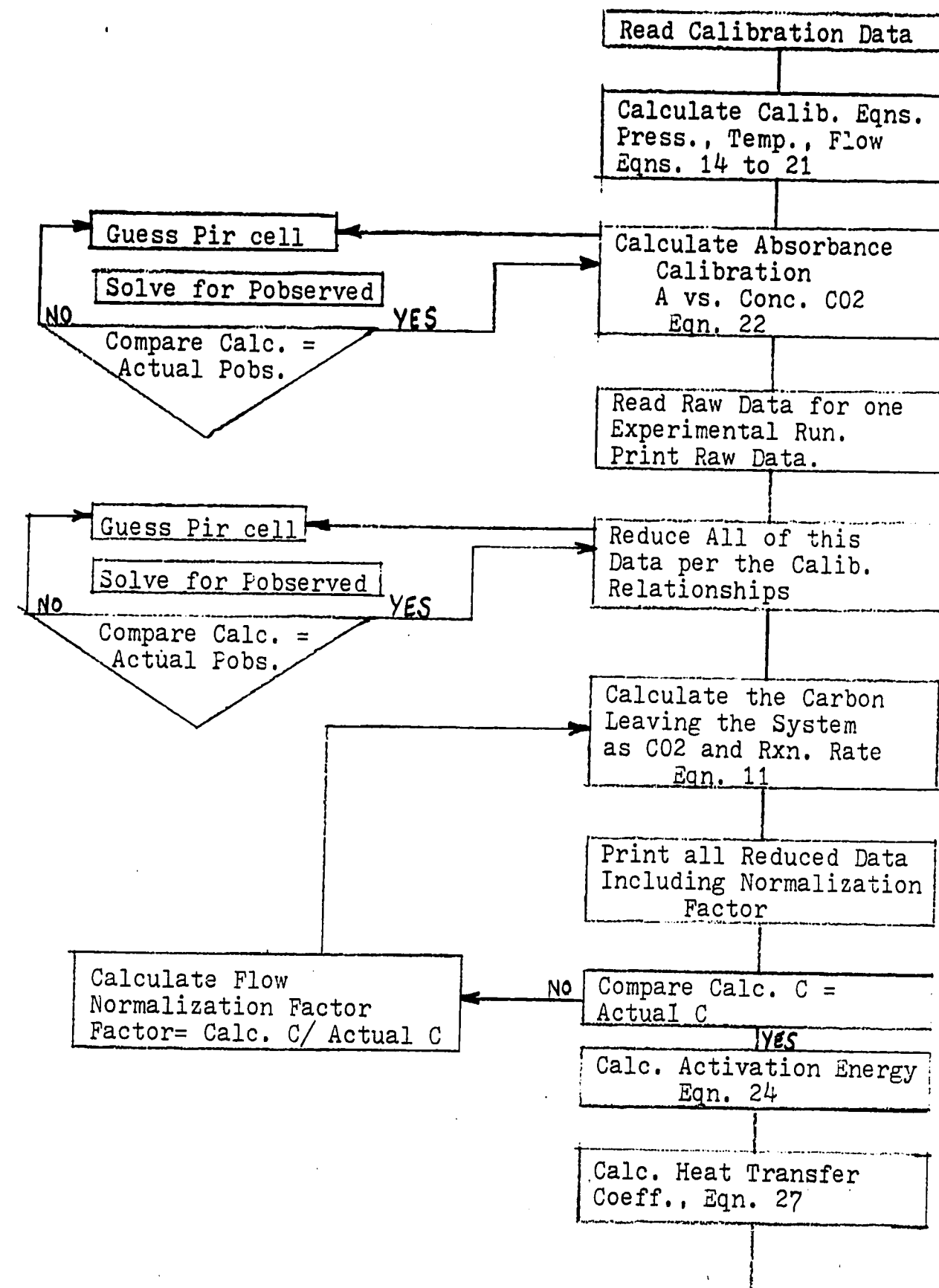
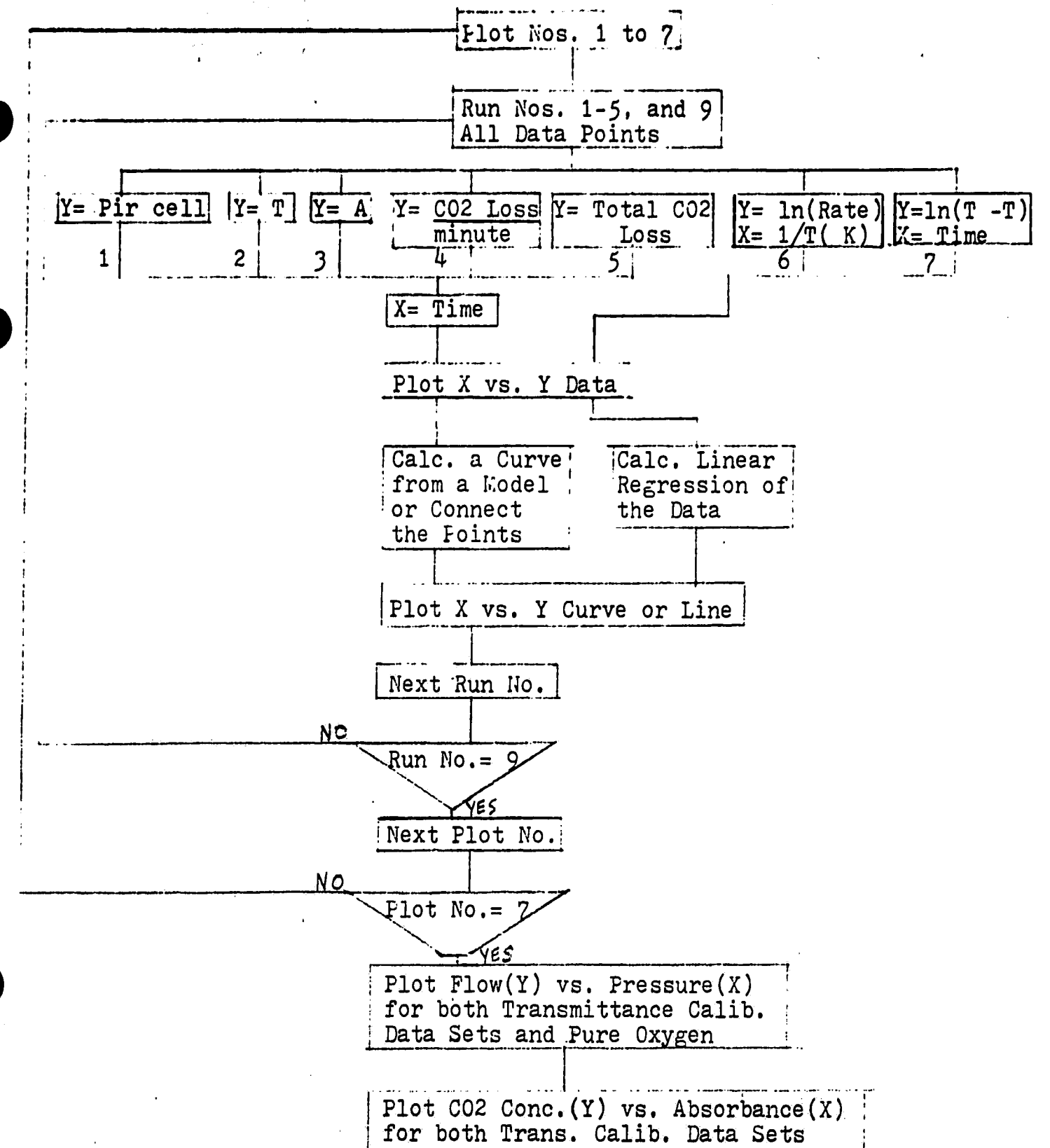


FIGURE 20



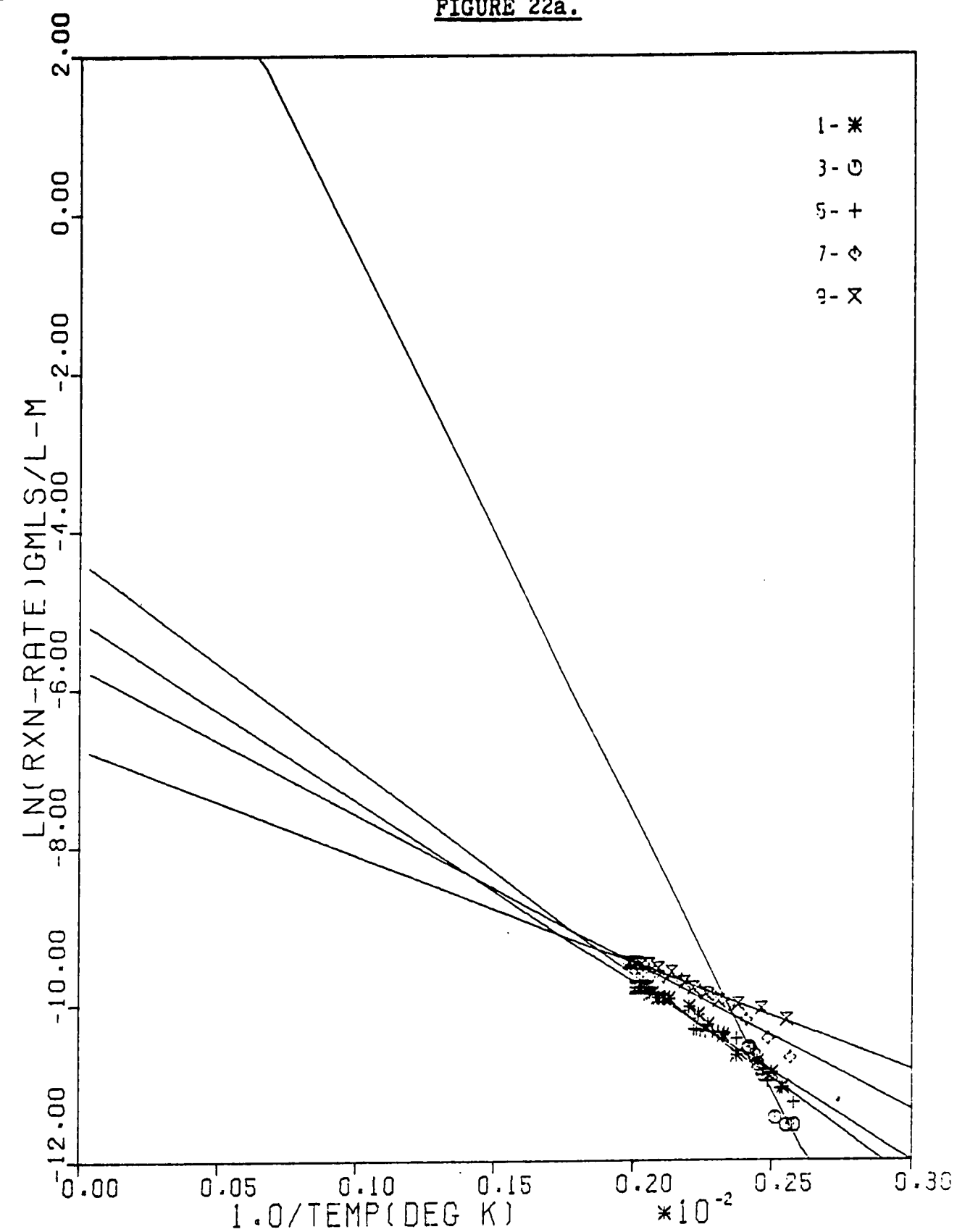
Data Analysis

The major cross check on the reaction rate calculation was the measurement of the weight of carbon removed from the polymer. Since the carbon-hydrogen ratio in polyisoprene is 1:1.6, the molecular weight of a fundamental unit of the polymer is 13.6 grams/grammole and the carbon removed from the polymer is simply $12/13.6$ of the weight of polymer removal. Another value for the carbon leaving the polymer and the system is provided by the carbon dioxide material balance equation where the carbon weight is $12/44$ of the total calculated weight of carbon dioxide leaving the system (44 is the molecular wt. of CO_2). Ideally these two independently measured values should be identical. Table 21 shows how these carbon values actually compared in this work. The extremely poor match in the values for run 2 at 200 watts was probably because the low transmittance signal being measured was swamped by the size of the experimental error. Therefore, the rate data for 200 watts appear to be invalid and will be excluded from this analysis. The trend of the remainder of the data on Table 21 reveals that the 55 cc/min. flow rate runs 1,3,4 have calculated carbon losses up to 30% above the polymer weight loss value while the 27 cc/min. runs 5,9 have calculated carbon losses up to 30% below the polymer weight loss value. The cause of this deviation is believed to be an inaccuracy in the slope of the flow vs. pressure curve (Fig. AP IV-4) used in the carbon dioxide calculation. If the slope of this line is

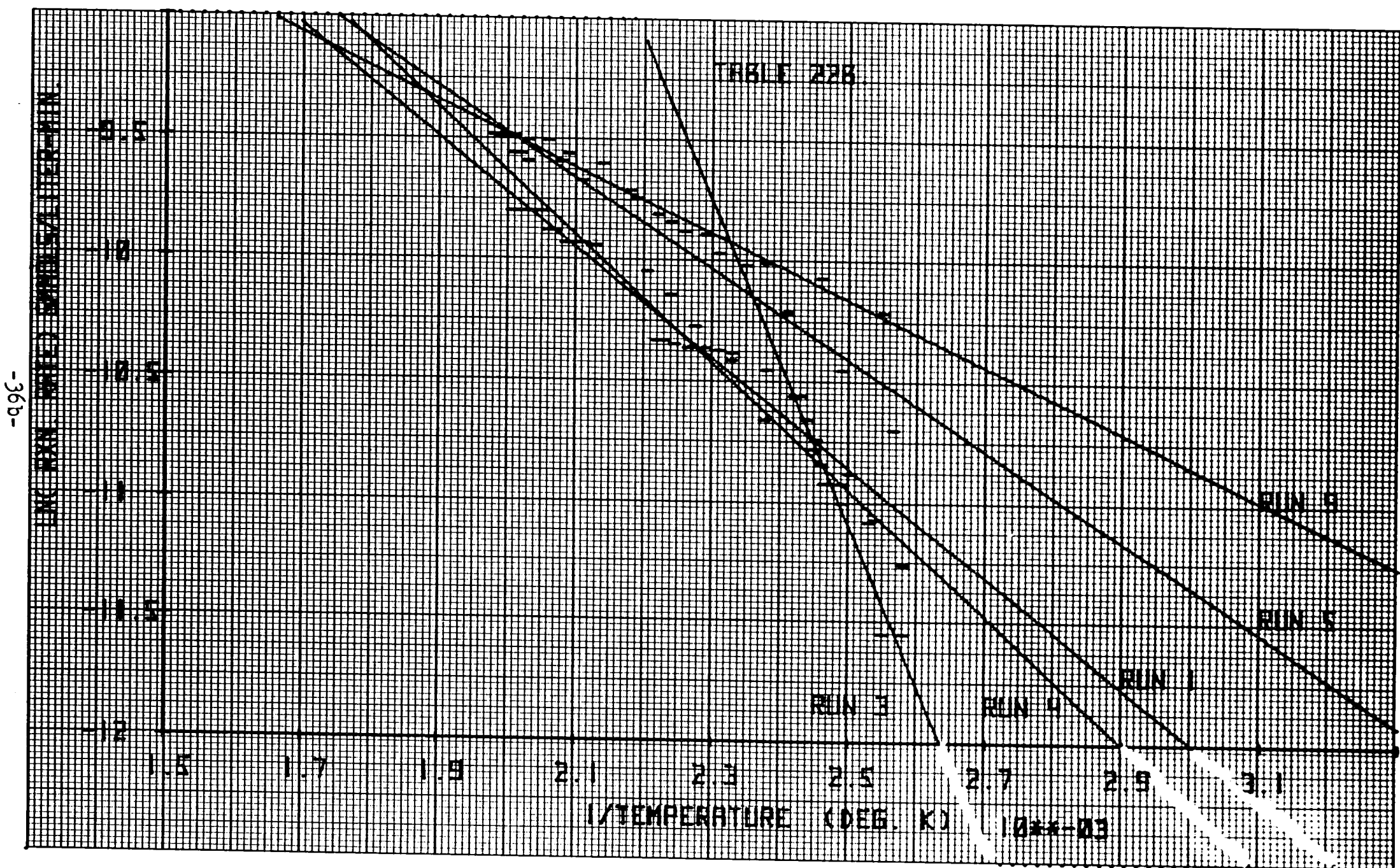
TABLE 21

<u>Run No.</u>	<u>Carbon Wt. Loss from the Polymer (grams)</u>	<u>Carbon Loss Calc. from CO2 Conc. (grams)</u>	<u>Normalization Factor Calc./Actual</u>
3	0.0779	0.0762	.978
4	0.0880	0.0856	.972
1	0.149	0.195	1.31
5	0.235	0.171	.728
9	0.250	0.234	.936

FIGURE 22a.



THE SYMBOL NUMBERS ON THE GRAPH CORRESPOND TO RUN NUMBERS AS FOLLOWS:
 SYMBOL 1 - RUN 1, SYMBOL 3 - RUN 3, SYMBOL 5 - RUN 5, SYMBOL 7 - RUN 7, SYMBOL 9 - RUN 9.
 THE RXN RATE HAS UNITS OF GMMOLES/LITER-MINUTE



decreased from 33.3 to approximately 23.2, then the trend in this data would disappear. The only justification for considering such a change is the effect water vapor might have in altering this line. The flow vs. pressure measurements for O₂, CO₂, and H₂O vapor are plotted on Fig. AP IV-6. However, the water vapor data taken to construct this plot are not as reliable as the oxygen and carbon dioxide values due to the ease with which the water vapor could condense in the system even under vacuum conditions. It is doubtful whether a reliable flow-pressure curve could be constructed for this room temperature system. Rather than manipulate the slope of the flow-pressure line, the same result can be achieved by normalizing the calculated exhaust flow rate. This was accomplished by dividing each flow rate by the ratio of the total calculated carbon loss to the measured carbon weight loss. For example, since the carbon loss ratio for run no. 1 was 1.31, all of the exhaust flow rates calculated were divided by 1.31. With the exhaust flow rates and consequently the reaction rates normalized, it became possible to plot the reaction rate data vs. $1/T(^{\circ}K)$ in order to determine the temperature dependence of the rate. This plot of runs 1, 3, 4, 5, and 9 is Fig. 22a and b. Since the plot shows the data to be linear, the rate controlling step in the polymer breakdown must either be zero order or the concentration must be constant to satisfy equation (2),

$$\text{Rate} = A * \exp(-E_{act}/R * T) * f(C) \quad (2)$$

If $f(C) = (C)^n$ as proposed by D'Allelio and Parker [36], then only when $n=0$ and $f(C) = (C)^0 = 1.0$ or when C = a constant and $f(C) = (C)^n = J$, a different constant, will eqn. (2) yield a linear temperature dependence for the reaction rate. Since the rate in eqn. (2) is dC/dt , a generalized integration of this eqn. can be carried out with the substitution of the constant J for $f(C)$ as follows,

$$dC/dt = A * \exp(-E_{act}/R * T) * J$$

$$C = J * A * \exp(-E_{act}/R * T) * t$$

$$\ln(\Delta C/\Delta t) = \ln(J * A * \exp(-E_{act}/R * T))$$

$$\ln(\text{Rate}) = -E_{act}/R * T + \ln(J * A) \quad (24)$$

The meaning of the concentration independent reaction rate equation is that none of the chemical reactions, eqns. (2-10) are rate controlling in the polymer degradation process. Therefore, a thermophysical limit (i.e. diffusion, heat flux, or phase change) must be controlling the rate of the decomposition.

When thermal or physical processes are rate controlling in polymer degradation, the process is termed ablation. Ablation of polymers was studied extensively by researchers working on the space program in the 1960's [35,37]. These studies were directed toward finding materials which could

dissipate the maximum thermal load per pound on re-entry of a space vehicle. They discovered that the process of ablation consisted of; energy transfer to the polymer surface, rupture of the polymer bonds at the surface and/or in the bulk, melting and charring or sublimation of the surface layer, diffusion with possible reaction across a boundary layer into the gas phase, and possibly further reaction in the gas phase. In the present experiments although reaction is undoubtedly occurring in both the boundary layer and the bulk gas phase to form CO₂ and H₂O, these steps are not rate limiting as the rate-temperature data demonstrated.

In order to understand this physical process, the activation energy, E_{act} , and the frequency factor, A , are calculated for the various experiments. These values are easily obtained from Fig. 22a and b.

TABLE 23

Run #	Power (watts)	Flow (cc/min.)	E_{act} (cal./ gmmol)	A (gmmols/ min.)	Regression Fit (± 1.0 =perfect fit)
3	400	55	14000	690.0	-.97
4	600	55	5200	0.0128	-.95
1	800	55	4550	0.0059	-.99
5	800	30	3700	0.0033	-.98
9	800	27	2700	0.0012	-.99

From this chart it is readily apparent that chain rupture at the polymer surface cannot be rate controlling since the activation energies are far too low, 2-6 Kcal./gmmole. Chain rupture for cyclic polyisoprene would have energies of 80-120 Kcal./gmmole [38].

Although the 400 watt data give anomalous appearing values of Eact and A, the remainder of the data are in good agreement. The values are clustered by flow rate. At 27 cc/min. Eact averages 3200 ± 500 cal./gmmole while A averages 0.0022 ± 0.0010 gmmoles/min.. The higher flow, 55 cc/min., yields values of Eact of 4900 ± 400 cal./gmmole and A 0.0094 ± 0.0040 gmmoles/liter-min.. Since the values for the 600 and 800 watt runs are so close, it is assumed that no change in the degradation process occurs in this power region. However, the 400 watt data indicate that a significant change in the degradation process occurs at the lower power levels.

The lower activation energy and frequency factor for the low flow condition (low pressure) increases the rate of polymer decomposition at a fixed temperature by approximately 28%. For example, at 200 C, $V_r \cdot R(55 \text{ cc/min.}) = 0.00069$ while $V_r \cdot R(27 \text{ cc/min.}) = 0.00088$ gmmoles/min. Since it should be possible to explain this rate increase in terms of the degradation process, those ablation processes having activation energies of the magnitude 1-10 Kcal./gmmole will be explored. These processes are energy transfer to the

polymer surface, sublimation of the surface layer (charring was not observed in the polyisoprene experiments and melting is not favored under vacuum conditions), or diffusion into the bulk gas phase. Although the diffusion process cannot be eliminated rigorously from consideration, under vacuum conditions the resistance to diffusion must be extremely small due to the large mean free path of the chain fragments (e.g. an isoprene unit has a free path of 1-10 microns at 3 torr). In addition, a gaseous diffusion dependent rate would have a temperature dependence in a $3/2$ power of temperature not a logarithmic relationship. Therefore, the possible rate controlling processes are energy transfer and sublimation of the surface fragments. However, if gas phase thermal transfer were limiting, then the rate would have a $1/2$ power dependence on temperature. This energy transfer process even if not rate limiting is extremely important for the understanding of the plasma reactor. Therefore, it will be examined before proceeding with determination of the sublimation energies of the surface fragments.

Heat Transfer

Heat transfer to the polymer surface for bond rupture and sublimation is accomplished by ion and electron bombardment. From the data on temperature increase with time, the heat transfer to the surface can be determined. The temperature rise was found to follow the equation for transient heating with negligible internal resistance to conduction

compared to the resistance of the surface convection [39]. This eqn. was previously mentioned under the section, PROCEDURE. In more detail, it is,

$$(T_{\infty} - T) / (T_{\infty} - T_0) = \exp(-N \cdot t) \quad (23)$$

where $N = (Ar \cdot h / \rho \cdot CP \cdot V)_{Si}$ = a constant with the dimension of 1/time

h = the surface heat transfer coefficient,
cal./cm²-min.-°C

Ar / V = the area to volume ratio of the wafers, 100 cm⁻¹

CP = the heat capacity of the silicon, 0.168 cal./gm.-°C

ρ = the density of silicon, 2.33 grams/cm³

Using these values for the constants in the definition of N gives the simple relationship, $h = N/k_1 = N/51.09$ (cm² °C/cal.), where k_1 is a constant. These eqns. can be used to define for a specific power level, the actual thermal energy input to the wafer as well as the wafer time-temperature history, a result which allows extrapolation of the low power runs to low times where pyrometer data were not obtained. Taking the natural logarithm of both sides of eqn. (23) gives,

$$\ln(T_{\infty} - T) = -N \cdot t + \ln(T_{\infty} - T_0) \quad (27)$$

Thus plotting the wafer temperature(T) vs. time (t) experimental data as $\ln(T_{\infty} - T)$ vs. t for various values of T_{∞} should yield one value of T_{∞} which makes the plot linear.

Although this problem is in fact a two parameter search, i.e. h and T_{∞} , it was found that a straight line fit was very sensitive to T_{∞} for a small range of values of T . If further consideration is given to this phenomenon a logical reason for this effect might quickly become apparent. From the linear plot obtained, the slope of the line will be N whose value will determine the heat transfer coefficient, h , from eqn. (27). The intercept of this line then determines the value of the initial temperature, T_0 , seen by the wafers as opposed to room temperature from which they actually started. Using this information, the thermal energy flux from ion bombardment at any time is now,

$$q = h * A_r * (T_{\infty} - T) \quad (28)$$

And in order to obtain the total energy flux from zero to any time, t , it is only necessary to integrate eqn. (28) with time,

$$Q = \int_0^t q * dt = \int_0^t h * A_r * (T_{\infty} - T) * dt \quad (29)$$

where by rearranging eqn. (23) for the value of T ,

$$T = f(t) = T_{\infty} - (T_{\infty} - T_0) * \exp(-N * t) \quad (30)$$

and combining eqns. (29) and (30) yields,

$$Q = \int_0^t h * A_r * (T_{\infty} - T_0) * \exp(-N * t) * dt \quad (31)$$

Substituting $N = k_1 * h$ into eqn. (31) and multiplying by $-k_1/-k_1$ puts eqn. (31) into the analytically integral form $\exp(-u) * du$,

$$Q = Ar(T_{\infty} - T_0) * \int_0^t \exp(-k_1 * h * t) * -k_1 / -k_1 * dt \quad (32)$$

$$Q = Ar/k_1 * (T_0 - T_{\infty}) * \exp(-k_1 * h * (t - 0)) \quad (33)$$

$$Q = Ar/k_1 * (T_{\infty} - T_0) * (1.0 - \exp(-k_1 * h * t)) \quad (34)$$

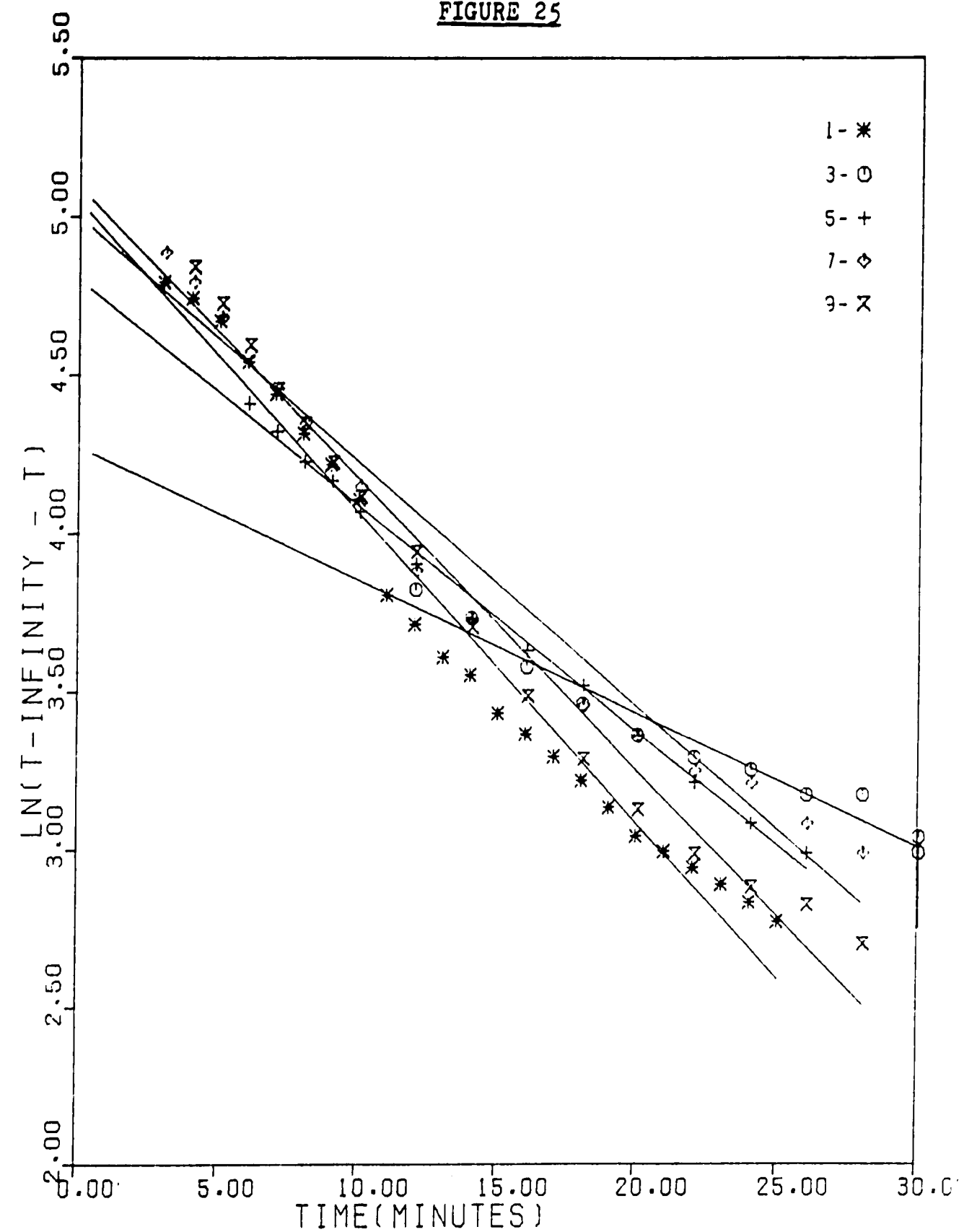
This equation with the constant values determined from the linear fit to eqn. (27) provides the description of the thermal flux to the polymer surface for any time or power level. The computer calculations carried out to analyze the rate data also included a section to determine all of the constants needed in eqn. (34) for each run. These constants are listed below on Table 24, and the plot from which they were obtained is Figure 25.

TABLE 24

Run #	T (Deg. C)	T (Deg. C)	N (1/min.)	h (cal./cm ² -min. °C)	Regression Fit (±1=perfect)
3	161	97	0.0358	0.0007	0.96
4	198	76	0.0715	0.0014	0.96
1	242	86	0.0976	0.0019	0.99
5	251	102	0.0766	0.0015	0.98
9	247	84	0.0920	0.0018	0.99

Although the heat transfer coefficient is constant at the two flow rates, 27 and 55 cc/min., it does increase slightly (25%) with an increase in power from 400-800 watts. Constancy of this heat transfer coefficient with flow rate compared with the significant change in reaction rate with

FIGURE 25



THE SYMBOL NUMBERS ON THE GRAPH CORRESPOND TO RUN NUMBERS AS FOLLOWS:-
 SYMBOL 1-RUN 1. SYM. 3-RUN 3. SYM. 5-RUN 5. SYM. 7-RUN 7. SYM. 9-RUN 9

THE Y-AXIS IS THE NAT. LOG OF THE BULK PLASMA GAS TEMP. - THE SILICON
 WAFER TEMPERATURE. T-INFINITY IS THE GAS TEMPERATURE.

-43a-

flow rate removes the possibility that heat transfer is the rate controlling process in photoresist decomposition.

Fragment Evaporation

Only surface fragment evaporation remains as an unexplored ablation process which might account for all of the data gathered on photoresist decomposition. The energy of evaporation of a long polymer chain cannot of course be determined since the energy to rupture the chain of the molecule is lower than its evaporation energy. However, the units in which this study is interested are the small surface fragments of the polymer. It is the resistance of these fragments to evaporation which are believed to be the rate limiting step to this process. An estimate of the evaporation energy of a monomer unit of a polymer may be obtained based on the monomer's solubility parameter, [40].

$$\delta = (\text{Evap.} / V_l)^{1/2} \quad (25)$$

$$\text{Evap.} = \delta^2 * V_l = \delta^2 * M_w / \rho \quad (26)$$

where Evap. = energy of vaporization, cal./gmole

δ = solubility parameter, (cal./cm³)^{1/2}

V_l = molar volume of the monomer, cm³/gmole

M_w = molecular weight of the monomer, grams/gmole

ρ = density of the monomer, grams/cm³

For isoprene δ has a value of 7.4, M_w is 68 gms./gmole, and ρ is 0.68 gms./cm³. Therefore, the vaporization energy is 5.5 Kcal./gmole which is the same order of magnitude as

the activation energy measured for the rate limiting degradation process. This evaporation energy analysis ought to be done with data on cyclic polyisoprene or the cyclic isoprene monomer. However, this data is not readily available.

CONCLUSIONS

The rate of breakdown of cyclic polyisoprene photoresist has been determined for a range of temperatures between 100-220 °C, two oxygen gas feed rates, three compositions of the feed gas, and three power levels. Calculations based on these data indicate a linear increase in the heat transfer coefficient to the silicon substrate with increasing power, $h = 0.0007 - 0.0019 \text{ cal./cm}^2 \text{ -min.- } ^\circ\text{C}$, while this coefficient is nearly constant versus oxygen feed rate (i.e. pressure). On the other hand, the activation energy for the polymer degradation process appears to be essentially constant versus power in the 600-800 watt rf power region. However, activation energy undergoes a significant decrease as oxygen feed rate (i.e. pressure) decreases indicating that the rate limiting step for the polymer decomposition is evaporation of chain fragments from the polymer surface. Further confirmation of this conclusion is provided by calculation of the theoretical evaporation energy for the polymer (i.e. isoprene monomer fragments). This polymer evaporation energy is calculated as 5.5 Kcal./gmole. while the measured activation energy for the degradation process is 2.5-5.5 Kcal./gmole. A large increase in the activation energy of the process to 14 Kcal./gmole. was observed at lower rf power levels (400 watts). This increase indicates that a change in the nature of the degradation process oc-

curs in low power oxygen plasmas. This data base on oxygen plasma decomposition of cyclic polyisoprene will be examined even more extensively in the future for further conclusions.

REFERENCES

1. M. Venugopalan, Reaction Under Plasma Conditions, Vol. II, New York: Wiley-Interscience, 1971, Pg. 145
2. R.H. Hansen, J.V. Pascale, T. Benedictis, and P.M. Rentzepis, " Effect of Atomic Oxygen on Polymers", J. of Polymer Science: Part A, Vol. 3, 1965, Pgs. 2205-2214.
3. J.R. Hollahan, J. of Chem. Ed., Vol. 43, 1966, Pg. A401
4. M.L. Kaplan, Science, Vol. 169, Sept. 1970, Pgs.1206-1207
5. " Introduction to Photoresist Stripping", Bulletin 8214-TA1: LFE Corp., June 1975
6. D.C. Frost, " Ionization and Dissociation of O₂ by Electron Impact", Amer. Chem. Soc. J., Vol. 80, Dec. 1958, Pgs.6183-6187
7. G.S. Egerton and A.G. Morgan, " The Role of Singlet Oxygen and Hydrogen Peroxide in the Photosensitized Degradation of Polymers", J. of the Soc. of Dyers and Colorers, Aug. 1971, Pgs.268-277
8. A.T. Bell, " Models for High Frequency Electric Discharge Reactors ", Chemical Engineering Progress Symposium Series, Vol. 67, No. 112, Pgs.1-11

9. A.M. Mearns and A.J. Morris, "Oxidation Reactions in a Microwave Discharge: Factors Affecting the Efficiency of Oxygen Atom Production", *ibid.* , Pgs.37-46
10. V.H. Dibeler and J.A. Walker, " Mass-Spectrometric Study of Photoionization. VI O₂, CO₂, COS, and CS₂", *J. of the Opt. Soc. of Amer.*, Vol. 57, Aug. 1967, No. 8, Pgs. 1007-1012
11. L.W. Sieck and R. Gorden, jr., " Photoionization of CO₂-CO-O₂ Mixtures", *Journal of Research of the NBS-A, Physics and Chem.*, Vol. 78A, May-June 1974, No. 3, Pgs. 315-322
12. J.R. Hollahan and G.L. Carlson, " Hydroxylation of Polymethyl siloxane Surfaces by Oxidizing Plasmas", *J. of Appl. Poly. Sci.*, Vol. 14, 1970, Pgs. 2499-2508
13. C.Y. Kim and D.A.I. Goring, " Surface Morphology of Polyethylene After Treatment in a Corona Discharge", *ibid.*, Vol. 15, 1971, Pgs. 1357-1364
14. N.J. DeLollis, " The Use of Radio-Frequency Activated Gas Treatment to Improve Bondability", *Rubber Chem. and Tech.*, Vol. 46, June 1973 , Pgs. 549-554
15. C.Y. Kim, J. Evans, and D.A.I. Goring, " Corona-Induced Autohesion of Polyethylene", *J. Appl. Poly. Sci.*, Vol. 15, 1971, Pgs.1365-1375

16. A. Bradley and J.D. Fales, " Prospects for Industrial Applications of Electrical Discharge", Chemical Technology, April 1971, Pgs. 232-237
17. M. White, "Thin Polymer Films", Thin Solid Films, Vol. 18, 1973, Pgs. 157-172
18. J.R. Hall, C.A.L. Westerdahl, A.T. Devine, and M.J. Bodnar, " Activated Gas Plasma Surface Treatment of Polymers for Adhesive Bonding", J. of Applied Polymer Science, Vol. 13, 1969, Pgs.2085-2096
19. S. Morita, G. Sawa, M. Ieda, " Influence of Oxygen on Electrical Properties of Styrene Thin Film Polymerized in a Glow Discharge", J. of Appl. Poly. Sci., Vol. 44, May 1973, No. 5, Pgs. 2435-2436
20. M. Akahane, K. Kanda, K. Yahagi, " Effect of Dielectric Constant on Surface Discharge of Polymer Insulators in Vacuum", J. Appl. Phys., Vol. 44, June 1973, No. 6, Pg.2927
21. R.L. Zapp and J.H. Peery, " The Ozone Attack on Swollen Elastomeric Networks", J. of Appl. Poly. Sci., Vol. 13, 1969, Pgs. 2097-2112
22. Venugopalan, op. cit., Vol. I, Pgs. 22 and 62-66
23. Venugopalan, op. cit., Vol. II, Pg. 171

24. J.R. Hollahan and A.T. Bell, Techniques and Applications of Plasma Chemistry, New York: John Wiley and Sons, 1974, Pgs. 3-26
25. Ibid., Pgs. 116-140 and 351-355
26. Ibid., Pgs. 125-127
27. Ibid., Pg. 138
28. Ibid., Pg. 91
29. Ibid., Pg. 69 and 104
30. R.H. Still and P.B. Jones, " Thermal Degradation of Polymers", J. of Appl. Poly. Sci., Vol. 13, 1969, Pgs. 2033-2043
31. J.M. Smith, Chemical Engineering Kinetics, New York: McGraw-Hill, 1956, Pg. 187
32. Ibid., Pg. 196
33. M.R. Havens, M.E. Biolsi, and K.G. Mayhan, " Survey of Low Temperature Rf Plasma Polymerization and Processing", J. of Vacuum Science and Technology , Vol. 13, March/April 1976, No. 2, Pgs. 575-584
34. Hollahan and Bell, Techniques, op. cit., Pg. 136
35. G.F. D'Allelio and J.A. Parker, Ablative Plastics, New York: Marcel Dekker, 1971, Pgs. 1-35, 437-485

36. H. Friedman, J. Poly. Sci., Polymer Symposium No. 6, 1963, Pgs. 532- 539. Cited in D'Allelio and Parker, Ablative Plastics, Pg. 3
37. P.J. Blatz and W.H. Andersen, " Fundamental Problems Relating to the Fabrication of Plastics for High Temperature Application", Combustion and Propulsion (5th AGARDograph Colloquium), New York, 1963, Pgs. 317-320
38. Ibid., Pg. 327
39. B. Gebhart, Heat Transfer, New York: McGraw-Hill, 1961, Pg. 83
40. D.H. Solomon, The Chemistry of Organic Film Formers, New York: John Wiley and Sons, 1967, Pgs. 30-31

BIBLIOGRAPHY

- Akahane, M., Kanda, K., Yahagi, K., " Effect of Dielectric Constant on Surface Discharge of Polymer Insulators in Vacuum", J. Applied Physics, 44, No. 6, 2927, (1973).
- Baddour, R.F., Timmins, R.S., (Ed.), The Applications of Plasmas to Chemical Processing, Cambridge, Mass.: The M.I.T. Press, (1967).
- Barnes, R.B., Gore, R.C., " Infrared Spectroscopy", Analytical Chemistry, 21, No. 1, 7-12, (1949).
- Barr, E.S., " Historical Survey of the Early Development of the Infrared Spectral Region", American J. of Physics, 28, 42-54, (1960).
- Barrow, G.M., Physical Chemistry, New York: McGraw-Hill, (1961).
- Bauman, R.P., Absorption Spectroscopy, New York: John Wiley and Sons, (1962).
- Bell, A.T., " Models for High Frequency Electric Discharge Reactors", Chemical Engineering Progress Symposium Series, 67, No. 112, 1-11.
- Bellamy, L.J., The Infrared Spectra of Complex Molecules, New York: John Wiley and Sons, (1958).

- Bevilacqua, E.M., " Degradation of Polyisoprene Networks by Oxygen", J. of the ACS, 80, 5364-5367, (1968).
- Blatz, P.J., Andersen, W.H., " Fundamental Problems Relating to the Fabrication of Plastics for High Temperature Application", Combustion and Propulsion, 5th AGARDograph Colloquium, New York: Pergamon Press, (1963).
- Blok, J., LeGrand, D.G., " Dielectric Breakdown of Polymer Films", J. of Appl. Phys., 40, No. 1, 288-293, (1969).
- Bradley, A., Fales, J.D., " Prospects for Industrial Applications of Electrical Discharge", Chem. Tech., 232-237, (April 1971).
- Burch, D.E., Gryvnak, D.A., Patty, R.R., " Absorption of Infrared Radiation by CO2 and H2O. Experimental Techniques", J. of the Optical Society of America, 57, No. 7, 885-895, (1967).
- Carstenson, P., " Free Radicals in Diene Polymers Induced by Ultraviolet Irradiation I. An ESR Study of Cis-1,4-Polyisoprene ", Rubber Chemistry and Technology, 918-932.
- Chan, M.G., Hawkins, W.L., " The Relationship Between Rate of Reaction with Oxygen and Chemical Change in Polymers.....", Polymer Engineering and Science, 264-268, (Oct. 1967).

- Cross, A.D., An Introduction to Practical Infrared Spectroscopy, London: Butterworths Scientific Publications, (1960).
- D'Allelio, G.F., Parker, J.A., Ablative Plastics, New York: Marcel Dekker, Inc., (1971).
- DeForest, W., Photoresist, New York: McGraw-Hill, (1975).
- DeLollis, N.J., " The Use of Radio Frequency Activated Gas Treatment to Improve Bondability", Rubber Chem. and Tech., 46, 549-554, (1973).
- Dibeler, V.H., Walker, J.A., " Mass Spectrometric Study of Photoionization VI. O₂, CO₂, COS, and CS₂", J. of the Opt. Soc. of Amer., 57, No. 8, 1007-1012, (1967).
- Doebelin, E.D., Measurement Systems: Application and Design, New York: McGraw-Hill, 408-416, (1966).
- Dushman, S., Scientific Foundations of Vacuum Technique, New York: John Wiley and Sons, (1962).
- Egerton, G.S., Morgan, A.G., " The Role of Singlet Oxygen and Hydrogen Peroxide in Photosensitized Degradation of Polymers", Journal of the Society of Dyers and Colorers, 268-277, (Aug. 1971).
- Forman, R., " Electrical Conduction and Breakdown in High Pressure (0.25-300 mmHg) Rare Gases", J. of Appl. Phys., 32, 1651-1658, (1961).

- Frost, D.C., McDowell, C.A., " The Ionization and Dissociation of Oxygen by Electron Impact", J. of the ACS, 80, 6183-6187, (1958).
- Gebhart, B., Heat Transfer, New York: McGraw-Hill, (1971).
- Hall, J.R., Westerdahl, C.A.L., Devine, A.T., and Bodnar, M.J., " Activated Gas Plasma Surface Treatment of Polymers for Adhesive Bonding", J. of Appl. Poly. Sci., 13, 2085-2096, (1969).
- Hansen, R.H., Pascale, J.V., DeBenedictis, R., " Effect of Atomic Oxygen on Polymers", J. of Poly. Sci., part A, 3, 2205-2214, (1965).
- Havens, M.R., Biolsi, M.E., Mayhan, K.G., " Survey of Low Temperature Rf Plasma Polymerization and Processing", J. of Vacuum Science and Technology, 13, No.2, 575-584, (1976).
- Hollahan, J.R., Bell, A.T., Techniques and Applications of Plasma Chemistry, New York: John Wiley and Sons, (1974).
- Hollahan, J.R., Carlson, G.L., " Hydroxylation of Polymethylsiloxane Surfaces by Oxidizing Plasmas", J. of Appl. Poly. Sci., 14, 2499-2508, (1970).
- Hollahan, J.R., J. Chem. Ed., 43, A401, (1966).

- Hull, L.A., Hisatsune, I.C., Heicklen, J., " Low Temperature Infrared Studies of Simple Alkene-Ozone Reactions", J. of the ACS, 94, No. 14, 4856-4863, (1972).
- Jones, W.N., Dennison, J.E., Broyde, B., " Effects of Ozone on the Crosslinking of Photoresists", Solid State Technology, 56-58, (Jan. 1974).
- Kaplan, M.L., " Oxidation of a Polymer Surface with Gas Phase Singlet Oxygen ", Science, 169, 1206-1207, (1970).
- Kim, C.Y., Goring, D.A.I., " Surface Morphology of Polyethylene After Treatment in a Corona Discharge ", J. of Appl. Poly. Sci., 15, 1357-1364, (1971).
- Kim, C.Y., Evans, J., Goring, D.A.I., " Corona Induced Autohesion of Polyethylene ", J. of Appl. Poly. Sci., 15, 1365-1375, (1971).
- Lee, W.G., Paine, J.A., " Stability of Nitric Oxide Calibration Gas Mixtures in Compressed Gas Cylinders ", Reprint from Special Technical Publication 598, Philadelphia: American Society for Testing and Materials, (1976).
- Legg, B.J., Parkinson, K.J., " Calibration of Infrared Gas Analysers for Use with Carbon Dioxide ", Journal of Scientific Instruments, 1, 1003-1006, (1968).

LFE Corporation, " Effects of Bare Silicon Back in Plasma Etching ", Bulletin 8241-TA1.

LFE Corp., " Photoresist Removal with and without Equi-Etch Chamber Insert ", Bulletin 8216-TA1, (Aug. 1975).

LFE Corp., " Comparison of LFE DS-180' to O2 ", Bulletin 8215-TA1, (Aug. 1971).

LFE Corp. , " Introduction to Photoresist Stripping ", Bulletin 8214-TA1, (June 1975).

Madorsky, S.L., " Thermal Degradation of Polymers at Low Rates ", J. of Research of the National Bureau of Standards, Research Paper 2957, 62, No. 6, 219-228, (1959).

Madorsky, S.L., Thermal Degradation of Organic Polymers, New York: Interscience Publishers, (1964).

Maguire, T., " Space Researchers Shed Light on Plasma Sheath ", Electronics, 35, 20-21, (1962).

McLafferty, F.W., McAdoo, D.J., Smith, J.S., " Unimolecular Gaseous Ion Reactions of Low Activation Energy. Five Membered-Ring Formation ", J. of the ACS, 91, 5400-5401, (1969).

McTaggart, F.K., Plasma Chemistry in Electrical Discharges, New York: Elsevier Publishing, (1967).

- Mearns, A.M., Morris, A.J., " Oxidation Reactions in a Microwave Discharge: Factors Affecting Efficiency of Oxygen Atom Production ", Chemical Engineering Progress Symposium Series, 67, No. 112, 37-46.
- Meek, J.M., Craggs, J.D., Electrical Breakdown of Gases, London: Oxford Press, (1953).
- Molee, C.S., Muller, M., " Gas and Pollution Analysis Using Infrared Sensors ", Design News, Pg. 57, (Aug. 1976).
- Morrison, R.T., Boyd, R.N., Organic Chemistry, Boston: Allyn and Bacon, (1966).
- Morita, S., Sawa, G., Ieda, M., " Influence on Electrical Properties of Styrene Thin Film Polymerized in a Glow Discharge ", J. of Appl. Phys., 44, No. 5, 2435-2436, (1973).
- Pease, R.N., Equilibrium and Kinetics of Gas Reactions, Princeton, N.J.: Princeton University Press, (1942).
- Price, D.A., Moruzzi, J.L., " Ionization in Mixtures of Oxygen and Carbon Monoxide ", J. of Phys. D: Appl. Phys., 6, 14-16, (1973).
- Scheppele, S.E., et. al., " Internal Energy Distribution and the Fragmentation of Gaseous Organic Ions.....", J. of the ACS, 95, No. 16, 5105-5115, (1973).

Schissel, P.O., " Production of Oxygen and Carbon Monoxide from Carbon Dioxide in an Ionization Gauge ", J. of Appl. Phys., 2659-2660, (1962).

Segal, C.L., High Temperature Polymers, New York: Marcel Dekker, (1967).

Sieck, L.W., Gorden, R. Jr., " Photoionization of CO₂-CO-O₂ Mixtures ", J. of Research of the NBS-A. Physics and Chemistry, 78A, No. 3, 315-322, (1974).

Smith, J.M., Chemical Engineering Kinetics, New York: McGraw-Hill, (1956).

Sokolowski, M., et. al., " Ion Treatment of Silicon in a Glow Discharge ", Thin Solid Films, 30, 29-35, (1975).

Southworth, R.W., Deleeuw, S.L., Digital and Numerical Methods, New York: McGraw-Hill, (1965).

Spedding, P.L., " Features of Design and Operation of Electrochemical Reactors ", Chem. Eng. Prog. Symp. Ser., 67, No. 112

Stine, K.E., Modern Practices in Infrared Spectroscopy, Fullerton, Calif.: Beckman Instruments Inc., (1970).

Venugopalan, M., (Ed.), Reactions Under Plasma Conditions, Vol. I and II, New York: Wiley-Interscience, (1971).

Von Engel, A., Ionized Gases, Clarendon Press, (1965).

Vriens, L., " Energy Balance in Low Pressure Gas Discharges
", J. of Appl. Phys., 44, 3980-3989, (1973).

Wall, L.A., Florin, R.E., " Effect of Structure on the Thermal
Decomposition of Polymers ", J. of Research of the
NBS, Research Paper 2860, 60, No. 5, 451-458, (1958).

Warshaw, D., " Ionized Band Encircles the Earth ", Radio
Electronics, 31, 38-39, (1960).

Weast, R.C., Selby, S.M., Handbook of Chemistry and Physics,
Cleveland: The Chemical Rubber Co., (1966).

Weber, H.C., Meissner, H.P., Thermodynamics for Chemical
Engineers, New York: John Wiley and Sons, (1957).

White, M., " Thin Polymer Films ", Thin Solid Films, 18,
157-172, (1973).

Zapp, R.L., Peery, J.H., " The Ozone Attack on Swollen
Elastomeric Networks ", J. of Appl. Poly. Sci., 13,
2097-2112, (1969).

APPENDIX I

Calibration of the Thermocouple Pressure Gauges

When the experiments were performed, careful readings were taken from the thermocouple pressure gauge at the reactor end of the transfer line from the reactor to the IR measuring cell. However, the IR cell pressure is needed for the calculation of both the gas flow rate and the carbon dioxide mole fraction in the exhaust stream. Therefore, in order to correlate the measured pressures with the IR gas cell pressure, a threaded tee was mounted in the cell and simultaneous readings of the reactor gauge and the IR cell gauge were made. These data appear in Table AP I-4 under the heading, simultaneous IR tc - rxn tc gauges.

Since a McLeod gauge was chosen as the absolute pressure standard and the apparatus was too cumbersome to move, it was necessary to use a portable mechanical vacuum gauge as the intermediary between the standard and the thermocouple gauges. The calibration procedure consisted of attaching this mechanical gauge to the McLeod apparatus, pumping the system to a pressure below 0.01 torr, sealing the system off from the vacuum pump to check for air leaks in the apparatus, and then taking simultaneous readings of the McLeod and mechanical gauges while nitrogen was bled into the apparatus. Nitrogen was used to perform the calibration because it is inert to the mercury of the McLeod gauge.

Once the mechanical gauge was calibrated, it was attached to the side of the threaded tee in the IR cell while the other side held the thermocouple gauge used to measure the IR cell pressure in the calibration mentioned above. The procedure followed was identical to the McLeod calibration with the exception that the gas used was oxygen. Oxygen was used both because it was the reactive gas for the experiment and its use avoided an extra calibration step (air to oxygen). Next the reactor gauge was calibrated to the IR cell gauge using the same technique. Before each reading in these calibrations was taken, the system was allowed to stabilize for 3 minutes at the new pressure level. All of these calibration data are listed on Table AP I-4 .

APPENDIX I-A

Iteration Procedure to Determine Total Pressure

Since a thermal conductivity pressure gauge responds to the thermal conductivity of a gas as well as its pressure, a means must be utilized to remove the gas composition effects from the gauge readings. The tables relating the observed pressure readings to the actual pressure of CO₂ or H₂O provide part of the solution, Tables AP I-1 and 2. These tables permit any actual partial pressure of carbon dioxide or water vapor to be converted to the observed partial pressure reading on the meter. A second part of the solution is the calibration equation relating observed total pressure at the reactor to the actual total pressure in the infrared measuring cell. (See Appendix I) This equation is,

$$P_{\text{observed reactor (torr)}} = 1.0/0.497 * (P_{\text{actual ir}} - 0.0027) \quad (\text{I-1})$$

However, equation (I-1) is limited to the gas used in the calibration, oxygen. Therefore, before using eqn. (I-1), the partial pressure of carbon dioxide and water must be converted to the observed partial pressure on an oxygen basis. This conversion is done using Tables AP I-1 and 2 mentioned above.

The only unknown quantities are the actual partial pressures of carbon dioxide, water, and oxygen. Since the relationship between partial pressures and total pressure is,

$$P_{\text{total}} = \sum Y_i \cdot P_{\text{total}} = (Y_{\text{CO}_2} + Y_{\text{H}_2\text{O}} + Y_{\text{O}_2}) \cdot P_{\text{total}} \quad (\text{I-2})$$

OR

$$1.0 = Y_{\text{CO}_2} + Y_{\text{H}_2\text{O}} + Y_{\text{O}_2} \quad (\text{I-3})$$

And since equation (I-3) can be simplified by use of the stoichiometric link between carbon dioxide and water vapor,

$$Y_{\text{H}_2\text{O}} = 0.8 \cdot Y_{\text{CO}_2} \quad (\text{I-4})$$

to yield,

$$Y_{\text{O}_2} = 1.0 - 1.8 \cdot Y_{\text{CO}_2} \quad (\text{I-5})$$

Now a knowledge of the value of Y_{CO_2} fixes all of the mole fractions in the IR cell. The only remaining unknowns now are Y_{CO_2} and the total pressure in the IR cell. An independent equation relating these two variables is,

$$Y_{\text{CO}_2} = C_{\text{CO}_2} / C_{\text{total}} = 24.631 \cdot 760.0 \cdot C_{\text{CO}_2} / P_{\text{total}} \quad (\text{I-6})$$

where 24.631 is the molar volume of an ideal gas at 27 °C.

Since the concentration of carbon dioxide is a monitored parameter of the system through the absorbance calibration, this iteration scheme is ready for use.

Iteration Procedure (SUBROUTINE PFIND) -----

1. Knowing C_{CO_2} , Guess Pir cell
2. Calculate Y_{CO_2} from eqn. (I-6)
3. Calculate Y_{O_2} from eqn. (I-5) and Y_{H_2O} from eqn. (I-4)
4. Compute partial pressures, $P_{CO_2} = Y_{CO_2} \cdot P_{ir \text{ cell}}$, etc.
5. Use the tables (AP I-1 and 2) to determine the observed pressures for CO_2 and H_2O on an oxygen basis.
Of course, the observed and partial pressures of O_2 are identical.
6. Sum the observed partial pressures.
7. Calculate the observed pressure at the reactor from eqn. (I-1)
8. Compare the monitored value of reactor press. with the calc. value from step 7.
9. If the two values in step 8. differ by more than 0.2%, then Pir cell is adjusted and iteration returns to step 2.

This iteration scheme with trivial modification was used to determine the total IR cell pressure for the calibration of the spectrometer using carbon dioxide - oxygen mixtures. Also this iteration could be generalized for this apparatus and any reacting polymer and product gases

provided that: the exhaust concentration of the product gases was monitored, the stoichiometric ratio of the reactant atoms in the polymer is known, and that the thermal conductivity effect of the gases on the thermocouple gauge is known (Fig. AP I-3).

Of course, this appendix section would have been unnecessary had a composition independent pressure gauge been used. However, pressure transducers for the vacuum region studied (0-10 torr) are very expensive and/or are no more accurate.

TABLE AP I-1

PRESSURE OBSERVED O2 (TORR)	PRESSURE ACTUAL CO2 (TORR)
0.1230E+00	0.8100E-01
0.2310E+00	0.1860E+00
0.3280E+00	0.2780E+00
0.4300E+00	0.3710E+00
0.5500E+00	0.4860E+00
0.6440E+00	0.5850E+00
0.7500E+00	0.6870E+00
0.8620E+00	0.7950E+00
0.9820E+00	0.9000E+00
0.1090E+01	0.1020E+01
0.1180E+01	0.1130E+01
0.1300E+01	0.1250E+01
0.1385E+01	0.1360E+01
0.1500E+01	0.1490E+01
0.1625E+01	0.1600E+01
0.1710E+01	0.1725E+01
0.1780E+01	0.1840E+01
0.1900E+01	0.2000E+01
0.2000E+01	0.2190E+01
0.2150E+01	0.2375E+01
0.2630E+01	0.3100E+01
0.3230E+01	0.3900E+01
0.3710E+01	0.4750E+01
0.4250E+01	0.5900E+01
0.4750E+01	0.6200E+01
0.5300E+01	0.8800E+01
0.6500E+01	0.1364E+02

A-6a

APCO2=0.1596E+00 BPCO2=0.9096E+00 CPCO2=-.3313E-01 STDEV=0.2024E-01

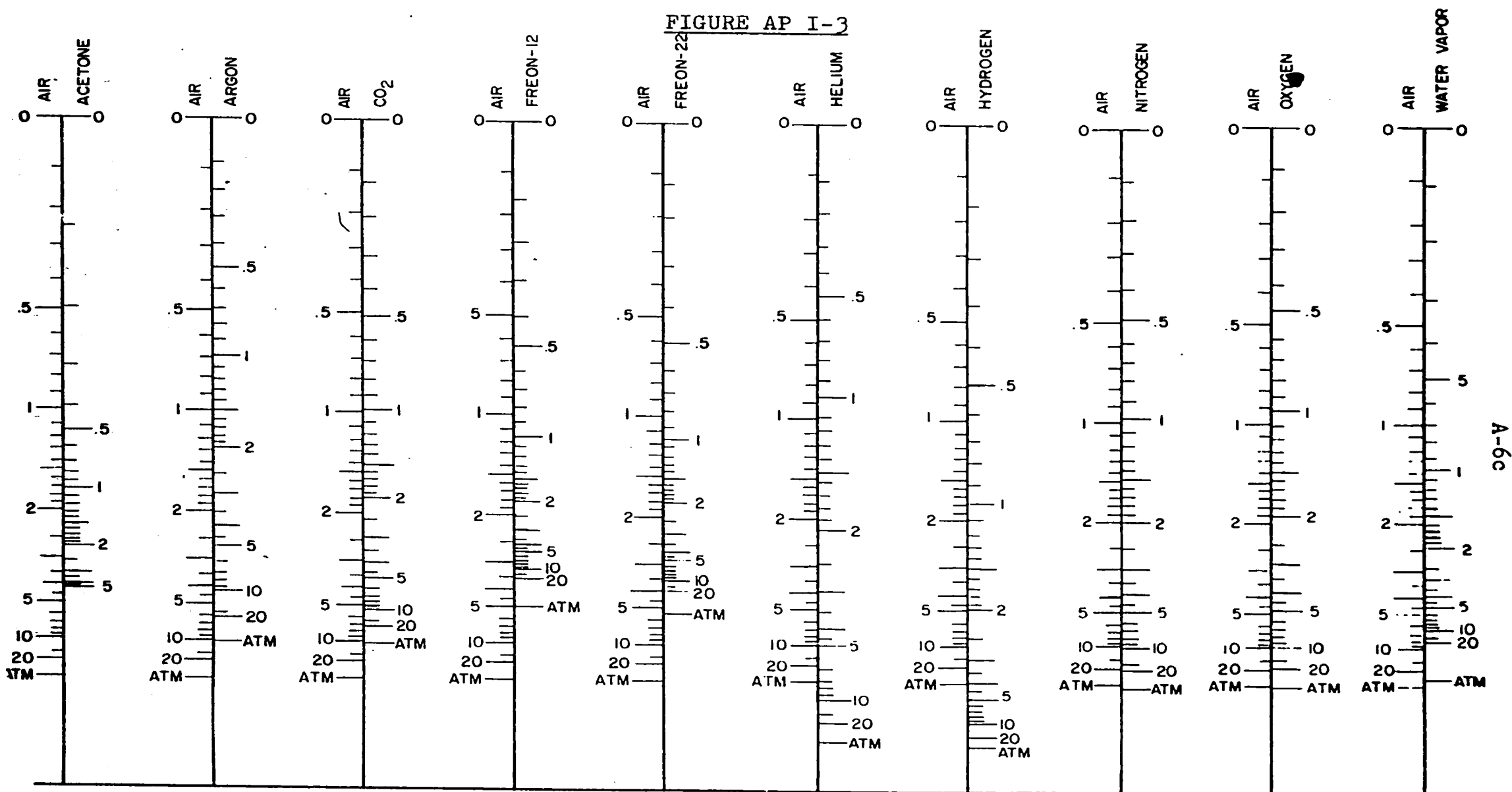
TABLE AP I-2

PRESSURE OBSERVED O2 (TORR)	PRESSURE ACTUAL H2O (TORR)
0.1230E+00	0.9200E-01
0.2330E+00	0.1730E+00
0.3280E+00	0.2330E+00
0.4300E+00	0.2890E+00
0.5500E+00	0.3570E+00
0.6440E+00	0.4200E+00
0.7500E+00	0.4750E+00
0.8620E+00	0.5500E+00
0.9820E+00	0.6270E+00
0.1090E+01	0.7000E+00
0.1180E+01	0.7700E+00
0.1300E+01	0.8600E+00
0.1385E+01	0.9250E+00
0.1500E+01	0.1040E+01
0.1625E+01	0.1130E+01
0.1710E+01	0.1220E+01
0.1780E+01	0.1315E+01
0.1900E+01	0.1400E+01
0.2000E+01	0.1500E+01
0.2150E+01	0.1590E+01
0.2630E+01	0.2050E+01
0.3230E+01	0.2650E+01
0.3710E+01	0.3300E+01
0.4250E+01	0.4150E+01
0.4750E+01	0.5000E+01
0.5300E+01	0.6000E+01
0.6500E+01	0.7500E+01
0.7500E+01	0.1286E+02
0.8500E+01	0.1900E+02

APH20=0.3565E+00 BPH20=0.1049E+01 CPH20=-.3358E-01 STDDEV=0.4847E-01

A-6b

FIGURE AP I-3



NOMOGRAM SHOWING CALIBRATION OF HASTINGS VACUUM GAUGES WHICH USE THE DV-4D GAUGE TUBE FOR GASES OTHER THAN AIR. TO FIND THE PRESSURE IN A GAS OTHER THAN AIR, LOCATE THE OBSERVED READING ON THE "AIR" SIDE OF THE APPROPRIATE SCALE AND READ, ON THE OPPOSITE SIDE OF THE SCALE, THE TRUE PRESSURE IN MILLIMETERS OF MERCURY FOR THE GAS BEING MEASURED.

TELEDYNE HASTINGS-RAYDIST
HAMPTON, VIRGINIA

TABLE AP I-4

PRESSURE CALIBRATION DATA

ALL PRESSURES ARE IN TORR

NP IS THE NUMBER OF DATA POINTS TAKEN

NP0=12

NP1= 7

NP2= 9

NCOR= 8

MCLEND GAUGE	MECHANICAL GAUGE	MECHANICAL GAUGE	IR THERMOCOUPLE GAUGE	IR THERMOCOUPLE GAUGE	REACTOR THERMOCOUPLE GAUGE	SIMULTANEOUS IR TC GAUGE	RXN TC GAUGE
1.0000	0.8000	2.0000	3.1000	0.7500	0.9600	0.9300	1.2500
1.9000	1.8000	2.2000	3.1500	1.0000	1.3000	1.1500	1.6000
3.0000	2.9500	2.3000	3.3000	1.1500	1.3700	2.8500	4.0000
4.0000	4.2000	2.5000	3.6000	1.2000	1.6000	3.5500	4.9500
5.0000	5.3000	2.7000	3.8500	1.8600	2.3500	4.2500	6.0000
5.9000	6.3000	4.3500	5.8000	1.9500	2.4500	4.7000	6.5000
6.6000	7.2000	5.7000	7.6500	4.6000	5.4000	5.0000	7.0500
7.4000	7.9500			4.7000	5.5000	5.6500	8.2000
8.0000	8.7000			7.0000	8.6500		
8.2000	8.8000						
9.0000	9.7000						
9.6000	10.4000						

SLOPE PM0= 0.8931 INTERCEPT PB0= 0.2849 FIT OF LINE= 0.9998

SLOPE PM1= 0.8005 INTERCEPT PB1= -0.3752 FIT OF LINE= 0.9989

SLOPE PM2= 0.8335 INTERCEPT PB2= -0.0496 FIT OF LINE= 0.9988

SLOPE PMCOR= 0.6950 INTERCEPT PBCOR= 0.0739 FIT OF LINE= 0.9993

POM= 0.5960 POB= -0.0856 POCIRM= 0.4969 POCIRB= 0.0027

APPENDIX II

Calibration of the Iron-Constantan Thermocouples and the Infrared Pyrometer

In order to calibrate the temperature measuring equipment, a controlled temperature plate ("hot chuck") was obtained. This instrument is a Rucker and Kolls model 135 hot chuck probe station which consists of a flat metal disc into which two heating elements and an iron-constantan thermocouple are inserted, and an API model 227 solid state temperature controller. The API controller drives the heating elements based on an error signal between the thermocouple and the controller set point (set point range= 0-300 deg. c). Stability of the controller is a temperature of 151.3 ± 1.1 deg. C (8.08 ± 0.06 millivolts) at the low end of the range, whereas at the high end temperature stability was 266.1 ± 2.2 deg. C (14.45 ± 0.12 millivolts). The calibration was accomplished by melting a small amount of a pure chemical on the surface of the hot chuck. Chemicals were chosen which had melting points over the temperature region of this study: Ice m.p. 0 deg. C, Water b.p. 100 deg. C, Indium m.p. 156.4 deg. C, Silver Nitrate m.p. 212 deg. C, and Bismuth m.p. 271.3 deg. C. These calibration data are recorded in Table AP II-2 and plotted on Fig. AP II-3. In order to calibrate the other thermocouples to the hot chuck, it was only necessary to attach the experimental ther-

thermocouples to the chuck and chart the calibrated chuck thermocouple against the new unit. Both the reactor and exhaust gas thermocouples read identically during calibration. This data is plotted in Fig. AP II-5.

In calibrating the IR pyrometer to the hot chuck thermocouple, the method consisted of attaching an unoxidized silicon wafer to the hot chuck surface, focusing the pyrometer on the wafer, and reading the thermocouple versus the pyrometer at an "assumed" silicon emissivity of 0.45. Comparing the thermocouple data and pyrometer readings, a better choice of effective emissivity was made. During these initial setup operations, the pyrometer developed a defective chopper, and subsequently was repaired. Therefore, it was necessary to repeat the emissivity calibration described above. The effective emissivity was now found to be 0.50 (See Fig. AP II-4). This value is closer to the literature value of the emissivity (i.e. $e = 0.65$, F.G. Allen BTL-AL, Memorandum, 1957) than was the earlier optimum, $e = 0.31$, and was therefore considered more accurate.

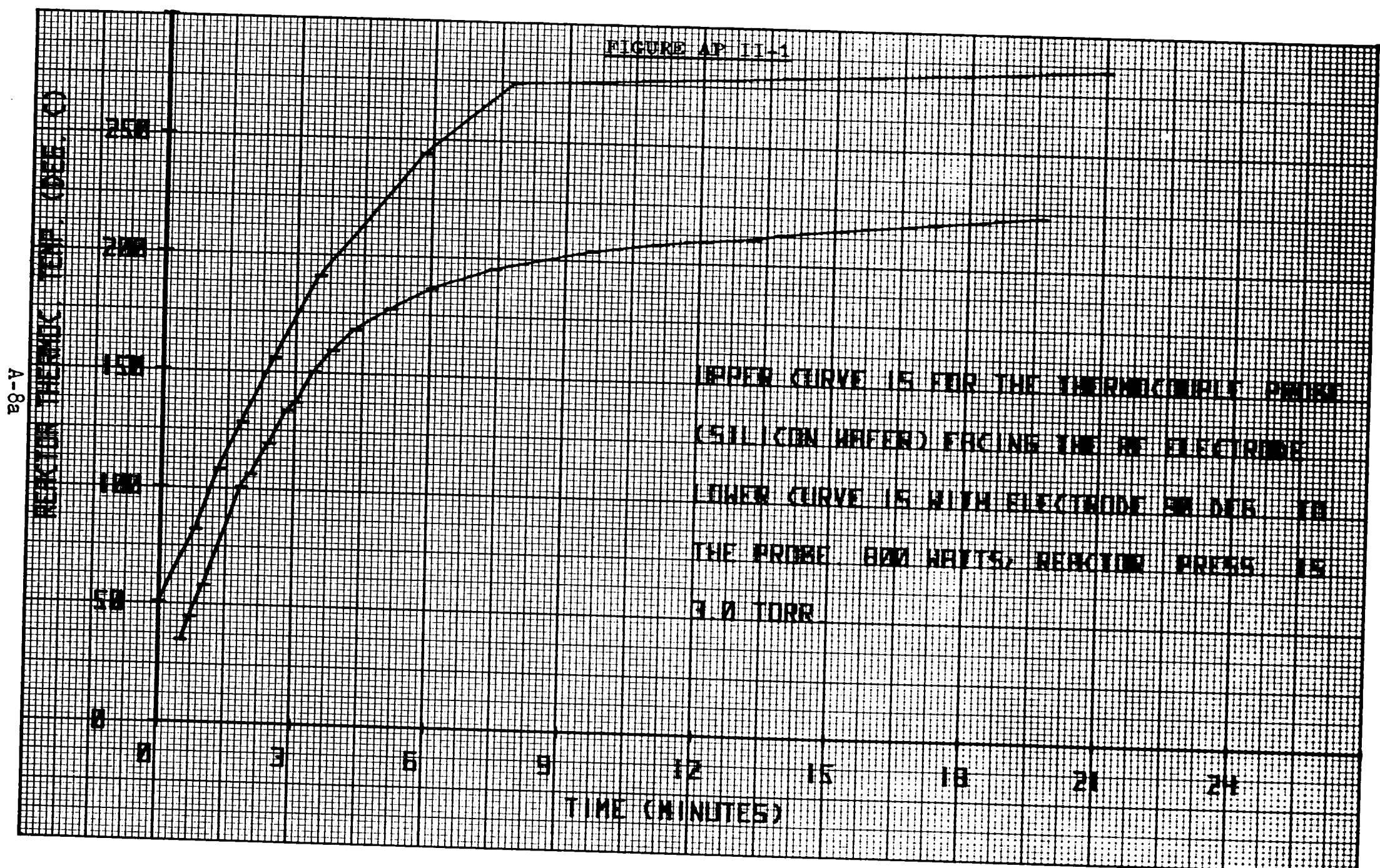


TABLE AP II-2

TEMPERATURE CALIBRATION DATA

ALL TEMPERATURES ARE IN DEG. C

NT IS THE NUMBER OF DATA POINTS TAKEN

NT0= 5

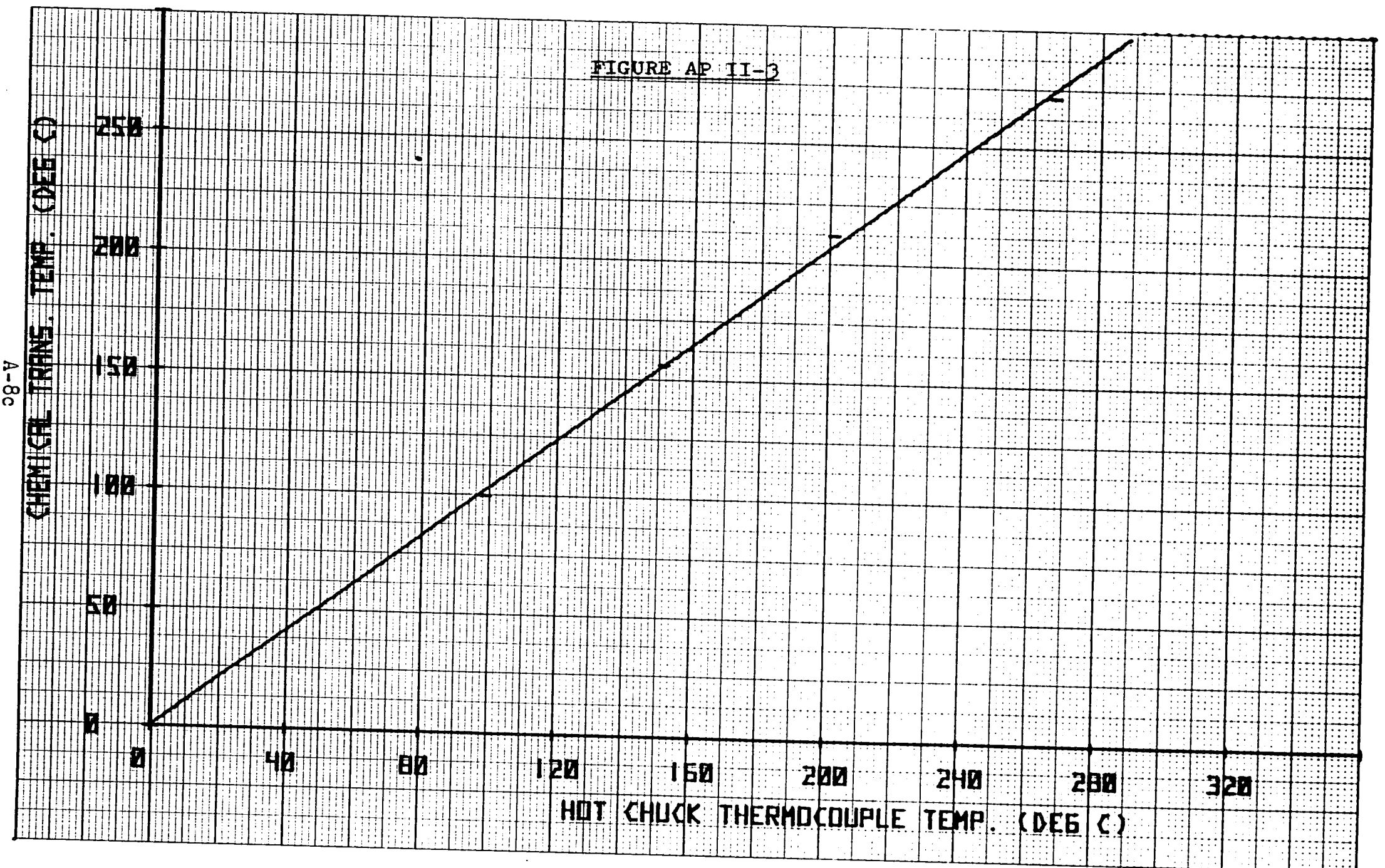
NT1= 8

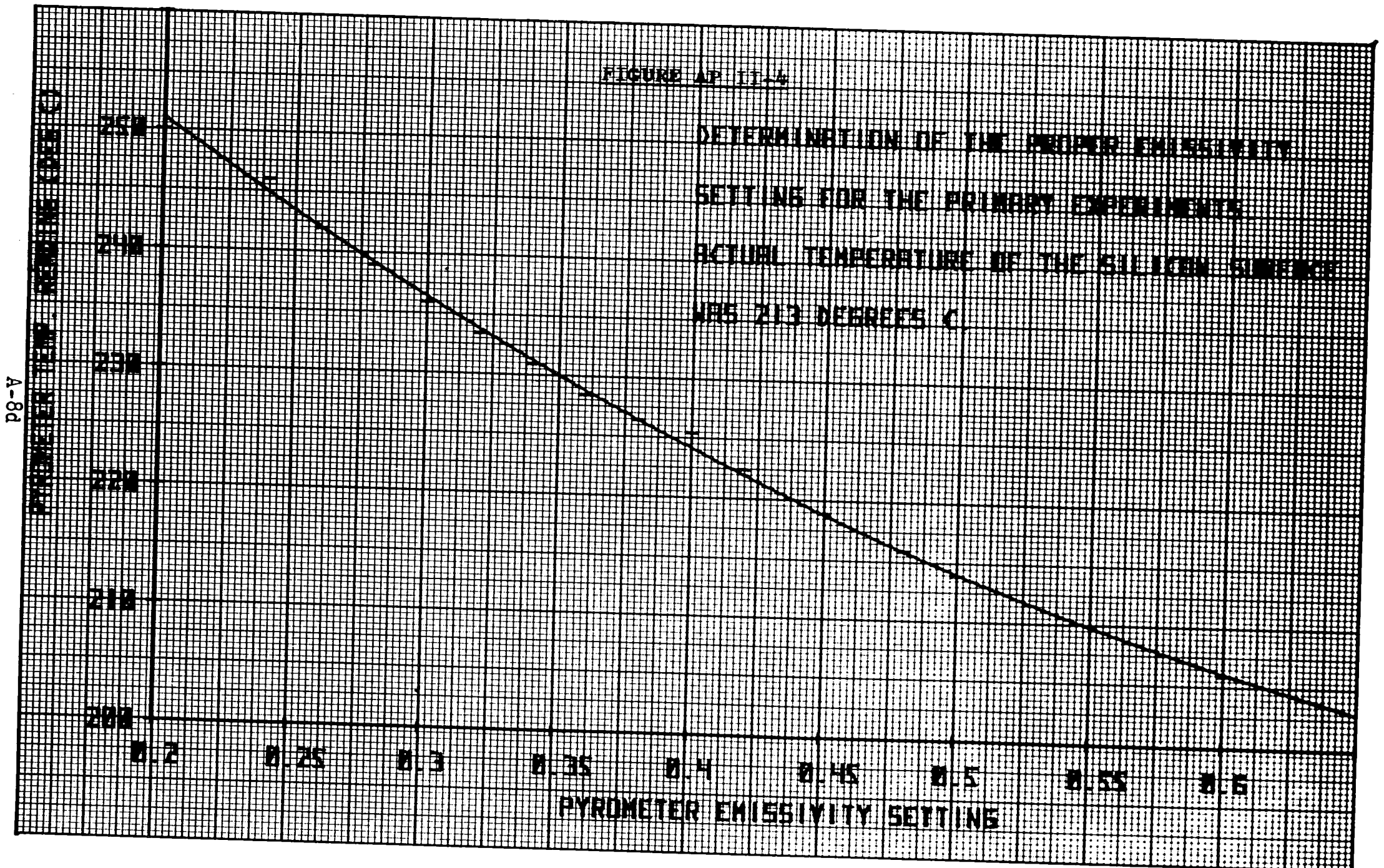
CHEN MELTING POINT (DEG C)	HOT CHUCK TEMPERATURE	HOT CHUCK TEMPERATURE	IR PYROMETER
0.0	0.0	136.1000	135.0000
100.0000	81.4000	155.2800	156.5000
156.4000	151.6600	179.4400	182.0000
212.0000	201.6600	205.8300	208.5000
271.3000	266.3899	232.5000	235.0000
		258.6001	260.5000
		284.1699	286.0000
		303.8899	305.0000

SLOPE TM0= 1.0050 INTERCEPT T80= 7.0165 FIT OF LINE= 0.9977

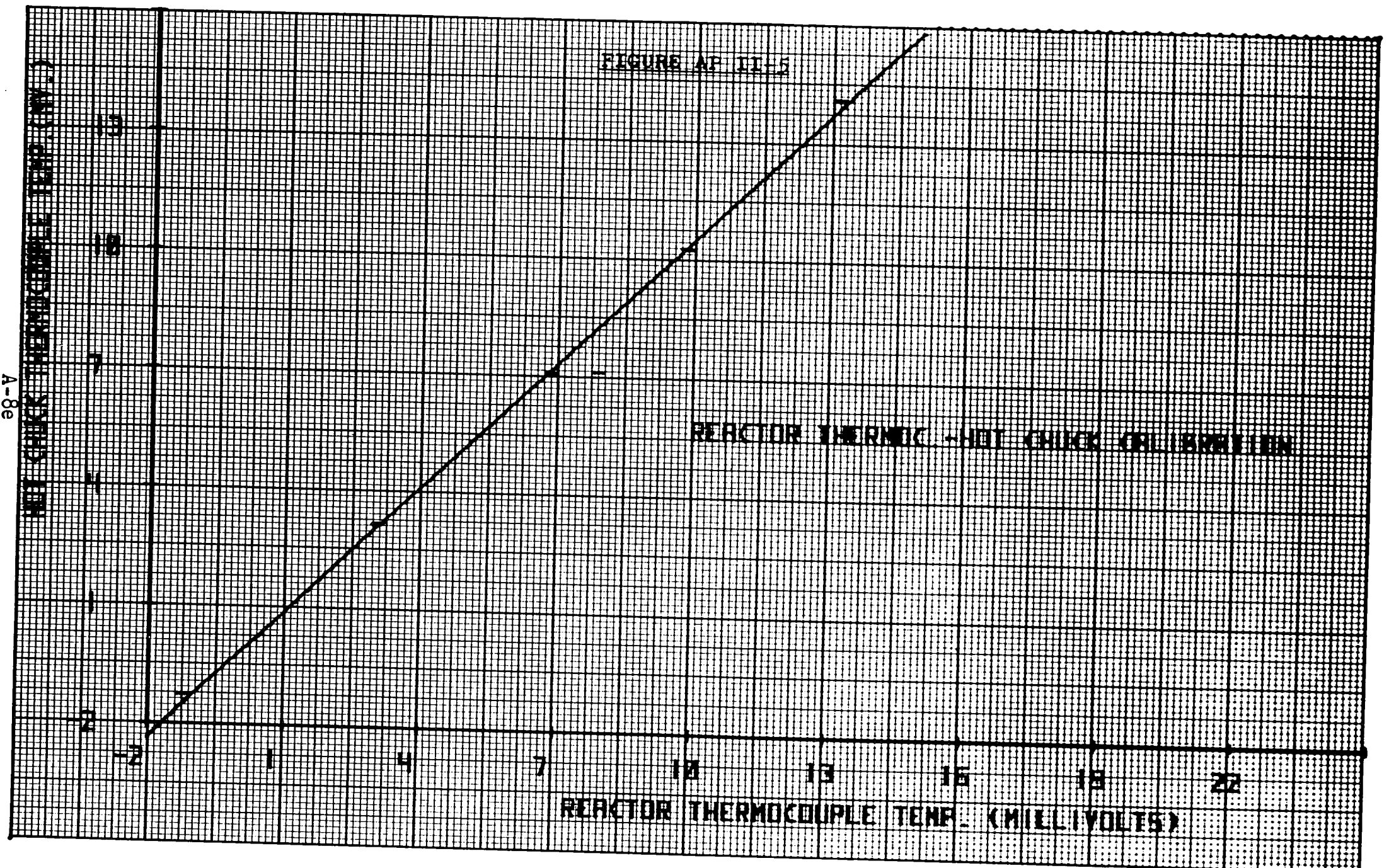
SLOPE TM1= 0.9922 INTERCEPT T81= 0.1318 FIT OF LINE= 0.9998

TOM= 0.9972 T08= 7.1489





K&E 20 X 7 X TO THE INCH 46 1240
K&E MODEL & ESSER CO.



K&E 20 X 7 X TO THE INCH 46 1240
K&E & ESSER CO.

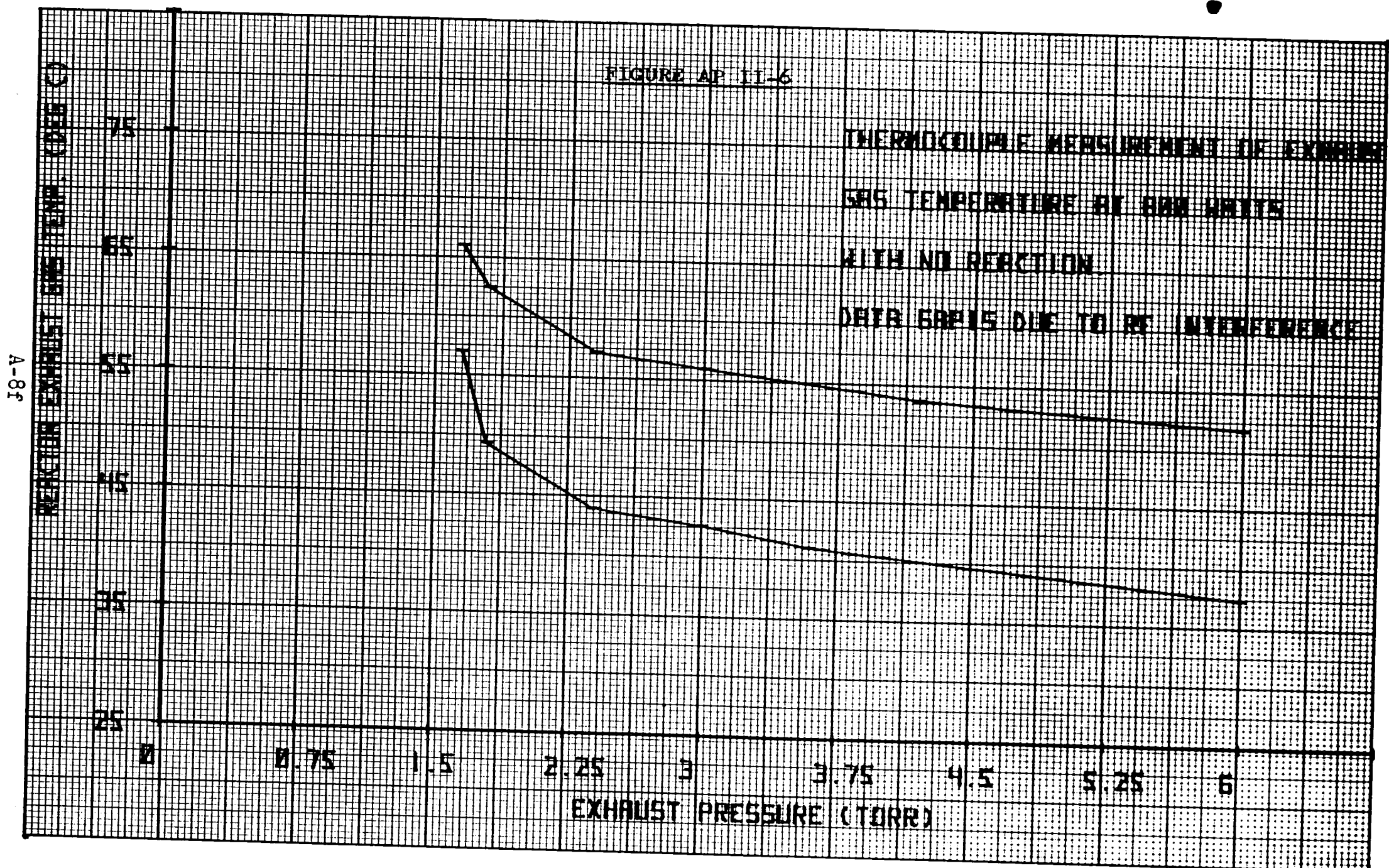


FIGURE AP III-1

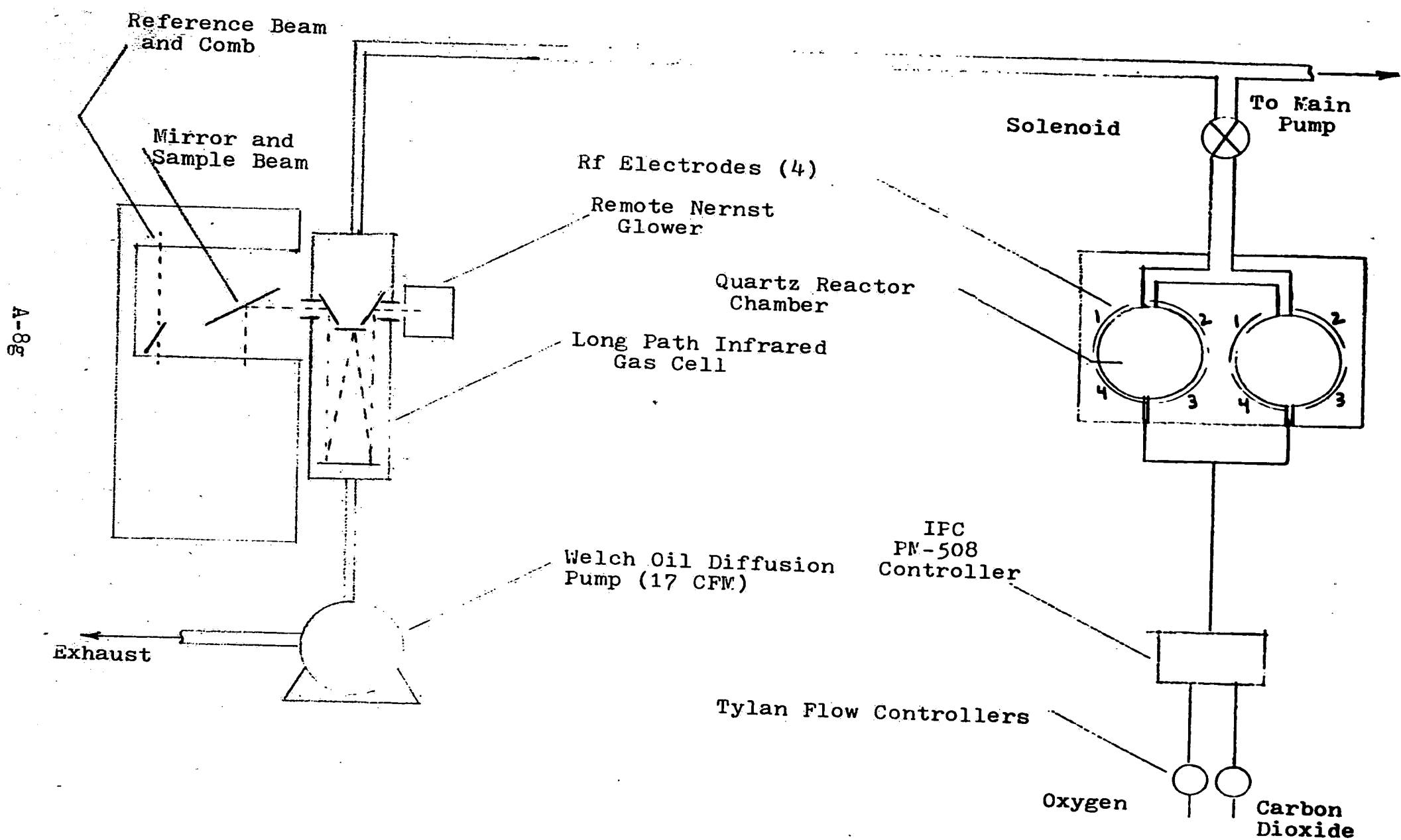
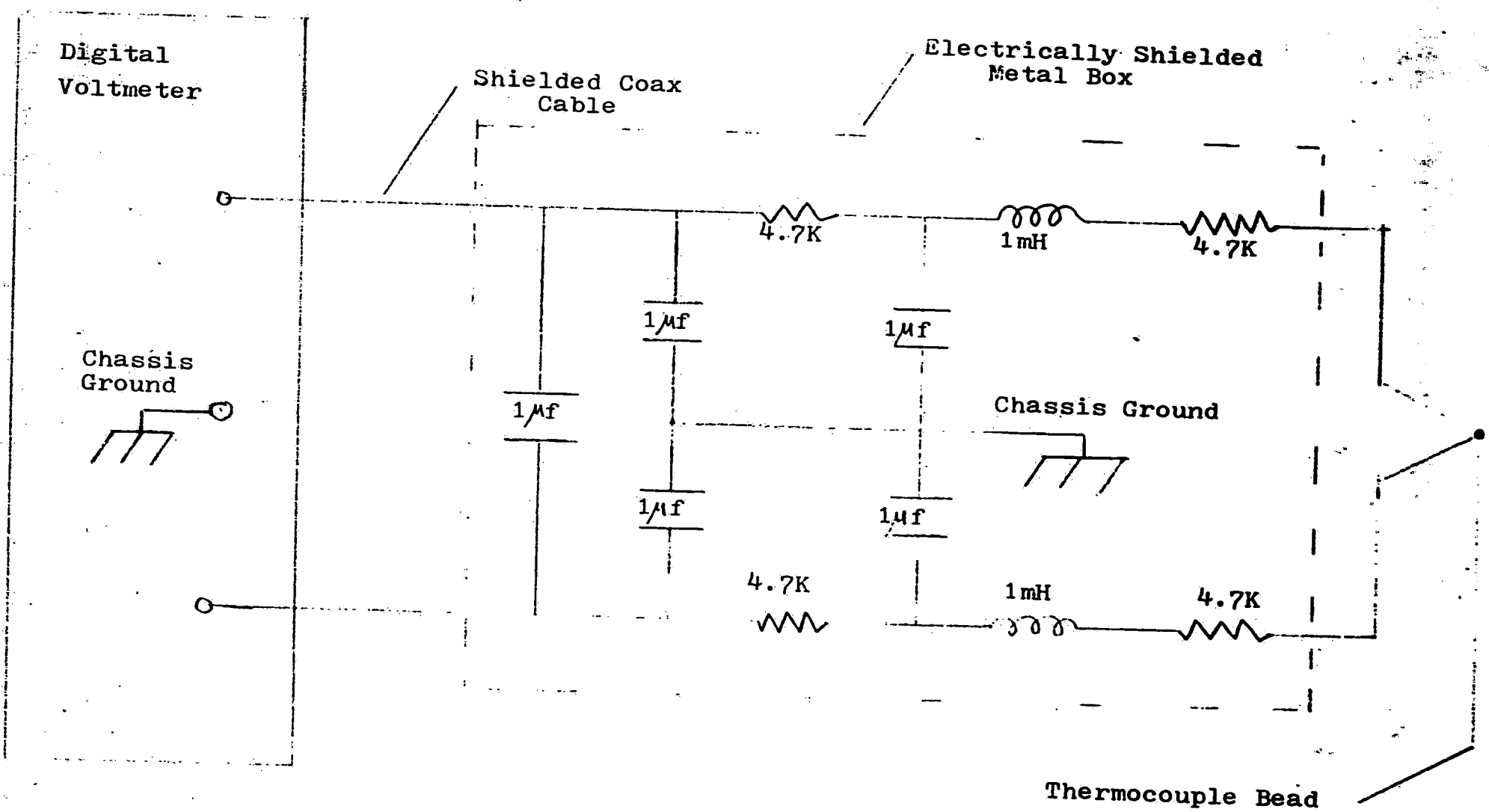


FIGURE AP III-2



APPENDIX IV

Calibration of the Tylan Mass Flow Controllers

Although the primary (absolute) standard for flow calibration is measured liquid displacement for an interval of time, this technique was not used. It was decided that a calibrated Brooks ball and tube flowmeter would be accurate enough for this work. The Brooks R-2-15-D tube with a glass ball was used by connecting it in series with the mass flow controller being calibrated. Since the controller is driven by a 0-5 volt DC signal, an external power supply was used to drive the controller while a digital voltmeter read both this external signal supplied to the controller and the controller response in volts. Ideally, both the control voltage and the signal put out by the controller (in response to the control voltage) will be identical. However, for the high flow region of the carbon dioxide controller, significant deviation from ideality was measured, Table AP IV-2. Also monitored to complete the calibration was the height of the ball in the graduated tube and the flow displayed by the controller, Table AP IV-2 and 3. Nitrogen gas was used for the calibration because its controller correction factor is the same as oxygen, 1.00. Conversion of the ball height measurement to actual flow was done with the Brooks calibration curve for the R-2-15-D tube.

TABLE IV-1
CONVERSION FACTORS

DESCRIPTION	SYMBOL	Specific Heat, Cp Cal/gm-°C	Density g/100°C	Conversion Factor
Acetylene	C2H2	.383	1.1709	.61
Air	--	.248	1.2929	1.00
Ammonia	NH3	.5232	.7710	.68
Argon	A	.1253	1.7837	1.36
Arsine	AsH3	.118	3.484	.66
Carbon Dioxide	CO2	.1989	1.9769	.74
Carbon Monoxide	CO	.2478	1.2504	1.00
Chlorine	CL2	.115	3.214	.79
Diborane	B2H6	.5012	1.2352	.44
Dichlorosilane	H2SiCL2	.080	4.74	.72
Ethane	C2H6	.4097	1.3566	.49
Ethylene	C2H4	.3592	1.2604	.60
Germane	GeH4	.1335	3.43	.60
Helium*	He	1.248	.1785	1.43
Hydrogen*	H2	3.389	.0899	1.02
Hydrogen Bromide	HBr	.0820	3.6445	1.04
Hydrogen Chloride	HCL	.1939	1.6392	.98
Hydrogen Selenide	H2Se	.100	3.612	.81
Krypton	Kr	.0600	3.700	1.49
Methane	CH4	.5271	.7168	.72
Nitric Oxide	NO	.2328	1.3407	.99
Nitrogen	N2	.2477	1.2506	1.00
Nitrous Oxide	N2O	.2004	1.997	.73
Oxygen	O2	.2177	1.4290	1.00
Phosphine	PH3	.261	1.5178	.69
Propane	C3H8	.3882	2.0199	.35
Propylene	C3H6	.3541	1.46	.53
Silane	SiH4	.3186	1.44	.59
Silicon Tetrachloride	SiCL4	.169	7.569	.21
Sulfur Dioxide	SO2	.1516	2.927	.66
Sulfur Hexafluoride	SF6	.1590	6.139	.28
Tungsten Hexafluoride	WF6	.0954	13.296	.22
Xenon	Xe	.0400	5.897	1.36

Each flow controller is calibrated at the factory for a particular gas and flow range as etched on the outside surface. For conversion to another gas, multiply the output reading by the ratio of the conversion factor (above) for the desired gas to the conversion factor for the calibrated gas.

For example:

Controller calibrated for oxygen

When flow is argon, output reads 50 SCCM

$$\text{Corrected flow} = 50 \times \frac{1.36}{1.00} = 68 \text{ SCCM of argon}$$

*Conversion of controller to or from hydrogen or helium may seriously alter dynamic response or stability.

NOTE: Standard Pressure is defined as 760 mmHg (14.7 psig). Standard Temperature is defined as 0°C as of 4/1/73. (Previous to this date was 59°F).

Published by Tylan
Corporation

TABLE AP IV-2

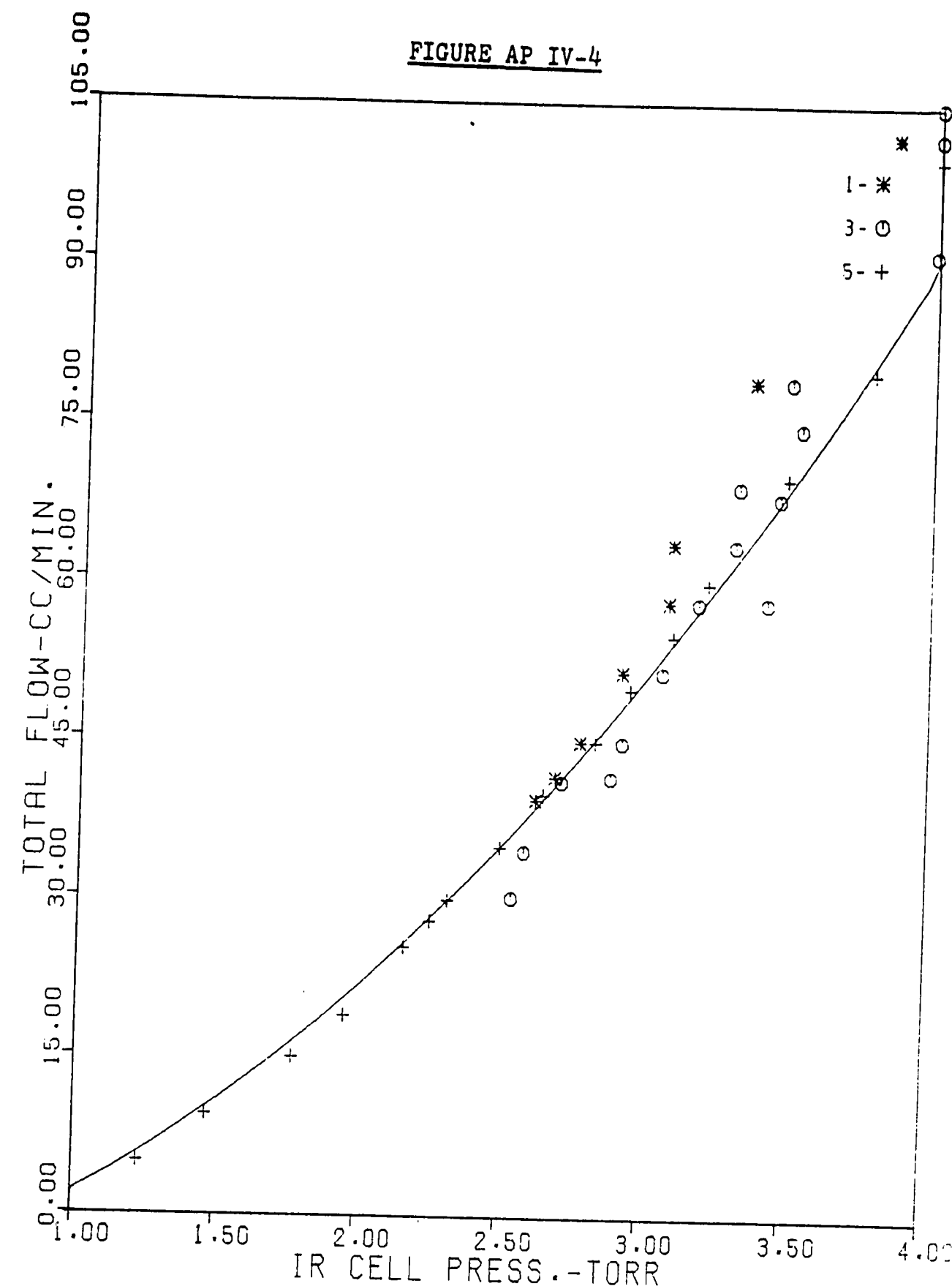
Calibration Data for the Carbon Dioxide Mass Flow Controller

<u>Controller Display (cc/min.)</u>	<u>Control Voltage (volts DC)</u>	<u>Display Voltage (volts DC)</u>	<u>Ball Height (cm.)</u>	<u>O2 Flow Corresponding to Ball Height (70 F) (cc/min.)</u>
140	5.0	4.05	10.5	220
---	4.5	3.90	10.25	214
---	4.0	3.88	10.20	214
135	3.5	3.50	9.70	195
115	3.0	3.00	8.80	166
96	2.5	2.5	8.00	142
77	2.0	2.0	7.10	116
57	1.5	1.5	6.0	87
38	1.0	1.0	4.75	58
---	0.75	0.74	3.9	44.5
---	0.60	0.59	3.4	35
19.5	0.50	0.49	2.85	28
11.5	0.30	0.29	----	----
---	0.25	0.24	1.5	14
3.5	0.10	0.09	0.5	7

TABLE AP IV-3

Calibration Data for the Oxygen Mass Flow Controller

Controller Display (cc/min.)	Control Voltage (volts DC)	Display Voltage (volts DC)	Ball Height (cm.)	O2 Flow Corresponding to Ball Height (70 F) (cc/min.)
205	5.0	5.0	12.5	290
---	4.5	4.5	11.5	255
---	4.0	4.0	10.5	220
---	3.5	3.5	9.75	195
---	3.0	3.0	9.0	170
103	2.5	2.5	8.0	140
---	2.0	2.0	7.0	112
---	1.5	1.5	6.0	87
---	1.0	1.0	4.75	58
---	0.5	0.5	3.0	28
---	0.0	0.0	0.0	0



THIS PLOT SHOWS THE TOTAL FLOW OF CO₂ PLUS O₂ VERSUS IR CELL PRESSURE FOR THE TWO TRANSMITTANCE CALIBRATION RUNS AND A MEASUREMENT OF FLOW VS. PRESSURE FOR O₂. SYMBOL1 IS CALIBRATION1, SYMBOL3 IS CALIBRATION2, AND SYMBOL5 IS THE FLOW VS. PRESS. CURVE USED IN THE CALCULATIONS. THE LINES ON THIS PLOT WERE CALCULATED FROM THE RELATIONSHIP $Y=A+B \cdot X+C \cdot X^2$ WHERE A, B, AND C ARE CONSTANTS.

SYMBOL1 IS CALIBRATION1 DATA. SYMBOL3 IS DATA FROM CALIBRATION2

A-11a

TABLE AP IV-5

<u>Feed Rate O2</u> <u>(cc/min.)</u>	<u>Pressure IR</u> <u>Cell (torr)</u>	<u>Feed Rate CO2</u> <u>(cc/min.)</u>	<u>Pressure IR</u> <u>Cell (torr)</u>	<u>Feed Rate H2O</u> <u>(cc/min.)</u>	<u>Pressure IR</u> <u>Cell (torr)</u>
0.0	0.69	0.0	0.58	0.0	0.58
5.0	1.23	3.70	1.01	6.75	0.90
9.5	1.47	7.03	1.22	15.00	1.35
15.0	1.77	11.47	1.42	22.5	1.72
19.0	1.95	15.54	1.57	29.6	2.0
25.5	2.16	20.0	1.82	38.25	2.39
28.0	2.25	25.9	1.98	45.0	2.65
30.0	2.31	29.6	2.20	90.75	4.60
35.0	2.49	33.3	2.31		
40.0	2.64	37.0	2.44		
45.0	2.82	37.74	2.53		
50.0	2.94	44.4	2.62		
55.0	3.09	51.8	2.75		
60.0	3.21	59.2	2.98		
70.0	3.48	74.0	3.23		
80.0	3.78	88.8	3.47		
100.0	4.26				

A-11b

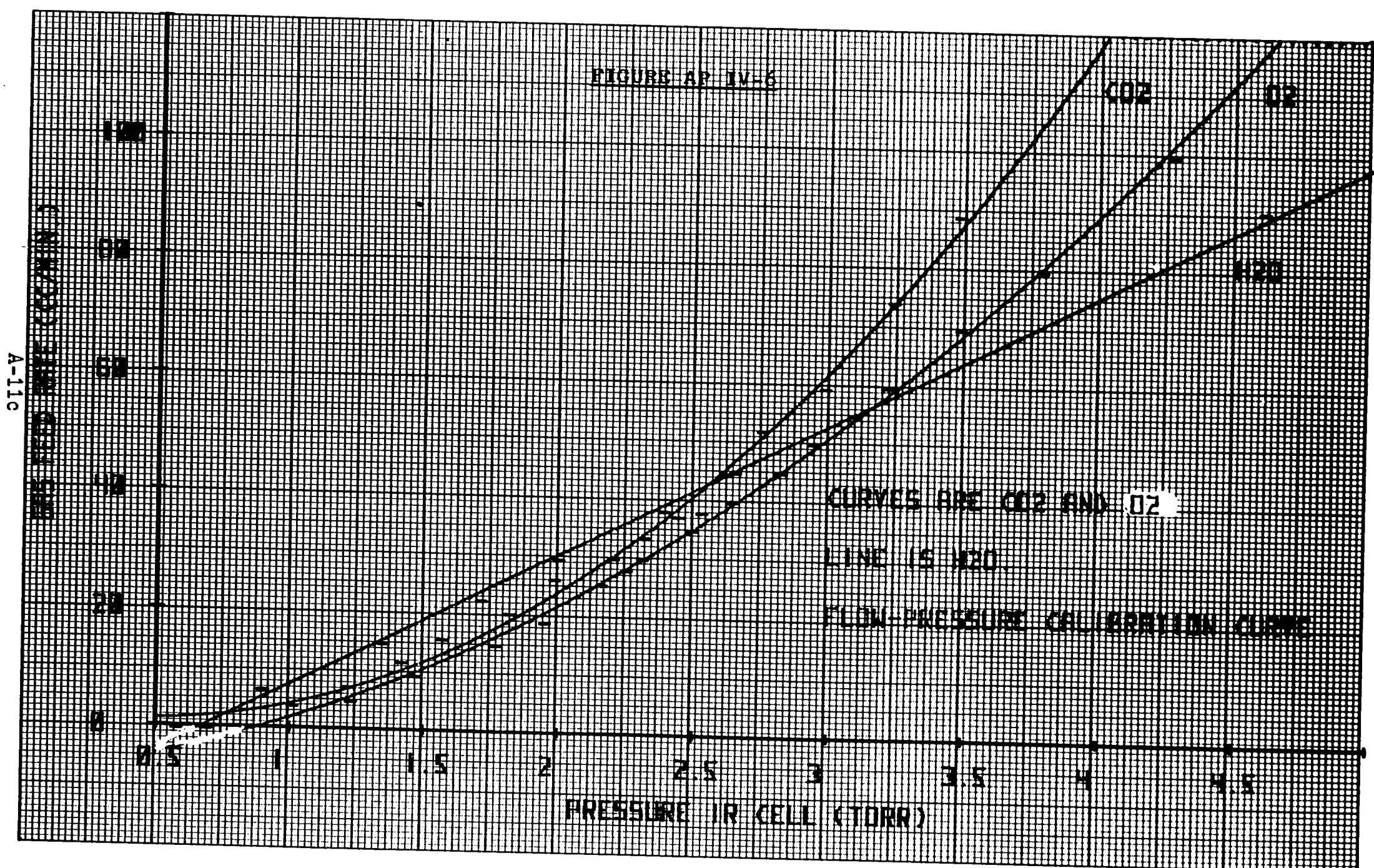


TABLE AP IV-7

FLOW 02 CC/MINUTE	PRESSURE IR-TORR
0.0	0.6900E+00
0.5000E+01	0.1230E+01
0.9500E+01	0.1470E+01
0.1500E+02	0.1770E+01
0.1900E+02	0.1950E+01
0.2550E+02	0.2160E+01
0.2800E+02	0.2250E+01
0.3000E+02	0.2310E+01
0.3500E+02	0.2490E+01
0.4000E+02	0.2640E+01
0.4500E+02	0.2820E+01
0.5000E+02	0.2940E+01
0.5500E+02	0.3090E+01
0.6000E+02	0.3210E+01
0.7000E+02	0.3480E+01
0.8000E+02	0.3780E+01
0.1000E+03	0.4260E+01

FOR TRANS. CAL. 18 FLOW(Y-AXIS) VS. PRESS.(X-AXIS) COFFS. ARE A=-.7993E+01 R=0.5329E+01 C=0.4789E+01 STDDEV=0.3146E+00

A-11d

APPENDIX IV-A

Tylan Mass Flow Controller - theory of operation

The temperature of a gas stream is measured before and after a heat source using thermocouples. The difference in these two temperatures is a function of the density, heat capacity, flow rate, and controller configuration. For a given controller and a particular gas, Tylan Corp. adjusts electronically the difference signal, ΔT , so that the ratio, $\Delta T/f(\rho, CP, Kc)$, is equal to the actual volume flow rate in cc/min. at STP flowing through the controller. Once the controller is calibrated at the factory, it should be immune to variations in the environment where it is used since the variations of gas density and heat capacity near room temperature are small.

These Tylan flow controllers can be used with a different gas than the one for which they were calibrated with equal accuracy by adjusting the displayed flows (flow readings) using the conversion factor chart shown in Table AP IV-1. The equation used to derive these factors is,

$$\text{Factor} = K * (0.3098 / \rho * CP) \quad (\text{IV-1})$$

where K = a constant dependent on gas type; K is 1.04 for monatomic gases, 1.0 for diatomic, 0.94 for triatomic, and 0.88 for polyatomic.

ρ = gas density, grams/liter, at STP (0 °C, 760 mmHg)

CP = gas heat capacity, calories/gram- °C

APPENDIX V

Calibration of the Perkin-Elmer 457 Spectrometer and Infrared Gas Cell

Calibration of the CO₂ detection apparatus shown in Fig. AP III-1, consisted of the following: the spectrometer was set at 2349 cm⁻¹ by filling the system with CO₂ and locating the point of maximum absorbance near 2350 cm⁻¹, the remote Nernst glower variac was set at 90 out of 140, and the secondary or gas cell vacuum pump was turned on. With the gas cell (IR cell) at low pressure, 4-5 torr, the remote glower, IR cell, and concave mirror were adjusted to the maximum obtainable absorbance (minimum transmittance). During these adjustments, the IR cell pathlength was 10 cm. and the "comb" was not in the reference beam. Next the response time of the spectrometer at various gas cell pathlengths. For a cell path of 10 meters, the time for the transmittance to stabilize at a new level after a step change in CO₂ concentration (pure O₂ to 44% CO₂ in oxygen) was 10-12 minutes. This response was far too slow to adequately measure real time CO₂ concentration. However, with a pathlength of 6.4 meters, the stabilization time for the same step change was only 3-4 minutes. This time was probably close to the actual mixing time for full changeover of the gas composition. Although shorter pathlengths continued to reduce the response time of the spectrometer, they

attenuated the sensitivity more than could be tolerated in this experiment. Therefore, the IR gas cell was set at 6.4 meters pathlength for all of the experiments.

In order to prevent any doubts about the relationship between calibration and experimental absorbance measurements, the absorbance maximization procedure described above was carried out before calibrations on different days and a recalibration was performed the day when the primary experiments were run. The maximization performed with the IR cell set at 6.4 meters included using the "comb" in the reference beam to attenuate the beam's intensity and hence improve the strength of the measured signal. Usually, the comb was set such that an 80-90 % transmittance baseline was obtained. This transmittance baseline was checked both before and after every experimental run for assurance that the baseline had not drifted.

A cylinder of pure CO₂ was used to perform the calibration. Delivery pressure was 5 psig and the gas was at room temperature. This carbon dioxide was supplied to one Tylan flow controller, while oxygen was fed into the other. Both gases were mixed after the flow controllers and fed together through the whole apparatus (reaction chambers, transfer line) to the IR cell. The calibration procedure for the primary experiments consisted of: turning on the flow controllers to a set flow, allowing the system 5 minutes to stabilize before each reading, and then reading flows ,

total pressure, and transmittance simultaneously. While the oxygen flow remained fixed, the CO₂ flow was varied over a range of flow from 2-60 cc/min.. Once the range of CO₂ flow had been covered, the oxygen flow was changed and the range of CO₂ values repeated.

Calculations to reduce the data were the following:

1. Use the flow calibration eqns. (20) and (21) to obtain the actual flows of CO₂ and O₂.
2. Calculate the mole fraction of CO₂, $Y_{CO_2} = \frac{CO_2 \text{ Flow}}{\text{Total Flow}}$.
3. Put the relative transmittance readings on an absolute basis by dividing them by the baseline transmittance.
4. Convert the transmittance values to absorbance, $A = -\log_{10}(\text{Trans.})$
5. Calculate the actual IR cell pressure using Appendix I-A.
6. Finally, Calculate the CO₂ concentration using the ideal gas molar volume at room temperature (27 °C).

$$C_{CO_2}(\text{gmmoles/liter}) = \frac{P_{\text{gas cell}}}{760.0} \times 24.631 \quad (V-1)$$

where $P_{\text{gas cell}}$ is in torrs.

All the calibration data are charted on Table AP V-1 and graphed on Fig. AP V-2. A least square straight line was fitted to the absorbance vs. concentration data to yield the important relationship,

$$\text{Cco}_2(\text{gmmoles/liter}) = 0.0008022 * \text{Absorbance} - 0.00002139$$

(22)

'FIT' OF LINE=0.9935E+00

TABLE AP V-1b

TRANSMITTANCE CALIBRATION DATA

THE NUMBER OF DATA POINTS TAKEN=16

THE BASELINE TRANSMITTANCE (ZERO CO₂)= 0.8300

CONCENTRATION IS IN GRAMMOLES/LITER

PRESSURE IS IN TORR

A-17b

RAW FLOW CO ₂ CC/MINUTE	RAW FLOW O ₂ CC/MINUTE	RAW REACTR PRES.-TORR	RELATIVE TRANSMITT.	ABSOLUTE % CO ₂	ABSOLUTE CONC. CO ₂	ABSOLUTE TRANSMITT.	ABSOLUTE ABSORBANCE	ABSOLUTE IR PRESS.	TOTAL FLOW CC/MINUTE
0.2900E+02	0.2700E+02	0.6700E+01	0.5950E+00	0.4608E+00	0.8151E-04	0.7169E+00	0.1446E+00	0.3311E+01	0.6911E+02
0.3800E+02	0.2700E+02	0.6900E+01	0.5600E+00	0.5243E+00	0.9837E-04	0.6747E+00	0.1709E+00	0.3486E+01	0.7899E+02
0.5900E+02	0.2700E+02	0.7500E+01	0.5000E+00	0.6349E+00	0.1358E-03	0.6024E+00	0.2201E+00	0.4004E+01	0.1021E+03
0.1300E+02	0.2700E+02	0.6300E+01	0.6400E+00	0.2770E+00	0.4519E-04	0.7711E+00	0.1129E+00	0.3054E+01	0.5154E+02
0.7000E+01	0.2700E+02	0.6000E+01	0.6750E+00	0.1710E+00	0.2663E-04	0.8133E+00	0.8977E-01	0.2915E+01	0.4495E+02
0.4000E+01	0.2700E+02	0.5900E+01	0.6900E+00	0.1055E+00	0.1621E-04	0.8313E+00	0.8023E-01	0.2877E+01	0.4155E+02
0.1900E+02	0.2700E+02	0.6500E+01	0.6250E+00	0.3590E+00	0.6092E-04	0.7530E+00	0.1232E+00	0.3177E+01	0.5812E+02
0.2400E+02	0.2700E+02	0.6700E+01	0.6050E+00	0.4143E+00	0.7308E-04	0.7289E+00	0.1373E+00	0.3302E+01	0.6162E+02
0.2400E+02	0.3500E+02	0.7200E+01	0.6000E+00	0.3530E+00	0.6647E-04	0.7229E+00	0.1409E+00	0.3525E+01	0.7466E+02
0.3900E+02	0.3500E+02	0.7900E+01	0.5600E+00	0.4700E+00	0.1002E-03	0.6747E+00	0.1709E+00	0.3991E+01	0.9113E+02
0.8500E+02	0.3500E+02	0.8500E+01	0.4600E+00	0.6590E+00	0.1649E-03	0.5542E+00	0.2563E+00	0.4684E+01	0.1416E+03
0.1800E+02	0.3500E+02	0.7100E+01	0.6130E+00	0.2904E+00	0.5357E-04	0.7386E+00	0.1316E+00	0.3453E+01	0.6807E+02
0.9000E+01	0.3500E+02	0.7000E+01	0.6700E+00	0.1699E+00	0.3100E-04	0.8072E+00	0.9300E-01	0.3416E+01	0.5818E+02
0.3000E+01	0.1950E+02	0.5200E+01	0.7250E+00	0.1091E+00	0.1755E-04	0.8735E+00	0.5874E-01	0.2532E+01	0.3020E+02
0.7000E+01	0.1950E+02	0.5300E+01	0.6800E+00	0.2222E+00	0.3053E-04	0.8193E+00	0.8657E-01	0.2572E+01	0.3460E+02
0.1300E+02	0.1950E+02	0.5600E+01	0.6450E+00	0.3466E+00	0.5004E-04	0.7771E+00	0.1095E+00	0.2702E+01	0.4119E+02

FOR TRANS. CAL. 2 FLOW (Y-AXIS) VS. PRESS. (X-AXIS)

COEFS. ARE A=-.9665E+02

B=0.4898E+02

C=0.0

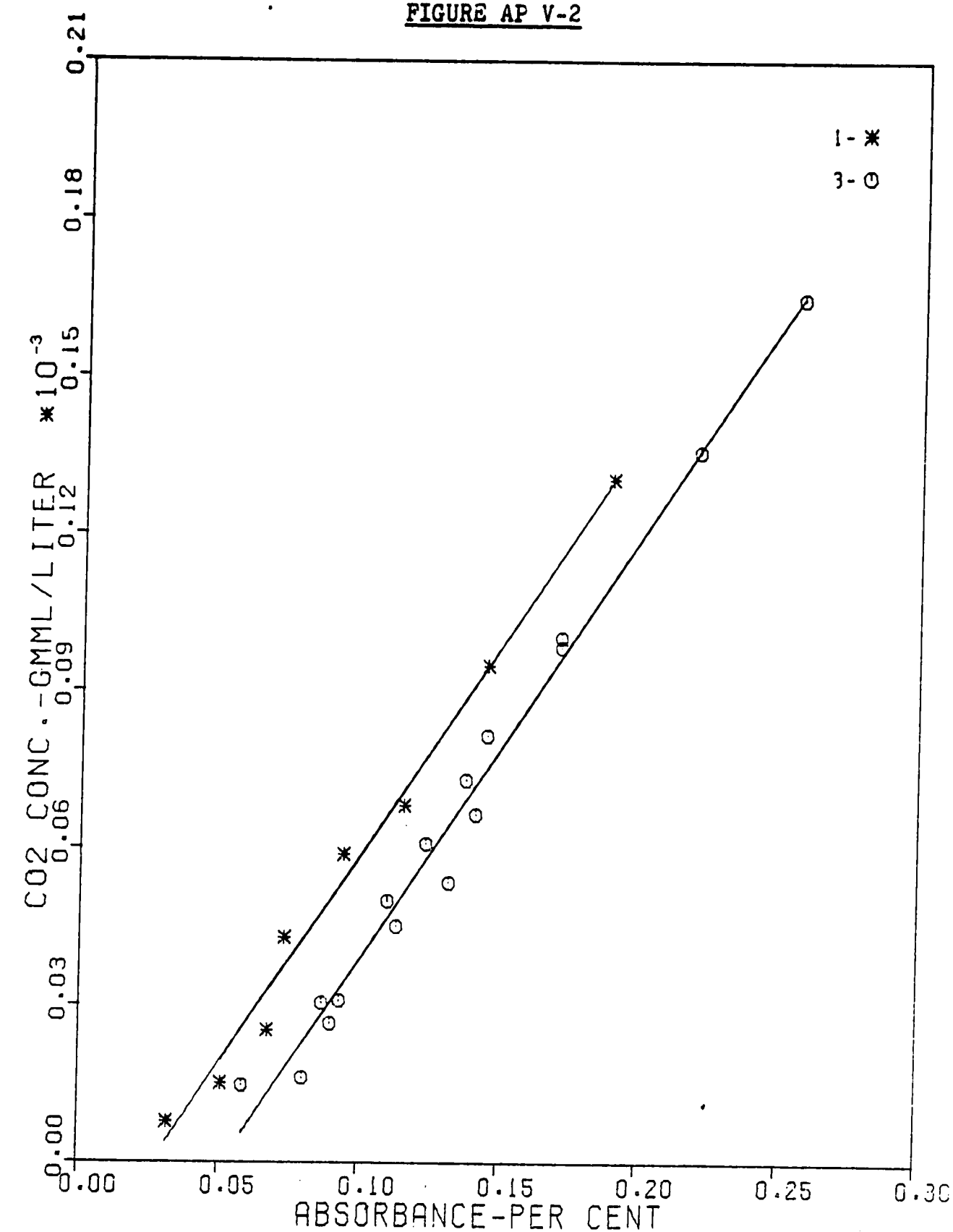
STDEV=0.9819E+00

SLOPE CONOM=0.8090E-03

INTERCEPT CONOM=-.4195E-04

FIT OF LINE=0.9921E+00

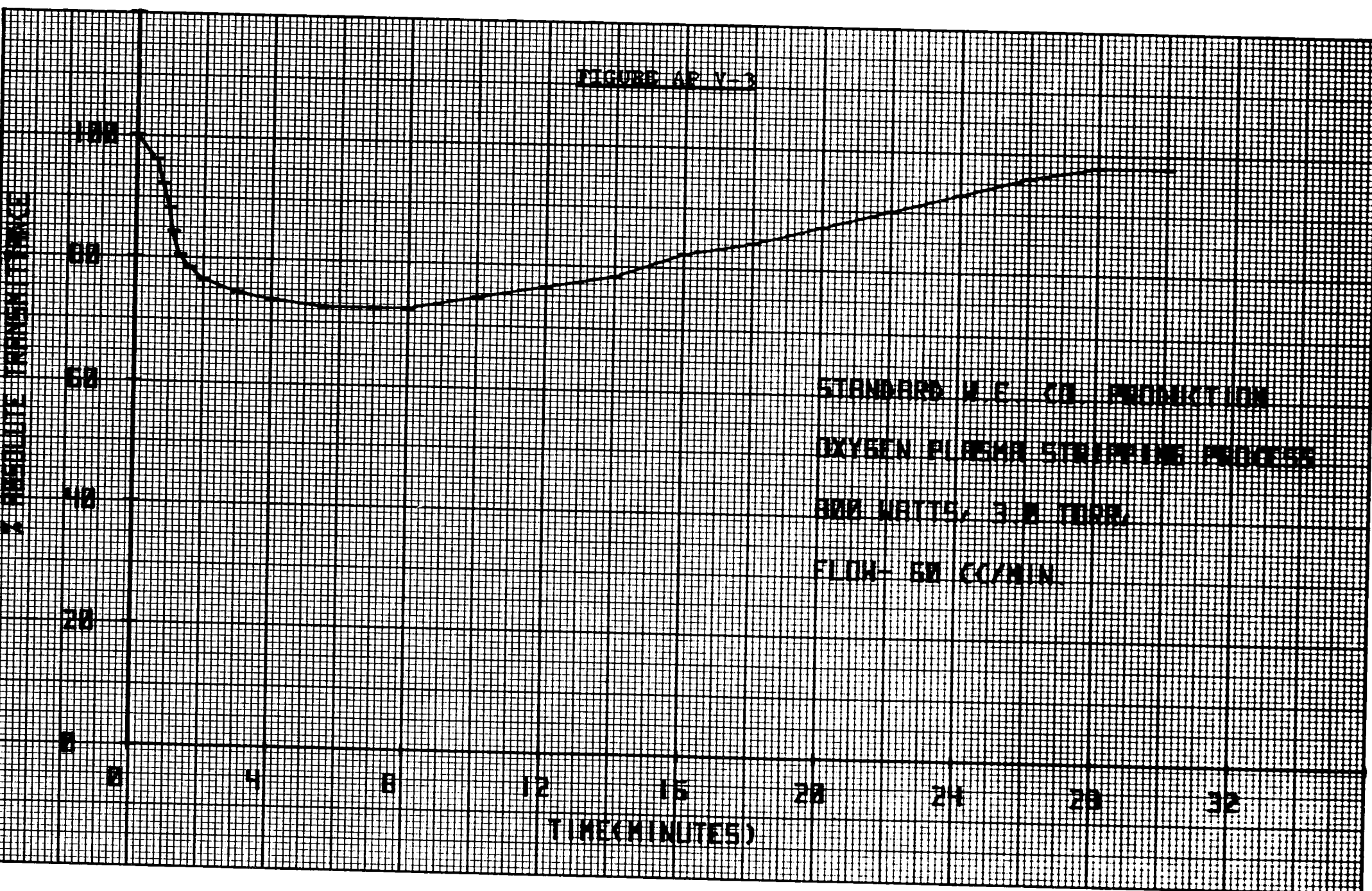
FIGURE AP V-2



THIS PLOT SHOWS THE ABSORBANCE VS. CO2 CONCENTRATION (GRAMMOLES/LITER) RELATIONSHIP DETERMINED BY THE TRANSMITTANCE CALIBRATION. THE LINES ON THIS PLOT WERE CALCULATED FROM THE RELATIONSHIP $Y = A - B \times X$ WHERE A AND B ARE CONSTANTS

A-17c

FIGURE AP V-3



STANDARD W. E. CO. PRODUCTION
OXYGEN FLUORENCE STRIPPING PROCESS
300 WATTS, 3.5 TORR
FLOW- 50 CC/MIN.

APPENDIX VI

THIS PROGRAM CALCULATES CALIBRATION LINES FOR PRESSURE, WAFER TEMP	MSDG 1
, CO2-O2 FLOW, AND TRANSMITTANCE FOR A SYSTEM CONSISTING OF AN IPC	MSDG 2
PLASMA REACTOR MODEL 2000 WITH OUTPUT GAS HOOKED TO AN INFRARED	MSDG 3
0-10 METER PATHLENGTH CELL. VACUUM IS DRAWN ON THE PLASMA REACT.	MSDG 4
THROUGH THE IR CELL BY A 17 CFM WELCH ROUGHING PUMP. FOLLOWING	MSDG 5
THE CALIBRATION SECTION OF THE PROGRAM, THE INSTRUMENT READINGS	MSDG 6
OF THE EXPERIMENTS ARE CONVERTED TO ABSOLUTE, THEN ALL OF THE	MSDG 7
DATA IS CROSS-CORRELATED FOR EMPIRICAL GRAPHS, RELATIONS, AND	MSDG 8
RATE OF REMOVAL CALCULATIONS.	MSDG 9
COMMON POM, POB, POCIRM, POCIRB, TOM, TOB, CONOM, CONOB	MSDG 10
COMMON FLOWA, FLOWB, FLOWC	MSDG 11
DIMENSION POMCL(50), POMECH(50), P1MECH(50), P1TCIR(50), P2TCIR(50)	MSDG 12
DIMENSION P2TCRT(50), PCORIR(50), PCORRT(50), TOCHEM(20), TOHCTC(20)	MSDG 13
DIMENSION T1HCTC(50), T1PYR(50)	MSDG 14
DIMENSION CO2CON(50)	MSDG 15
DIMENSION BLINE(10), F2(10), CONM(2), CONB(2)	MSDG 16
DIMENSION FCREM(2,30), FOREM(2,30), RLTRM(2,30)	MSDG 17
DIMENSION PREM(2,30)	MSDG 18
DIMENSION CONF(2), CO2PR(2,30), CO2CN(2,30), ABSRB(2,30), NDATA(10)	MSDG 19
DIMENSION AA(3), BB(3), CC(3), CDLTOT(10,40), FCO2CB(2,30)	MSDG 20
DIMENSION FO2CB(2,30), PIRCB(2,30), PRCTCB(2,30), XPLOT(102)	MSDG 21
DIMENSION YPLOT(102), NTRAN(5), CO2PER(50), ABSORB(50), ABSB(10,40)	MSDG 22
DIMENSION TIME(10,40), POWLEV(10), WTLOSS(10), PIR(10,40)	MSDG 23
DIMENSION PRACT(10,40), TPYROM(10,40), CDLSPM(10,40), CDLOSS(10,40)	MSDG 24
DIMENSION TRANS(10,40), R(10,40), FLOW2(10,40), YCO2(10,40)	MSDG 25
DIMENSION DUMX(40), DUMY(40)	MSDG 26
DIMENSION TRUE(10)	MSDG 27
DIMENSION DUMF(40), DUMP(40), EACT(10), FREQF(10), HEATCO(10)	MSDG 28
DIMENSION TMPZER(10)	MSDG 29
DIMENSION FITTMP(10)	MSDG 30
DIMENSION COABA(10), COABB(10), COABY(10), COPRA(10), COPRB(10)	MSDG 31
DIMENSION COPRY(10), COTMPA(10), COTMPB(10), COTMPY(10), COTOTA(10)	MSDG 32
DIMENSION COTOTB(10), COTOTC(10)	MSDG 33
DIMENSION CDL(100), FLWA(2), FLWB(2), FLWC(2), FITT(2)	MSDG 34
DIMENSION POB1(10,40), CO2C(10,40), DCO2DT(10,40), YO2(10,40)	MSDG 35
DIMENSION DUMC(40), DUMH(40)	MSDG 36
DIMENSION DUMO(40), DO2DT(10,40)	MSDG 37
DIMENSION COMNT(240)	MSDG 38
REAL LGLG, LINR	MSDG 39
DATA FLIP, BLANK, 'FLIP', ' /	MSDG 40
	MSDG 41
	MSDG 42
	MSDG 43
	MSDG 44
	MSDG 45
	MSDG 46
	MSDG 47
	MSDG 48
	MSDG 49
	MSDG 50

	DATA SLGX,SLGY,LINR,LGLG,END/'SLGX','SLGY','LINR','LGLG','END '/	MSDG 51
	CALL PLOTS(0,0,9)	MSDG 52
	THIS SECTION READS THE CALIBRATION PRESSURE READINGS BETWEEN THE	MSDG 53
	ABSOLUTE PRESSURE MCLEOD GAUGE(P0),THE MECHANICAL GAUGE,THE MODEL	MSDG 54
	DV-4DM HASTINGS-RAYDIST THERMOCOUPLE GAUGES (ONE IN REACTOR,ONE IN	MSDG 55
	IR CELL). IT PERFORMS LINEAR REGRESSIONS TO ENABLE THE REACTOR	MSDG 56
	PRESSURE DATA TO BE CONVERTED TO ABSOLUTE REACTOR PRESSURES USING	MSDG 57
	(FUNCTION P0RT) AND ABSOLUTE IR CELL PRESS. (FUNTION P0IRRT) .	MSDG 58
		MSDG 59
		MSDG 60
		MSDG 61
		MSDG 62
		MSDG 63
		MSDG 64
	READ(5,10) NP0	MSDG 65
	10 FORMAT(I2)	MSDG 66
	READ(5,15) (P0MCL(I),P0MECH(I),I=1,NP0)	MSDG 67
	15 FORMAT(4(2F10.4))	MSDG 68
	READ(5,10) NP1	MSDG 69
	READ(5,15) (P1MECH(I),P1TCIR(I),I=1,NP1)	MSDG 70
		MSDG 71
	READ(5,10) NP2	MSDG 72
	READ(5,15) (P2TCIR(I),P2TCRT(I),I=1,NP2)	MSDG 73
		MSDG 74
	READ(5,10) NCOR	MSDG 75
	READ(5,15) (PCORIR(I),PCORRT(I),I=1,NCOR)	MSDG 76
		MSDG 77
	WRITE(6,40)	MSDG 78
	WRITE(6,41) NP0,NP1,NP2,NCOR	MSDG 79
	40 FORMAT(1H1,50X,'PRESSURE CALIBRATION DATA'/1X,49X,25('-')//,	MSDG 80
	1 42X,'ALL PRESSURES ARE IN TORR'//)	MSDG 81
		MSDG 82
	41 FORMAT(42X,'NP IS THE NUMBER OF DATA POINTS TAKEN'///1X,11X,'NP0='	MSDG 83
	1 ,I2,12X,12X,'NP1=',I2,24X,'NP2=',I2,24X,'NCOR=',I2///1X)	MSDG 84
		MSDG 85
	WRITE(6,854)	MSDG 86
	WRITE(6,855)	MSDG 87
	WRITE(6,856)	MSDG 88
	WRITE(6,857)	MSDG 89
		MSDG 90
	WRITE OUT THE PRESSURE CALIBRATION DATA	MSDG 91
		MSDG 92
		MSDG 93
	854 FORMAT(1X,42X,9X,'IR',13X,'IR',11X,'REACTOR',11X,'SIMULTANEOUS')	MSDG 94
		MSDG 95
	855 FORMAT(1X,4X,'MCLEOD',7X,'MECHANICAL',5X,'MECHANICAL',4X,'THERMOCOMSDG	MSDG 96
	1UPLE',3X,'THERMOCOUPLE',3X,'THERMOCOUPLE',7X,'IR TC',9X,'RXN TC')	MSDG 97
		MSDG 98
	856 FORMAT(1X,4X,'GAUGE',5X,7(5X,'GAUGE',5X))	MSDG 99
		MSDG100
	857 FORMAT(1X,1X,11('-'),2X,7(2X,11('-'),2X))	MSDG101
		MSDG102
		MSDG103
		MSDG104

DO 68 KK=1,50	
IF (KK.GT.NP0.AND.KK.GT.NP1.AND.KK.GT.NP2 .AND.KK.GT.NCOR) GO TO 69	MSDG105
WRITE (6,50)	MSDG106
50 FORMAT (1H)	MSDG107
52 FORMAT (1H+, F10.4,5X,F10.4,2X)	MSDG108
53 FORMAT (1H+,30X,F10.4,5X,F10.4,2X)	MSDG109
54 FORMAT (1H+,60X,F10.4,5X,F10.4,2X)	MSDG110
55 FORMAT (1H+,90X,F10.4,5X,F10.4,2X)	MSDG111
	MSDG112
	MSDG113
DO 200 KKK=1,4	MSDG114
	MSDG115
GO TO (201,202,203,204),KKK	MSDG116
	MSDG117
GO TO 200	MSDG118
201 IF (KK.GT.NP0) GO TO 200	MSDG119
WRITE (6,52) POMCL (KK), POMECH (KK)	MSDG120
202 IF (KK.GT.NP1) GO TO 200	MSDG121
WRITE (6,53) P1MECH (KK), P1TCIR (KK)	MSDG122
GO TO 200	MSDG123
203 IF (KK.GT.NP2) GO TO 200	MSDG124
WRITE (6,54) P2TCIR (KK), P2TCRT (KK)	MSDG125
GO TO 200	MSDG126
204 IF (KK.GT.NCOR) GO TO 200	MSDG127
WRITE (6,55) PCORIR (KK), PCORRT (KK)	MSDG128
	MSDG129
	MSDG130
200 CONTINUE	MSDG131
68 CONTINUE	MSDG132
69 CONTINUE	MSDG133
	MSDG134
	MSDG135
	MSDG136
LINEAR REGRESSION ANALYSIS OF PRESSURE DATA	MSDG137
	MSDG138
CALL REGLNR (POMCL, POMECH, NP0, PM0, PB0, PFIT0)	MSDG139
CALL REGLNR (P1MECH, P1TCIR, NP1, PM1, PB1, PFIT1)	MSDG140
CALL REGLNR (P2TCIR, P2TCRT, NP2, PM2, PB2, PFIT2)	MSDG141
	MSDG142
P0= M0*(M1*(M2*PRT + B2) + B1) + B0	MSDG143
	MSDG144
P0M=PM0*PM1*PM2	MSDG145
P0B=PM0*PM1*PB2 + PM0*PB1 + PB0	MSDG146
	MSDG147
CALL REGLNR (PCORIR, PCORRT, NCOR, PMCOR, PBCOR, PFITC)	MSDG148
	MSDG149
P0IR= M0*(M1*(MCOR*PRT + BCOR) + B1) + B0	MSDG150
	MSDG151
P0CIRM=PM0*PM1*PMCOR	MSDG152
P0CIRB=PM0*PM1*PBCOR + PM0*PB1 + PB0	MSDG153
	MSDG154
WRITE (6,66)	MSDG155
WRITE (6,70) PM0, PB0, PFIT0, PM1, PB1, PFIT1, PM2, PB2, PFIT2, PMCOR, PBCOR,	MSDG156
1 PFITC	MSDG157
	MSDG158

C	66	FORMAT(1X, //)	MSDG159
	70	FORMAT(1X, 19X, 'SLOPE PM0=', F10.4, 5X, 'INTERCEPT PB0=', F10.4, 5X,	MSDG160
	1	'FIT OF LINE=', F10.4//1X, 19X, 'SLOPE PM1=', F10.4, 5X, 'INTERCEPT	MSDG161
	2	PB1=', F10.4, 5X, 'FIT OF LINE=', F10.4//1X, 19X, 'SLOPE PM2=', F10.4,	MSDG162
	3	5X, 'INTERCEPT PB2=', F10.4, 5X, 'FIT OF LINE=', F10.4//1X, 19X,	MSDG163
	4	'SLOPE PMCOR=', F10.4, 5X, 'INTERCEPT PBCOR=', F10.4, 5X,	MSDG164
	5	'FIT OF LINE=', F10.4// //)	MSDG165
C			MSDG166
		WRITE(6, 72) POM, POB, POCIRM, POCIRB	MSDG167
	72	FORMAT(1X, 19X, 'POM=', F10.4, 5X, 'POB=', F10.4, 5X, 'POCIRM=', F10.4,	MSDG168
	1	5X, 'POCIRB=', F10.4)	MSDG169
C			MSDG170
		READ THE FLOW (DUMF) VS. PRESSURE (DUMP) DATA FOR OXYGEN.	MSDG171
C		THIS DATA IS ABSOLUTE PER THE CALIBRATIONS ESTABLISHED IN THIS	MSDG172
C		COMPUTER PROGRAM. THIS DATA WAS REDUCED BY HAND.	MSDG173
C			MSDG174
		READ(5, 15) (DUMF(I), DUMP(I), I=1, 17)	MSDG175
		NTR=17	MSDG176
		IOR=1	MSDG177
C			MSDG178
C		FLOW VS. PRESSURE DATA IS FITTED TO A QUADRATIC EQN. BELOW	MSDG179
C			MSDG180
		CALL QUADFT(DUMF, DUMP, NTR, IOR, A, B, C, FIT)	MSDG181
		FLOWA=A	MSDG182
		FLOWB=B	MSDG183
		FLOWC=C	MSDG184
		WRITE(6, 73)	MSDG185
		DO 91 I=1, 17	MSDG186
		WRITE(6, 74) DUMF(I), DUMP(I)	MSDG187
	91	CONTINUE	MSDG188
		WRITE(6, 66)	MSDG189
		WRITE(6, 363) I, FLOWA, FLOWB, FLOWC, FIT	MSDG190
	363	FORMAT(1X, 'FOR TRANS. CAL.', I2, 'FLOW(Y-AXIS) VS. PRESS. (X-AXIS)	MSDG191
	1	COEFS. ARE A=', E10.4, 5X, 'B=', E10.4, 5X, 'C=', E10.4, 5X, 'STDDEV=',	MSDG192
	2	E10.4/)	MSDG193
	73	FORMAT(1H1, 'FLOW O2 CC/MINUTE', 5X, 'PRESSURE IR-TORR'//)	MSDG194
	74	FORMAT(1X, 4X, E10.4, 11X, E10.4)	MSDG195
C			MSDG196
		READ ON THE THERMOCOUPLE GAUGE, OBSERVED PRESSURE (OXYGEN	MSDG197
C		CALIBRATION BASIS) (DUMO) VS. ACTUAL PURE CO2 PRESSURE (DUMC)	MSDG198
C			MSDG199
		READ(5, 15) (DUMO(I), DUMC(I), I=1, 27)	MSDG200
		NTR=27	MSDG201
		IOR=1	MSDG202
C			MSDG203
		FIT ABOVE DATA TO A QUADRATIC EQN. . HOWEVER, IN THIS PROGRAM	MSDG204
C		THIS DATA IS USED AS A LOOK-UP TABLE DUE TO POOR QUADR. FIT	MSDG205
C		OVER LARGE RANGE.	MSDG206
C			MSDG207
		CALL QUADFT(DUMO, DUMC, NTR, IOR, A, B, C, FIT)	MSDG208
		APCO2=A	MSDG209
		BPCO2=B	MSDG210
		CPCO2=C	MSDG211
			MSDG212

WRITE(6,75)	MSDG213
75 FORMAT(1H1,'PRESSURE OBSERVED O2',5X,'PRESSURE ACTUAL CO2',/,	MSDG214
1 7X,'(TORR)',7X,5X,7X,'(TORR) '//)	MSDG215
DO 92 I=1,27	MSDG216
WRITE(6,74) DUMO(I),DUMC(I)	MSDG217
92 CONTINUE	MSDG218
WRITE(6,66)	MSDG219
WRITE(6,93) APCO2,BPCO2,CPCO2,FIT	MSDG220
C READ OBSERVED PRESSURE (O2 BASIS) (DUMO) VS. ACTUAL PRESSURE	MSDG221
C PURE WATER VAPOR PRESSURE (DUMH)	MSDG222
C	MSDG223
93 FORMAT(1X,'APCO2=',E10.4,2X,'BPCO2=',E10.4,2X,'CPCO2=',E10.4,2X,	MSDG224
1 'STDDEV=',E10.4)	MSDG225
READ(5,15) (DUMO(I),DUMH(I),I=1,29)	MSDG226
NTR=29	MSDG227
IOR=1	MSDG228
C	MSDG229
C FIT DATA TO QUADRATIC. HOWEVER, DATA USED AS LOOK-UP TABLE	MSDG230
C	MSDG231
CALL QUADFT(DUMO,DUMH,NTR,IOR,A,B,C,FIT)	MSDG232
APH20=A	MSDG233
BPH20=B	MSDG234
CPH20=C	MSDG235
WRITE(6,76)	MSDG236
76 FORMAT(1H1,'PRESSURE OBSERVED O2',5X,'PRESSURE ACTUAL H2O',/,	MSDG237
1 7X,'(TORR)',7X,5X,7X,'(TORR) '//)	MSDG238
DO 94 I=1,29	MSDG239
WRITE(6,74) DUMO(I),DUMH(I)	MSDG240
94 CONTINUE	MSDG241
WRITE(6,66)	MSDG242
WRITE(6,95) APH20,BPH20,CPH20,FIT	MSDG243
95 FORMAT(1X,'APH20=',E10.4,2X,'BPH20=',E10.4,2X,'CPH20=',E10.4,2X,	MSDG244
1 'STDDEV=',E10.4)	MSDG245
C	MSDG246
C THIS SECTION READS THE CALIBRATION TEMPERATURE READINGS BETWEEN	MSDG247
C THE ABSOLUTE TEMP. CHEMICAL MELTING POINTS(T0),THE IRON-CONSTANTAN	MSDG248
C	MSDG249
C HOT CHUCK THERMOCOUPLE,AND THE IR INDUSTIES INFRARED PYROMETER.	MSDG250
C	MSDG251
C IT PERFORMS LINEAR REGRESSIONS TO CONVERT PYROMETER READINGS TO	MSDG252
C	MSDG253
C ABSOLUTE TEMP. USING FUNCTION TOPYR . THE THERMOCOUPLE READINGS	MSDG254
C	MSDG255
C	MSDG256
C	MSDG257
C LAVE BEEN CONVERTED FROM MVOLTS (CORRECTED FOR AIR TEMP.) TO	MSDG258
C TEMPERATURE USING A TABLE.	MSDG259
READ(5,10) NT0	MSDG260
READ(5,15) (TOCHEM(I),T0HCTC(I),I=1,NT0)	MSDG261
C	MSDG262
READ(5,10) NT1	MSDG263
C	MSDG264
READ(5,15) (T1HCTC(I),T1PYR(I),I=1,NT1)	MSDG265
	MSDG266

C	WRITE(6,80)	MSDG267
	80 FORMAT(1H1,50X,'TEMPERATURE CALIBRATION DATA'/1X,49X,30('-')//,	MSDG268
	1 1X,41X,'ALL TEMPERATURES ARE IN DEG. C',//)	MSDG269
	WRITE(6,82)NT0,NT1	MSDG270
	82 FORMAT(42X,'NT IS THE NUMBER OF DATA POINTS TAKEN'///1X,11X,	MSDG271
	1 'NT0=',I2,24X,'NT1=',I2///1X)	MSDG272
	WRITE(6,84)	MSDG273
	84 FORMAT(1X,'CHEM MELTING',5X,'HOT CHUCK',6X,'HOT CHUCK')	MSDG274
	WRITE(6,86)	MSDG275
	86 FORMAT(1X,'POINT(DEG C)',4X,'TEMPERATURE',4X,'TEMPERATURE',3X,	MSDG276
	1 'IR PYROMETER')	MSDG277
	WRITE(6,88)	MSDG278
	88 FORMAT(1X,1X,11('-'),2X,3(2X,11('-'),2X))	MSDG279
C		MSDG280
C		MSDG281
C		MSDG282
	DO 100 KK=1,50	MSDG283
C		MSDG284
	90 IF(KK.GT.NT0.AND.KK.GT.NT1) GO TO 101	MSDG285
	WRITE(6,50)	MSDG286
C		MSDG287
C		MSDG288
	DO 250 KKK=1,2	MSDG289
C		MSDG290
	GO TO(255,256),KKK	MSDG291
C		MSDG292
	255 IF(KK.GT.NT0) GO TO 250	MSDG293
	WRITE(6,52)TOCHEM(KK),TOHCTC(KK)	MSDG294
	GO TO 250	MSDG295
	256 IF(KK.GT.NT1) GO TO 250	MSDG296
	250 CONTINUE	MSDG297
	WRITE(6,53)T1HCTC(KK),T1PYR(KK)	MSDG298
C		MSDG299
	100 CONTINUE	MSDG300
	101 CONTINUE	MSDG301
C		MSDG302
	LINEAR REGRESSION ANALYSIS OF TEMPERATURE DATA	MSDG303
	CALL REGLNR(TOCHEM,TOHCTC,NT0,TM0,TB0,TFIT0)	MSDG304
	CALL REGLNR(T1HCTC,T1PYR,NT1,TM1,TB1,TFIT1)	MSDG305
C		MSDG306
	TOM= TM0*TM1	MSDG307
	T0B= TM0*TB1 + TB0	MSDG308
C		MSDG309
	WRITE(6,66)	MSDG310
	WRITE(6,120) TM0,TB0,TFIT0,TM1,TB1,TFIT1,TOM,T0B	MSDG311
	120 FORMAT(1X,19X,'SLOPE TM0=',F10.4,5X,'INTERCEPT TB0=',F10.4,5X,	MSDG312
	1 'FIT OF LINE=',F10.4//1X,19X,'SLOPE TM1=',F10.4,5X,'INTERCEPT TB'	MSDG313
	21=',F10.4,5X,'FIT OF LINE=',F10.4//1X,19X,'TOM=',F10.4,5X,	MSDG314
	3 'T0B=',F10.4)	MSDG315
C		MSDG316
C		MSDG317
	THIS SECTION READS EQUILIBRIUM VALUES SIMULTANEOUSLY OF CO2 AND O2	MSDG318
		MSDG319
		MSDG320

C	FLOW, REACTOR PRESS., REL. PERCENT TRANSMITTANCE, AND THE ZERO CO2	MSDG321
C	CONC. BASELINE TRANSMITTANCE.	MSDG322
C		MSDG323
C	THE CO2 AND O2 FLOWS ARE	MSDG324
C		MSDG325
C	CORRECTED FOR THE TYLAN H2 FLOW CONTROLLER USING TYLAN'S PUBLISHED	MSDG326
C	FACTORS (FUNCTION F0CO2 AND FUNCTION F0O2). THE PRESS. READING IS	MSDG327
C		MSDG328
C	CONVERTED TO ACTUAL IR CELL PRESS. SUBRTNE PCBFND NEXT THE FLOW	MSDG329
C	% CO2 AND THE IR CELL PRESSURE ARE USED TO CALCULATE THE ACTUAL	MSDG330
C		MSDG331
C	CO2 CONC. (GM-MOLES/LITER) IN THE CELL WHICH IS FED WITH THE	MSDG332
C		MSDG333
C	ABSORBANCE = -LOG(TRANSMITTANCE) INTO THE LINEAR REGRESSION	MSDG334
C		MSDG335
C	SUBROUTINE. THIS RELATION IS USED TO OBTAIN CO2 CONC. FROM TRANS.	MSDG336
C		MSDG337
C	DATA. TRANSMITTANCE = REL. TRANS./BASELINE TRANS. . THE BEAM PATH	MSDG338
C		MSDG339
C	IN THE IR CELL WAS SET AT 6.4 METERS LONG.	MSDG340
C		MSDG341
C	DO 190 J=1,2	MSDG342
C		MSDG343
C	CALIBRATIONS WERE DONE ON TWO DIFFERENT DAYS. J=1 IS THE DAY	MSDG344
C		MSDG345
C	WHEN THE PRIMARY EXPERIMENTS WERE DONE.	MSDG346
C		MSDG347
C	READ(5,10) NCAL	MSDG348
C	READ(5,10) NTRAN(NCAL)	MSDG349
C	READ(5,15) BLINET	MSDG350
C		MSDG351
C		MSDG352
C		MSDG353
C		MSDG354
C	900 WRITE(6,140)	MSDG355
C	BLINET=BLINET + 0.07	MSDG356
C	140 FORMAT(1H1,45X, 'TRANSMITTANCE CALIBRATION DATA'/1X,44X,30('-')//)	MSDG357
C		MSDG358
C	WRITE(6,145) NTRAN(NCAL),BLINET	MSDG359
C	145 FORMAT(1X///1X, 'THE NUMBER OF DATA POINTS TAKEN=',I2//1X,	MSDG360
C	1 'THE BASELINE TRANSMITTANCE (ZERO CO2)=' ,F10.4///1X,	MSDG361
C	2 'CONCENTRATION IS IN GRAMMOLES/LITER',//1X,'PRESSURE IS IN TORR'	MSDG362
C	3 ,///)	MSDG363
C		MSDG364
C		MSDG365
C	WRITE(6,150)	MSDG366
C	WRITE(6,151)	MSDG367
C		MSDG368
C	150 FORMAT(1X,'RAW FLOW CO2',1X,'RAW FLOW O2',1X,'RAW REACTR',3X,	MSDG369
C	1 'RELATIVE',2X,5(2X,'ABSOLUTE',2X),'TOTAL FLOW')	MSDG370
C		MSDG371
C	151 FORMAT(1X,1X,' CC/MINUTE',2X,' CC/MINUTE',2X,'PRES.-TORR',2X,	MSDG372
C		MSDG373
C		MSDG374

```

1 'TRANSMITT.',2X,' % CO2 ',2X,'CONC. CO2',2X,'TRANSMITT.',2X,MSDG375
2 'ABSORBANCE',2X,' IR PRESS.',2X,' CC/MINUTE' / 1X,9(2X,8('-')),2X)MSDG376
3 ,2X,8('-'))MSDG377

```

```

THIS SECTION READS THE RAW DATA THENMSDG378

```

```

THIS SEGMENT CONVERTS ALL THE UNCALIBRATED DATA TO ABSOLUTE VALUESMSDG379

```

```

AND THEN USES THESE TO CALCULATE CO2 CONC. , ABSORBANCE ,AND THEMMSDG380

```

```

LINEAR RELATIONSHIP BETWEEN THESE VARIABLES.MSDG381

```

```

NTR=NTRAN(NCAL)MSDG382

```

```

DO 30 I=1,NTRMSDG383

```

```

READ(5,15) FCO2,FO2,PRT,RELTMSDG384

```

```

RELT=RELT+0.07MSDG385

```

```

CO2PER(I) = F0CO2(FCO2) / (F0CO2(FCO2) + F0O2(FO2))MSDG386

```

```

TRAN=(RELT) / (BLINET)MSDG387

```

```

ABSORB(I) = -1.0* ALOG10(TRAN)MSDG388

```

```

FCO2CB(NCAL,I) = F0CO2(FCO2)MSDG389

```

```

FO2CB(NCAL,I) = F0O2(FO2)MSDG390

```

```

PREM(NCAL,I) = PRTMSDG391

```

```

FCREM(NCAL,I) = FCO2MSDG392

```

```

FOREM(NCAL,I) = FO2MSDG393

```

```

RLTREM(NCAL,I) = RELTMSDG394

```

```

CO2PR(NCAL,I) = CO2PER(I)MSDG395

```

```

ABSRB(NCAL,I) = ABSORB(I)MSDG396

```

```

YYCO2=CO2PER(I)MSDG397

```

```

CALL PCBFND(PRT,YYCO2,DUMO,DUMC ,PACTCB)MSDG400

```

```

CO2CON(I) = CO2PER(I) * (PACTCB/760.0) * (1.0/24.631)MSDG401

```

```

CO2CN(NCAL,I) = CO2CON(I)MSDG402

```

```

EQVPRT= (PACTCB-P0CIRB) / P0CIRMMSDG403

```

```

PIRCB(NCAL,I) = PACTCBMSDG404

```

```

PRCTCB(NCAL,I) = P0RT(EQVPRT)MSDG405

```

```

DUMY(I) = FCO2CB(NCAL,I) + FO2CB(NCAL,I)MSDG406

```

```

DUMX(I) = PIRCB(NCAL,I)MSDG407

```

```

30 WRITE(6,32 ) FCO2,FO2, PRT,RELT,CO2PER(I) ,CO2CON(I) ,TRAN,ABSORB(I)MSDG408

```

```

1 ,PIRCB(NCAL,I) ,DUMY(I)MSDG409

```

```

32 FORMAT(1X,10(1X,E10.4,1X))MSDG410

```

```

31 IOR=1MSDG411

```

```

LINEAR REGRESSION OF FLOW (DUMY) VS. PRESSURE (DUMX) FOR THEMSDG412
CALIBRATION DATAMSDG413

```

```

CALL REGLNR(DUMY,DUMX,NTR,CONOM,CONOB,CONFIT)MSDG414

```

```

FLWA(NCAL) = CONOBMSDG415

```

```

FLWB(NCAL) = CONOMMSDG416

```

```

FLWC(NCAL) = 0.0MSDG417

```

FITT(NCAL)=CONFIT	MSDG429
WRITE(6,66)	MSDG430
WRITE(6,363) NCAL,FLWA(NCAL),FLWB(NCAL),FLWC(NCAL),FITT(NCAL)	MSDG431
C	MSDG432
LINEAR REGRESSION OF CO2 CONCENTRATION VS. ABSORBANCE FOR THE	MSDG433
CALIBRATION DATA.	MSDG434
C	MSDG435
CALL REGLNR(CO2CON,ABSORB,NTR, CONOM,CONOB,CONFIT)	MSDG436
CONM(NCAL)=CONOM	MSDG437
CONB(NCAL)=CONOB	MSDG438
CONF(NCAL)=CONFIT	MSDG439
WRITE(6,160) CONOM,CONOB, CONFIT	MSDG440
160 FORMAT(1X,'SLOPE CONOM=',E10.4,5X,'INTERCEPT CONOB=',E10.4,5X,	MSDG441
1 'FIT OF LINE=',E10.4)	MSDG442
190 CONTINUE	MSDG443
C	MSDG444
C	MSDG445
C	MSDG446
C	MSDG447
C	MSDG448
C	MSDG449
C	MSDG450
C	MSDG451
C	MSDG452
C	MSDG453
C	MSDG454
C	MSDG455
DO 500 I=1,10	MSDG456
C	MSDG457
READ(5,400) NRUNNO, NDATA(NRUNNO),NOWAFS,POWLEV(NRUNNO),FO2,	MSDG458
1 BLINE(NRUNNO),WTLOSS(NRUNNO)	MSDG459
C	MSDG460
400 FORMAT(I2,1X,I2,1X,I2,2X,4F10.4)	MSDG461
II=NRUNNO	MSDG462
BLINE(II)=BLINE(II)+0.07	MSDG463
WRITE(6,640) NRUNNO,NDATA(II),NOWAFS,POWLEV(II),FO2,BLINE(II)	MSDG464
640 FORMAT(1H1,'RUN NUMBER',3X,I2/1X,'NO. DATA POINTS',3X,I2/1X,	MSDG465
1 'NUMBER OF WAFERS',3X,I2/1X,'POWER LEVEL RF WATTS',3X,F10.4/1X,	MSDG466
2 'O2 FEED RATE',3X,F10.6,3X,'CC/MINUTE'/1X,'BASELINE',	MSDG467
3 ' TRANSMITTANCE',3X,F10.4)	MSDG468
650 FORMAT(1H0///7X,' TIME ',11X,'RELATIVE TRANSMITTANCE',	MSDG469
1 4X,'REACTOR PRESSURE METER',10X,'PYROMETER METER')	MSDG470
652 FORMAT(9X,2X,'(MINUTES)',2X,37X,8X,'(TORR)'18X,'(DEG. CELSIUS)')	MSDG471
WRITE(6,650)	MSDG472
WRITE(6,652)	MSDG473
WRITE(6,660)	MSDG474
660 FORMAT(7X,15('-'),10X,24('-'),2X,24('-'),10X,17('-'))	MSDG475
C	MSDG476
CONOM=CONM(1)	MSDG477
CONOB=CONB(1)	MSDG478
ND=NDATA(II)	MSDG479
NJ=1	MSDG480
CDLTOT(II,1)=0.0	MSDG481
DO 600 K=1,ND	MSDG482

C	READ(5,15) TIME(II,K),RELT,PRT,TPYR	MSDG483
	RELT=RELT +0.07	MSDG484
		MSDG485
		MSDG486
		MSDG487
		MSDG488
	TPYROM(II,K)=TPYR(TPYR)	MSDG489
	IF(TPYROM(II,K) .LT. 100.0) TPYROM(II,K)=0.0	MSDG490
	ABSOB=-1.0*ALOG10((RELT)/(BLINE(II)))	MSDG491
	ABSB(II,K)=ABSOB	MSDG492
	POB1(II,K)=PRT	MSDG493
	DUMX(K)=TIME(II,K)	MSDG494
	TRANS(II,K)=(RELT)/(BLINE(II))	MSDG495
	621 CONTINUE	MSDG496
C		MSDG497
C		MSDG498
	WRITE(6,670) TIME(II,K),RELT,PRT,TPYR	MSDG499
	670 FORMAT(1X, 1X, 6X ,F10.4,5X,11X,5X,F10.4,7X,2X,6X,F9.4,23X,F10.4)	MSDG500
	600 CONTINUE	MSDG501
	READ(5,15) COPRA(II),COPRB(II),COPRY(II)	MSDG502
	READ(5,15) COTMPA(II),COTMPB(II),COTMPY(II)	MSDG503
	READ(5,15) COABA(II),COABB(II),COABY(II)	MSDG504
	FACTOR=1.0	MSDG505
C		MSDG506
C	THIS NEXT SECTION SENDS THE DATA THROUGH THE FULL SET OF	MSDG507
C	CALCULATIONS ONCE, THEN COMPARES THE CARBON DIOXIDE LEAVING	MSDG508
C	THE SYSTEM WITH THE ACTUAL CARBON LOST FROM THE POLYMER AND DOES	MSDG509
C	A SECOND SET SET OF CALCULATIONS USING FLOWS NORMALIZED BY THE	MSDG510
C	CARBON MATERIAL BALANCE. (FACTOR)	MSDG511
C		MSDG512
	731 CDLTOT(II,1)=0.0	MSDG513
	DO 680 K=1,ND	MSDG514
	PRT=POB1(II,K)	MSDG515
	ABSOB=ABSB(II,K)	MSDG516
	CO2C2=CDCON(ABSOB)	MSDG517
	IF(CO2C2 .LT. 0.0) CO2C2=0.0	MSDG518
	CALL PFIND(PRT,CO2C2,DUMO,DUMC,DUMH, PACT2)	MSDG519
	PIR(II,K)=PACT2	MSDG520
	YCO2(II,K)=CO2C2*760.0*24.631/PACT2	MSDG521
	CO2C(II,K)=CO2C2	MSDG522
	FLOW2(II,K)=FLOW(PACT2)	MSDG523
	FLOW2(II,K)=FLOW2(II,K)/FACTOR	MSDG524
	CDLSPM(II,K)=CO2C(II,K)*0.001*FLOW2(II,K)*(760.0/PIR(II,K))*44.0	MSDG525
	IF(K .EQ. 1) GO TO 685	MSDG526
	CDLOSS(II,K)=CDLSPM(II,K)*(TIME(II,K)-TIME(II,K-1))	MSDG527
	IF(CDLOSS(II,K) .LE. 0.0) CDLOSS(II,K)=0.0	MSDG528
	GO TO 682	MSDG529
	685 CDLOSS(II,1)=CDLSPM(II,1)*1.0	MSDG530
	IF(CDLOSS(II,1) .LE. 0.0) CDLOSS(II,1)=0.0	MSDG531
	CDLTOT(II,1)=CDLOSS(II,1)	MSDG532
	CDL(1)=CDLTOT(II,1)	MSDG533
	GO TO 683	MSDG534
	682 CDLTOT(II,K)=CDLTOT(II,K-1)+CDLOSS(II,K)	MSDG535
	CDL(K)=CDLTOT(II,K)	MSDG536

```

C
C THE SYSTEM VOLUME IS ESTIMATED AT 20.90 LITERS
C
683 DCO2DT(II,K)=CONOM*(COABA(II)*(+COABB(II))*EXP(-COABB(II)*TIME(II,
1 K)))/20.90
VT=20.90
C
C THE SYSTEM VOLUME IS ESTIMATED AT 20.90 LITERS
C
C THE REACTOR VOLUME IS 12.0 LITERS. HOW MUCH OF THIS IS
C EFFECTIVE VOLUME IS UNKNOWN
C
R(II,K)=(0.001*FLOW2(II,K)*(760.0/PIR(II,K)) *CO2C(II,K) + VT*
1 DCO2DT(II,K))/12.0
YO2(II,K)=1.0-1.8*YCO2(II,K)
IF(YO2(II,K).LT.0.0)YO2(II,K)=0.0
DO2DT(II,K)=(-0.001*FLOW2(II,K)*YO2(II,K)/24.631
1 +0.001*F002(FO2)/24.631-(7.0/5.0)*12.*R(II,K))/VT
680 CONTINUE
IOR=2
C
C FIT THE TOTAL CO2 LOSS DATA IN GRAMS VS. TIME TO A QUADRATIC
C EQN.
C
CALL QUADFT(CDL,DUMX,ND,IOR,A,B,C,FIT)
ND=NDATA(II)
F2(II)=F002(FO2)
COTOTA(II)=A
COTOTB(II)=B
COTOTC(II)=C
WRITE(6,640) II,NDATA(II),NOWAFS,POWLEV(II),F2(II),BLINE(II)
C
WRITE(6,700) FACTOR
700 FORMAT(1X,/,1X,'THE DATA ON THIS PAGE WAS REDUCED USING THE',
1 'CALIBRATION RELATIONS DEVELOPED EARLIER IN THIS PROGRAM',/1X,
2 'FLOW NORMALIZATION FACTOR WAS,',1X,F10.5/)
WRITE(6,710) WTLOSS(II),CDLTOT(II,ND)
710 FORMAT(1X,'THE MEASURED WT. LOSS IS',3X,F10.4,3X,'GRAMS',5X,
1 'THE CO2 LOSS CALCULATED FROM TRANSMITTANCE DATA IS',3X,F10.4,3X,
2 'GRAMS'//)
WRITE(6,720)
WRITE(6,721)
C
C THERE ARE TWELVE SPACES PER COLUMN; 10 DIGITS AND ONE
C SPACE ON EACH SIDE IN THE FORMATS BELOW.
C
720 FORMAT(1X,24X,1X,'TRANSMIT-',4X,'RXN-RATE',5X,'IR CELL',4X,
1 'CO2 MOLE',4X,'CO2 LOSS',3X,'TOTAL',6X,'WAFER',6X,'D(O2)/DT',
721 FORMAT(1X,4X,'TIME',5X,'ABSORBANCE',4X,'-TANCE',4X,'GRAMMOLES/',
1 3X,'PRESSURE',4X,'FRACTION',3X,'GRAMS',3X,'CO2 LOSS',2X,
2 'TEMPERATURE',1X,1X,'GRAMMOLES/')
WRITE(6,735)
735 FORMAT(1X,1X,'(MINUTES)',1X,24X,2X,'LITER-MIN.',
1 1X,3X,'(TORR)',16X,'PER MINUTE',1X,1X,'(GRAMS)',

```

2	1X, '(DEGREES C)', 1X, 1X, 'LITER-MIN.')	MSDG591
C		MSDG592
C		MSDG593
	WRITE(6,722)	MSDG594
722	FORMAT(1X, 1X, 10 ('-'), 1X, 9(1X, 10 ('-'), 1X) /)	MSDG595
725	FORMAT(1X, 1X, E10.4, 1X, 9(1X, E10.4, 1X))	MSDG596
	DO 502 J=1, ND	MSDG597
	WRITE(6,725) TIME(II,J), ABSB(II,J), TRANS(II,J), R(II,J), PIR(II,J),	MSDG598
1	YCO2(II,J), CDLSPM(II,J), CDLTOT(II,J), TPYROM(II,J), DO2DT(II,J)	MSDG599
502	CONTINUE	MSDG600
	WRITE(6,66)	MSDG601
	WRITE(6,602)	MSDG602
	WRITE(6,603) II, COABA(II), COABB(II), COABY(II)	MSDG603
603	FORMAT(1X, 'FOR RUN NO.', I2, 3X, 'THE COEFFICIENT VALUES ARE A=', E10.4,	MSDG604
1	5X, 'B=', E10.4, 5X, 'Y0=', E10.4 /)	MSDG605
602	FORMAT(1X, 'ABSORBANCE')	MSDG606
	WRITE(6,604)	MSDG607
604	FORMAT(1X, 'PRESSURE IR CELL')	MSDG608
	WRITE(6,603) II, COPRA(II), COPRB(II), COPRY(II)	MSDG609
	WRITE(6,606)	MSDG610
606	FORMAT(1X, 'TEMPERATURE')	MSDG611
	WRITE(6,603) II, COTMPA(II), COTMPB(II), COTMPY(II)	MSDG612
	WRITE(6,607) COTOTA(II), COTOTB(II), COTOTC(II)	MSDG613
607	FORMAT(1X, 'BEST QUADRATIC FIT OF THE TOTAL CO2 LOSS (GRAMS) WITH	MSDG614
1	TIME GIVES COEFS. A=', E10.4, 5X, 'B=', E10.4, 5X, 'C=', E10.4)	MSDG615
	FACTOR=((12.0/44.0)*CDLTOT(II,ND))/((12.0/13.6)*WTLOSS(II))	MSDG616
	IF(ABS(FACTOR) .LT. 0.01) GO TO 500	MSDG617
	IF(ABS(FACTOR-1.0) .LE. 0.01) GO TO 500	MSDG618
	GO TO 731	MSDG619
500	CONTINUE	MSDG620
	XD=8.5	MSDG621
	YD=11.0	MSDG622
C		MSDG623
C	THE INITIAL COMMENT CARD READ IS THE SCALE TYPE(LINEAR, LOG-LOG, ETC)	MSDG624
C	THE FIRST CARD READ AFTER THIS GIVES THE X-AXIS TITLE IN COL. 1-20	MSDG625
C	THE SECOND CARD GIVES THE Y-AXIS TITLE IN COLUMNS 1-20	MSDG626
C	THE THIRD TO TENTH CARDS ARE COMMENTS TO GO UNDER THE PLOT.	MSDG627
C	UNLESS ALL 8 COMMENT CARDS ARE USED, THE LAST CARD AFTER THE	MSDG628
	COMMENTS MUST BE AN END CARD, 'END ' IN COL. 1-4	MSDG629
	READ(5,172) COMNT(240)	MSDG630
	172 FORMAT(A4)	MSDG631
C		MSDG632
C	IR CELL PRESSURE VS. TIME, NEXT IS WAFER TEMP. VS. TIME, THEN	MSDG633
C	ABSORBANCE VS. TIME, CO2 LOSS/MINUTE VS. TIME, CO2 LOSS TOTAL VS.	MSDG634
C	TIME	MSDG635
C		MSDG636
	WRITE(6,372)	MSDG637
	K=1	MSDG638
	IFRAME=0	MSDG639
300	LC=-1	MSDG640
	COMNT(239)=BLANK	MSDG641
	CALL RDPLLOT(COMNT,NCT)	MSDG642
	DO 305 II=1,10	MSDG643
	ITMP=0	MSDG644


```

KTINF=0
IF (II.EQ.6.OR.II.EQ.7.OR.II.EQ.8.OR.II.EQ.10) GO TO 305
ND=NDATA(II)
IF (II.EQ. 2) ND=17
DO 312 I=1,ND
GO TO (315,320,325,330,335,336,337) ,K
315 YPLOT(I)=PIR(II,I)
YF=2.20
YS=0.20
GO TO 310
320 YPLOT(I)=TPYROM(II,I)
COEFA=COTMPA(II)
COEFB=COTMPB(II)
COEFY0=COTMPY(II)
YF=0.0
YS=40.0
GO TO 310
325 YPLOT(I)=ABSB(II,I)
COEFA=COABA(II)
COEFB=COABB(II)
COEFY0=COABY(II)
YF=0.0
YS=2.5E-02
GO TO 310
330 YPLOT(I)=CDLSPM(II,I)
YF=0.00
YS=0.006
GO TO 310
335 YPLOT(I)=CDLTOT(II,I)
YF=0.00
YS=0.13
310 XPLOT(I)=TIME(II,I)
XF=0.00
XS=7.00
GO TO 312
336 CONTINUE
IF (II.EQ. 2) GO TO 305
IF (I.EQ. 1) GO TO 332
IF (TPYROM(II,I) .GT. 100.0 .AND. TPYROM(II,I-1) .LT. 100.0
1 ) ITMP=I-1
332 CONTINUE
IF (ITMP.EQ. 0) GO TO 312
YPLOT(I-ITMP)=ALOG(R(II,I))
XPLOT(I-ITMP)=1.0/(TPYROM(II,I) + 273.0)
XF=0.0
XS=0.5E-03
YF=-12.0
YS=2.0
GO TO 312
337 CONTINUE
IF (II.EQ. 2) GO TO 305
IF (KTINF.EQ. 1) GO TO 339
IF (I.EQ. 1) GO TO 338
IF (TPYROM(II,I) .GT. 100.0 .AND. TPYROM(II,I-1) .LT. 100.0

```

```

MSDG645
MSDG646
MSDG647
MSDG648
MSDG649
MSDG650
MSDG651
MSDG652
MSDG653
MSDG654
MSDG655
MSDG656
MSDG657
MSDG658
MSDG659
MSDG660
MSDG661
MSDG662
MSDG663
MSDG664
MSDG665
MSDG666
MSDG667
MSDG668
MSDG669
MSDG670
MSDG671
MSDG672
MSDG673
MSDG674
MSDG675
MSDG676
MSDG677
MSDG678
MSDG679
MSDG680
MSDG681
MSDG682
MSDG683
MSDG684
MSDG685
MSDG686
MSDG687
MSDG688
MSDG689
MSDG690
MSDG691
MSDG692
MSDG693
MSDG694
MSDG695
MSDG696
MSDG697
MSDG698

```

```

! ) ITMP=I-1
338 CONTINUE
  IF(ITMP.EQ. 0) GO TO 312
  ITP=ITMP + 1
  KTFBES =1
  DO 308 KTF=1,20
    TINF=TPYROM(II,ND) + FLOAT(KTF)
    DO 346 LL=ITP,ND
      YPLOT(LL-ITMP) = ALOG(TINF-TPYROM(II,LL))
346 XPLOT(LL-ITMP)=TIME(II,LL)
      NPNTS=ND-ITMP
      CALL REGLNR(YPLOT,XPLOT,NPNTS,TSLOP,TINTCP ,FIT)
      FITTMP(KTF) = ABS(FIT)
      IF(KTF .GE. 2) GO TO 309
      FITBES =ABS(FITTMP(1))
309 CONTINUE
308 IF(ABS(FITTMP(KTF)) .GT. FITBES ) KTFBES =KTF
      KTINF=1
      TINF=TPYROM(II,ND) + FLOAT(KTFBES )
      WRITE(6,311) TINF,FITBES
311 FORMAT(1X, //1X, 'T (INFINITY) =', F10.4, 3X, 'FITCOEF=', E10.4, 3X)
339 YPLOT(I-ITMP) = ALOG(TINF-TPYROM(II,I))
      XPLOT(I-ITMP)=TIME(II,I)
      GO TO 312
312 CONTINUE
      NDREAL=ND
      IF(K .EQ. 6 .OR. K .EQ. 7) ND=ND-ITMP
      NDTMP=ND
      IF(II .GE. 2) LC=77
      IF(LC .EQ. 77) GO TO 316
      IFRAME=IFRAME+1
      IF(IFRAME .EQ. 1) GO TO 316
      IF(MOD(IFRAME,2) .EQ. 0) GO TO 317
      CALL PLOT(0,-(YD+1.0),-3)
      GO TO 316
317 CALL PLOT(-(XD+2.0),YD+1.0,-3)
316 CALL GENPLT(XPLOT,YPLOT, ND,LC,COMNT, NCT,XS,XF,YS,YF,XD,YD)
      ND=NDREAL
      IF(K .NE. 6) GO TO 321
      CALL REGLNR(YPLOT,XPLOT,
1 NDTMP,SLO,YINT,FITE)
      EACT(II)=1.986*(-SLO)
      FREQF(II) = EXP(YINT)
      WRITE(6,324) II,EACT(II),FREQF(II)
324 FORMAT(1X, //1X, 'THE ACTIVATION ENERGY FOR RUN', I2, ' =', E10.4,
1 'CALORIES', 3X, 'THE FREQUENCY FACTOR=', E10.4)
      DIV=3.0E-03/90.0
      TDIV=DIV
      DO 327 I=1,90
        YPLOT(I)=SLO*TDIV + YINT
        XPLOT(I)=TDIV
327 TDIV=TDIV + DIV
      GO TO 307
321 CONTINUE

```

MSDG699
 MSDG700
 MSDG701
 MSDG702
 MSDG703
 MSDG704
 MSDG705
 MSDG706
 MSDG707
 MSDG708
 MSDG709
 MSDG710
 MSDG711
 MSDG712
 MSDG713
 MSDG714
 MSDG715
 MSDG716
 MSDG717
 MSDG718
 MSDG719
 MSDG720
 MSDG721
 MSDG722
 MSDG723
 MSDG724
 MSDG725
 MSDG726
 MSDG727
 MSDG728
 MSDG729
 MSDG730
 MSDG731
 MSDG732
 MSDG733
 MSDG734
 MSDG735
 MSDG736
 MSDG737
 MSDG738
 MSDG739
 MSDG740
 MSDG741
 MSDG742
 MSDG743
 MSDG744
 MSDG745
 MSDG746
 MSDG747
 MSDG748
 MSDG749
 MSDG750
 MSDG751
 MSDG752

```

IF(K .NE. 7) GO TO 322
CALL REGLNR(YPLOT,XPLOT,NDTMP,TSLOP,TINTCP,FIT)
HEATCO(II) =-TSLOP*0.01957
TMPZER(II) =-EXP(TINTCP) + TINF
WRITE(6,341) II,HEATCO(II),TMPZER(II)
341 FORMAT(1X,/,1X,'THE HEAT TRANSFER COEFFICIENT, H, FOR RUN',
1 1X,I2,1X,'=',E10.4,'CALORIES/CM**2-MIN-DEG K',/1X,
2 'AND THE TIME(0) TEMPERATURE=',E10.4,'DEGREES C')
DIV=TIME(II,ND)/90.0
TDIV=DIV
DO 343 I=1,90
YPLOT(I)=TSLOP*TDIV + TINTCP
XPLOT(I)=TDIV
343 TDIV=TDIV + DIV
GO TO 307
322 CONTINUE
IF(K .EQ. 1 .OR. K .EQ. 4) GO TO 355
DIV=TIME(II,ND)/90.0
TDIV=DIV
IF(K .EQ. 5) GO TO 303
DO 318 I=1,90
YPLOT(I)=COEFA*(1.0-EXP(-COEFB*TDIV)) +COEFY0
XPLOT(I)=TDIV
318 TDIV=TDIV+DIV
GO TO 307
303 DO 313 I=1,90
YPLOT(I)=COTOTA(II)+COTOTB(II)*TDIV+COTOTC(II)*TDIV**2.0
XPLOT(I)=TDIV
TDIV=TDIV+DIV
313 CONTINUE
307 CONTINUE
NDIV=90
355 IF(K .EQ. 1 .OR. K .EQ. 4) NDIV=ND
LC=77
COMNT(239)=FLIP
CALL GENPLT(XPLOT,YPLOT,NDIV,LC,COMNT,NCT,XS,XF,YS,YF,XD,YD)
305 CONTINUE
K=K+1
IF(K .LE. 7) GO TO 300

C THIS SECTION READS AXES AND COMMENT CARDS FOR TWO PLOTS BASED ON THEM
C CALIBRATION DATA . THE FIRST IS TOTAL FLOW(CC/MIN.) VS. PRESSURE
C IN THE IR CELL,AND THE SECOND PLOT IS CO2 CONCENTRATION VS. ABSORB-
C ANCE.

K=1
340 LC=-1
CALL RDPLT(COMNT,NCT)
COMNT(239)=BLANK
DO 360 II=1,3
IF(K .EQ. 2 .AND. II .EQ. 3) GO TO 360
NTR=NTRAN(II)
IF(II .EQ. 3) NTR=17
DO 350 I=1,NTR

```

C TEMPERATURE AND PRESSURE.
C

```

WRITE(6,372)
372 FORMAT(1H1,1X)
WRITE(6,370)
370 FORMAT(1X,2('PYROMETER READING',5X,'REAL TEMP. (DEG C)',5X))
TEMP=95.0
DO 365 I=1,25
TEMP=TEMP+5.0
RLTEMP=TOM*TEMP+TOB
TMP=TEMP+130.0
RLTMP=TOM*TMP+TOB
WRITE(6,375) TEMP,RLTEMP,TMP,RLTMP
375 FORMAT(1X,2(3X,E10.4,12X,E10.4,9X))
365 CONTINUE
PRESS=1.9
WRITE(6,385)
385 FORMAT(1X,2('REACTOR METER',5X,'REAL RXTR PRESS.',5X,
1 'REAL IR PRESS.',5X))
DO 380 I=1,35
PRESS=PRESS+0.1
RLRCPR=POM*PRESS+POB
RLIRPR=POCIRM*PRESS+POCIRB
PRS=PRESS+3.6
RLRCPS=POM*PRS+POB
RLIRPS=POCIRM*PRS+POCIRB
WRITE(6,390) PRESS,RLRCPR,RLIRPR,PRS,RLRCPS,RLIRPS
390 FORMAT(1X,2(1X,E10.4,10X,E10.4,10X,E10.4,5X))
380 CONTINUE
391 CONTINUE
END
SUBROUTINE PCBFND (PRT,YYCO2,DUMO2,DUMCO2,PACTCB)
COMMON POM,POB,POCIRM,POCIRB,TOM,TOB,CONOM,CONOB
COMMON FLOWA,FLOWB,FLOWC
DIMENSION DUMO2(40),DUMCO2(40),DUMH2O(40)
PACTCB=0.2*PRT
10 PACTC2=YYCO2*PACTCB
PACTO2=PACTCB-PACTC2
DO 20 I=1,27
IF(DUMCO2(I).EQ. PACTC2) GO TO 40
IF(DUMCO2(I).GT. PACTC2) GO TO 30
20 CONTINUE
30 IF(I.EQ. 1)POBCO2=0.0
IF(I.EQ. 1)GO TO 50
FRACT=(PACTC2-DUMCO2(I-1))/(DUMCO2(I)-DUMCO2(I-1))
POBCO2=DUMO2(I-1) + FRACT*(DUMO2(I)-DUMO2(I-1))
GO TO 50
40 POBCO2=DUMO2(I)
50 CONTINUE
POBTST=(PACTO2+POBCO2-POCIRB)/POCIRM
APROCH=(PRT-POBTST)/PRT
IF(ABS(APROCH).LT. 0.002) GO TO 100
PACTCB=(1.0+0.2*APROCH)*PACTCB
GO TO 10

```

MSDG861
MSDG862
MSDG863
MSDG864
MSDG865
MSDG866
MSDG867
MSDG868
MSDG869
MSDG870
MSDG871
MSDG872
MSDG873
MSDG874
MSDG875
MSDG876
MSDG877
MSDG878
MSDG879
MSDG880
MSDG881
MSDG882
MSDG883
MSDG884
MSDG885
MSDG886
MSDG887
MSDG888
MSDG889
MSDG890
MSDG891
PCBF 1
PCBF 2
PCBF 3
PCBF 4
PCBF 5
PCBF 6
PCBF 7
PCBF 8
PCBF 9
PCBF 10
PCBF 11
PCBF 12
PCBF 13
PCBF 14
PCBF 15
PCBF 16
PCBF 17
PCBF 18
PCBF 19
PCBF 20
PCBF 21
PCBF 22
PCBF 23

```

100 CONTINUE
RETURN
END
SUBROUTINE PFIND(PRT,CO2C2,DUMO2,DUMCO2,DUMH2O,PACT2)
COMMON POM,POB,POCIRM,POCIRB,TOM,T0B,CONOM,CONOB
COMMON FLOWA,FLOWB,FLOWC
DIMENSION DUMO2(40),DUMCO2(40),DUMH2O(40)
PACT2=0.2*PRT
10 YCO22=CO2C2*760.0*20.397/PACT2
IF(YCO22.LT. 0.0) YCO22=0.0
IF(YCO22.GT. 0.56) GO TO 20
GO TO 30
20 PACT2=1.05*PACT2
GO TO 10
30 YH2O2=0.8*YCO22
YO22=1.0-1.8*YCO22
PACTC2=YCO22*PACT2
PACTHO=YH2O2*PACT2
PACTO2=YO22*PACT2
DO 40 I=1,27
IF(DUMCO2(I).GT. PACTC2) GO TO 65
IF(DUMCO2(I).EQ. PACTC2) GO TO 60
IF(DUMCO2(I).GT. PACTC2) GO TO 50
40 CONTINUE
50 FRACT=(PACTC2-DUMCO2(I-1))/(DUMCO2(I)-DUMCO2(I-1))
POBCO2=DUMO2(I-1) + FRACT*(DUMO2(I)-DUMO2(I-1))
GO TO 70
60 POBCO2=DUMO2(I)
GO TO 70
65 POBCO2=0.0
70 DO 75 I=1,29
IF(DUMH2O(I).GT. PACTHO) GO TO 92
IF(DUMH2O(I).EQ. PACTHO) GO TO 90
IF(DUMH2O(I).GT. PACTHO) GO TO 80
75 CONTINUE
80 FRACT=(PACTHO-DUMH2O(I-1))/(DUMH2O(I)-DUMH2O(I-1))
POBH2O=DUMO2(I-1) + FRACT*(DUMO2(I)-DUMO2(I-1))
GO TO 95
90 POBH2O=DUMO2(I)
GO TO 95
92 POBH2O=0.0
95 POBTST=(PACTO2+POBCO2+POBH2O-POCIRB)/POCIRM
APROCH=(PRT-POBTST)/PRT
IF(ABS(APROCH).LT. 0.002) GO TO 100
PACT2=(1.0+0.2*APROCH)*PACT2
GO TO 10
100 CONTINUE
RETURN
END
FUNCTION CDCON(ABSOB)
COMMON POM,POB,POCIRM,POCIRB,TOM,T0B,CONOM,CONOB
10 CDCON=CONOM*ABSOB+ CONOB
RETURN

```

```

PCBF 24
PCBF 25
PCBF 26
PFND 1
PFND 2
PFND 3
PFND 4
PFND 5
PFND 6
PFND 7
PFND 8
PFND 9
PFND 10
PFND 11
PFND 12
PFND 13
PFND 14
PFND 15
PFND 16
PFND 17
PFND 18
PFND 19
PFND 20
PFND 21
PFND 22
PFND 23
PFND 24
PFND 25
PFND 26
PFND 27
PFND 28
PFND 29
PFND 30
PFND 31
PFND 32
PFND 33
PFND 34
PFND 35
PFND 36
PFND 37
PFND 38
PFND 39
PFND 40
PFND 41
PFND 42
PFND 43
PFND 44
PFND 45
PFND 46
CDCN 1
CDCN 2
CDCN 3
CDCN 4
CDCN 5

```

END	CDCN	6
FUNCTION FLOW(PRES)	FLOW	1
COMMON POM,POB,POCIRM,POCIRB,TOM,T0B,CONOM,CONOB	FLOW	2
COMMON FLOWA,FLOWB,FLOWC	FLOW	3
FLOW=FLOWA+ FLOWB*PRES+ FLOWC*PRES**2.0	FLOW	4
RETURN	FLOW	5
END	FLOW	6
SUBROUTINE QUADFT(YQ,XQ,NDP,IORIGN, A, B, C,FIT)	QDFT	1
DIMENSION YQ(40),XQ(40),AA(10),SIG(40)	QDFT	2
IORIGN=2 IF THE SOLUTION IS TO BE FORCED THROUGH THE ORIGIN,0,0	QDFT	3
FITS DATA TO THE EQN. Y=A + B*X + C*X**2	QDFT	4
	QDFT	5
IF(IORIGN .NE. 2) GO TO 10	QDFT	6
NDP=NDP+1	QDFT	7
XQ(NDP)=0.0	QDFT	8
YQ(NDP)=0.0	QDFT	9
10 CONTINUE	QDFT	10
DO 20 I=1,NDP	QDFT	11
20 SIG(I)=0.0	QDFT	12
MOD=0	QDFT	13
NORD=2	QDFT	14
CALL POLFIT(XQ,YQ,SIG,NDP,NORD,MOD,AA,CHSQ)	QDFT	15
A=AA(1)	QDFT	16
B=AA(2)	QDFT	17
C=AA(3)	QDFT	18
SUM=0.0	QDFT	19
DO 30 I=1,NDP	QDFT	20
DIFF=YQ(I)-A-B*XQ(I)-C*XQ(I)**2.0	QDFT	21
SUM=SUM+ (ABS(DIFF))**2.0	QDFT	22
30 CONTINUE	QDFT	23
FIT=SQRT(SUM)/(NDP-3)	QDFT	24
IF(IORIGN .EQ. 2) NDP=NDP-1	QDFT	25
RETURN	QDFT	26
END	QDFT	27
SUBROUTINE POLFIT(X,Y,SIGMAY,NPTS,NORDER,MODE,A,CHISQR)	QDFT	28
	PLFT	1
	PLFT	2
	PLFT	3
SUBPROGRAM TO FIT PAIRS OF DATA POINTS TO A LEAST SQUARES POLYNOMIAL	PLFT	4
UP TO ORDER 10. MAXIMUM NUMBER OF PAIRS OF DATA POINTS IS LIMITED	PLFT	5
ONLY BY MAIN CALLING PROGRAM. THE ARGUMENTS ARE AS FOLLOWS.	PLFT	6
	PLFT	7
X = ARRAY NAME OF INDEPENDENT VARIABLE	PLFT	8
	PLFT	9
Y = ARRAY NAME OF DEPENDENT VARIABLE	PLFT	10
	PLFT	11
SIGMAY = ARRAY NAME FOR STANDARD DEVIATIONS ABOUT 'Y'	PLFT	12
	PLFT	13
NPTS = NUMBER OF PAIRS OF DATA POINTS	PLFT	14
	PLFT	15
NORDER = ORDER OF POLYNOMIAL TO BE FITTED TO DATA	PLFT	16
	PLFT	17
MODE - DETERMINES METHOD OF WEIGHTING LEAST-SQUARES FIT	PLFT	18
+1 (INSTRUMENTAL) WEIGHT(I)=1./SIGMA(Y)**2	PLFT	19

0 (NO WEIGHTING) WEIGHT(I)=1.	PLFT 20
-1 (STATISTICAL) WEIGHT(I)=1./Y(I)	PLFT 21
A - ARRAY NAME FOR COEFFICIENTS OF POLYNOMIAL	PLFT 22
CHISQR - REDUCED CHI SQUARE FOR FIT	PLFT 23
CALLING PROGRAM SHOULD DIMENSION 'X', 'Y', AND 'SIGMAY' AT LEAST	PLFT 24
'NPTS', AND 'A' AS 10.	PLFT 25
DATA ARE FIT TO A POLYNOMIAL OF SPECIFIED ORDER, 'NORDER'.	PLFT 26
DOUBLE PRECISION SUMX(19),SUMY(10),ARRAY(10,10),XTERM,YTERM,	PLFT 27
1CHISQ	PLFT 28
DIMENSION X(1),Y(1),SIGMAY(1),A(1)	PLFT 29
ACCUMULATE WEIGHTED SUMS	PLFT 30
NTERMS=NORDER+1	PLFT 31
NMAX=2*NTERMS-1	PLFT 32
DO 1 N=1,NMAX	PLFT 33
1 SUMX(N)=0.	PLFT 34
DO 2 J=1,NTERMS	PLFT 35
2 SUMY(J)=0.	PLFT 36
CHISQ=0.	PLFT 37
DO 11 I=1,NPTS	PLFT 38
XI=X(I)	PLFT 39
YI=Y(I)	PLFT 40
IF (MODE) 3,6,7	PLFT 41
3 IF (YI) 5,6,4	PLFT 42
4 WEIGHT=1./YI	PLFT 43
GO TO 8	PLFT 44
5 WEIGHT=1./(-YI)	PLFT 45
GO TO 8	PLFT 46
6 WEIGHT=1.	PLFT 47
GO TO 8	PLFT 48
7 WEIGHT=1./SIGMAY(I)**2	PLFT 49
8 XTERM=WEIGHT	PLFT 50
DO 9 N=1,NMAX	PLFT 51
SUMX(N)=SUMX(N)+XTERM	PLFT 52
9 XTERM=XTERM*XI	PLFT 53
YTERM=WEIGHT*YI	PLFT 54
DO 10 N=1,NTERMS	PLFT 55
SUMY(N)=SUMY(N)+YTERM	PLFT 56
10 YTERM=YTERM*XI	PLFT 57
CHISQ=CHISQ+WEIGHT*YI*YI	PLFT 58
11 CONTINUE	PLFT 59
CONSTRUCT MATRICES AND CALCULATE COEFFICIENTS	PLFT 60
DO 12 J=1,NTERMS	PLFT 61
DO 12 K=1,NTERMS	PLFT 62
N=J+K-1	PLFT 63
12 ARRAY(J,K)=SUMX(N)	PLFT 64
	PLFT 65
	PLFT 66
	PLFT 67
	PLFT 68
	PLFT 69
	PLFT 70
	PLFT 71
	PLFT 72
	PLFT 73

```

    DELTA=DETERM (ARRAY, NTERMS)
    IF (DELTA) 15, 13, 15
13  CHISQR=0.
    DO 14 J=1, NTERMS
14  A (J) =0.
    RETURN
15  DO 18 L=1, NTERMS
    DO 17 J=1, NTERMS
    DO 16 K=1, NTERMS
    N=J+K-1
16  ARRAY (J, K) =SUMX (N)
17  ARRAY (J, L) =SUMY (J)
18  A (L) =DETERM (ARRAY, NTERMS) /DELTA

```

CALCULATE CHI SQUARE

```

DO 19 J=1,NTERMS
CHISQ=CHISQ-2.*A(J)*SUMY(J)
DO 19 K=1,NTERMS
N=J+K-1
19 CHISQ=CHISQ+A(J)*A(K)*SUMX(N)
FREE=NPTS-NTERMS
CHISQR=CHISQ/FREE
RETURN
END

```

FUNCTION DETERM (ARRAY, NORDER)

FUNCTION SUBPROGRAM TO RETURN THE VALUE OF A DETERMINANT

CAUTION - THIS SUBPROGRAM DESTROYS THE INPUT MATRIX ARRAY

ARGUMENTS ARE AS FOLLOWS.

ARRAY - MATRIX WHOSE DETERMINANT IS SOUGHT, MAY BE DIMENSIONED BY CALLING PROGRAM TO A MAXIMUM OF 10 X 10.

NORDER - ORDER OF DETERMINANT, (DEGREE OF MATRIX)

```
DOUBLE PRECISION ARRAY(10,10),SAVE
DETERM=1.
DO 8 K=1,NORDER
```

INTERCHANGE COLUMNS IF DIAGONAL IS ZERO

```

IF (ARRAY (K,K) ) 5,1,5
1 DO 2 J=K,NORDER
  IF (ARRAY (K,J) ) 3,2,3
2 CONTINUE
  DETERM=0.
  RETURN
3 DO 4 I=K,NORDER
  SAVE=ARRAY (I,J)

```

PLFT 74
PLFT 75
PLFT 76
PLFT 77
PLFT 78
PLFT 79
PLFT 80
PLFT 81
PLFT 82
PLFT 83
PLFT 84
PLFT 85
PLFT 86
PLFT 87
PLFT 88
PLFT 89
PLFT 90
PLFT 91
PLFT 92
PLFT 93
PLFT 94
PLFT 95
PLFT 96
PLFT 97
PLFT 98
DTRM 1
DTRM 2
DTRM 3
DTRM 4
DTRM 5
DTRM 6
DTRM 7
DTRM 8
DTRM 9
DTRM 10
DTRM 11
DTRM 12
DTRM 13
DTRM 14
DTRM 15
DTRM 16
DTRM 17
DTRM 18
DTRM 19
DTRM 20
DTRM 21
DTRM 22
DTRM 23
DTRM 24
DTRM 25
DTRM 26
DTRM 27
DTRM 28

ARRAY (I,J) =ARRAY (I,K)	DTRM 29
4 ARRAY (I,K) =SAVE	DTRM 30
DETERM=-DETERM	DTRM 31
	DTRM 32
SUBTRACT ROW K FROM LOWER ROWS TO GET A DIAGONAL MATRIX	DTRM 33
	DTRM 34
5 DETERM=DETERM*ARRAY (K,K)	DTRM 35
IF (K-NORDER) 6,8,8	DTRM 36
6 K1=K+1	DTRM 37
DO 7 I=K1,NORDER	DTRM 38
DO 7 J=K1,NORDER	DTRM 39
7 ARRAY (I,J) =ARRAY (I,J) -ARRAY (I,K) *ARRAY (K,J) /ARRAY (K,K)	DTRM 40
8 CONTINUE	DTRM 41
RETURN	DTRM 42
END	DTRM 43
SUBROUTINE RDPLT (COMNT,NCT)	RDPL 1
DIMENSION COMNT (240)	RDPL 2
DATA END/'END '/	RDPL 3
DO 10 I=1,10	RDPL 4
N= (I-1) *20+1	RDPL 5
NN=N+19	RDPL 6
READ (5,15) (COMNT (NNI),NNI=N,NN)	RDPL 7
IF (COMNT (N) .EQ. END) GO TO 20	RDPL 8
15 FORMAT (20A4)	RDPL 9
10 CONTINUE	RDPL 10
20 NCT=I-1	RDPL 11
RETURN	RDPL 12
END	RDPL 13
SUBROUTINE REGLNR (Y,X,NDP,SLOPE,B,FIT)	RGLN 1
REGLNR PERFORMS A LINEAR REGRESSION ON Y-X DATA PAIRS AND RETURNS	RGLN 2
	RGLN 3
THE SLOPE,INTERCEPT (B) , AND DEGREE OF FIT TO THE MAIN PROGRAM. FOR	RGLN 4
	RGLN 5
FIT=+ OR - 1.0 , THE FIT IS PERFECT. FOR FIT=0.0 A STRAIGHT LINE	RGLN 6
	RGLN 7
DOES NOT FIT THE DATA. REGLNR IS NOW DIMENSIONED FOR 50 DATA PAIRS	RGLN 8
	RGLN 9
DIMENSION X (50),Y (50)	RGLN 10
XSUM=0.0	RGLN 11
YSUM=0.0	RGLN 12
DO 20 I=1,NDP	RGLN 13
YSUM=YSUM + Y (I)	RGLN 14
20 XSUM=XSUM + X (I)	RGLN 15
	RGLN 16
YBAR=YSUM/NDP	RGLN 17
XBAR=XSUM/NDP	RGLN 18
	RGLN 19
SLOPEN=0.0	RGLN 20
SLOPED=0.0	RGLN 21
FITRMY=0.0	RGLN 22
	RGLN 23
DO 30 II=1,NDP	RGLN 24
	RGLN 25
XDIFF=X (II) - XBAR	RGLN 26

	YDIFF=Y(II) - YBAR	RGLN 27
C		RGLN 28
	SLOPEN= SLOPEN + (XDIFF * YDIFF)	RGLN 29
	SLOPED= SLOPED + XDIFF**2	RGLN 30
	FITRMY= FITRMY + YDIFF**2	RGLN 31
30	CONTINUE	RGLN 32
C		RGLN 33
	SLOPE= SLOPEN/SLOPED	RGLN 34
C		RGLN 35
	FITN= SLOPEN	RGLN 36
	FITRMX= SLOPED	RGLN 37
	FITD= SQRT(FITRMX* FITRMY)	RGLN 38
		RGLN 39
	FIT= FITN/FITD	RGLN 40
C		RGLN 41
	B= YBAR - SLOPE * XBAR	RGLN 42
C		RGLN 43
	RETURN	RGLN 44
	END	RGLN 45
	FUNCTION FOCO2 (FCO2)	FOC2 1
	FOCO2=(1.484*0.74/1.00)*FCO2	FOC2 2
	RETURN	FOC2 3
	END	FOC2 4
	FUNCTION FOO2 (FO2)	FOO2 1
	FOO2=(1.38*1.00/1.00)*FO2	FOO2 2
	RETURN	FOO2 3
	END	FOO2 4
	FUNCTION PORT (PRT)	PORT 1
	COMMON POM,POB,POCIRM,POCIRB	PORT 2
	PORT= POM*PRT + POB	PORT 3
	RETURN	PORT 4
	END	PORT 5
	FUNCTION POIRRT (PRT)	PORR 1
	COMMON POM,POB,POCIRM,POCIRB	PORR 2
	POIRRT=POCIRM*PRT + POCIRB	PORR 3
	RETURN	PORR 4
	END	PORR 5
	FUNCTION TOPYR (TPYR)	TOPY 1
	COMMON POM,POB,POCIRM,POCIRB,TOM,TOB	TOPY 2
	TOPYR=TOM*TPYR + TOB	TOPY 3
	RETURN	TOPY 4
	END	TOPY 5
C		TOPY 6
	SUBROUTINE GENPLT(X,Y,NPTS,LC,COMNT,NC,XSCL,XFDIV,YSCL,YFDIV,XD,YDGNPL	1
2)		GNPL 2
C		GNPL 3
	THIS SUBROUTINE WILL PLOT X,Y DATA IN A LINEAR FORMAT	GNPL 4
	SCALED TO THE ARRAY LIMITS	GNPL 5
C		GNPL 6
C		GNPL 7
C		GNPL 8
C		GNPL 9
C		GNPL 10
C		GNPL 11
	DIMENSION X AND Y IN CALLING PROGRAM AT LEAST NPTS+2	
	THE ARRAY COMNT SHOULD BE DIMENSION FOR AT LEAST 240	
	IN THE CALLING PROGRAM	

C			GNPL 12
C		DEFAULT FOR PLOT DIMENSIONS ARE 8.5 X 11	GNPL 13
C			GNPL 14
C		A 77 IN THE LC INPUT OVERLAYS PLOTS	GNPL 15
C			GNPL 16
C		'LC' LINE CONTROL VALUES	GNPL 17
C		LC .GT. 0---LINE AND SYMBOLS	GNPL 18
C		LC .EQ. 0---LINE ONLY	GNPL 19
C		LC .LT. 0---SYMBOLS ONLY	GNPL 20
C		THE ABSOLUTE VALUE OF LC DETERMINES THE SPACING OF THE	GNPL 21
C		SYMBOLS, IF LC EQUALS 4 EVERY FOURTH SYMBOL IS PLOTTED	GNPL 22
C			GNPL 23
C		'PC' IS THE PLOT CONTROL CHARACTER	GNPL 24
C		PC = 0 PRODUCES A LINEAR PLOT	GNPL 25
C		PC = 1 PRODUCES A SEMILOG PLOT , LINEAR IN X	GNPL 26
C		PC = 2 PRODUCES A LOG-LOG PLOT	GNPL 27
C		PC = 3 PRODUCES A SEMILOG PLOT , LINEAR IN Y	GNPL 28
C			GNPL 29
		DIMENSION X(1),Y(1),COMNT(240),A(5),B(5),ISYM(15),D(3),C(5)	GNPL 30
		INTEGER PC	GNPL 31
		REAL*8 DAT1, TIME	GNPL 32
		DATA C/'LIN ', 'SLGY', 'LGLG', 'SLGX', 'SMOT' /	GNPL 33
		DATA DXD,DYD,Z,ONE,HLF,XH/8.5,11.,1.0E-10,1.0,0.5,0.140/	GNPL 34
		DATA ISYM/11,14,1,2,3,4,5,6,7,8,9,10,00,12,13/	GNPL 35
		DATA A,B/5*0.0,5*0.0/, BLANK/ ' ' /	GNPL 36
		DATA FLIP /'FLIP' /	GNPL 37
C			GNPL 38
C		MAXIMUM PLOT DIMENSIONS ARE 120 X 28 INCHES	GNPL 39
C			GNPL 40
		IF((LC .NE. 77) .AND. (COMNT(239) .EQ. FLIP)) LC = - 1	GNPL 41
		N=NPTS	GNPL 42
		T = COMNT(240)	GNPL 43
		PC = 0	GNPL 44
		DO 20 I=1,3	GNPL 45
		IF(T .EQ. C(I+1)) PC = I	GNPL 46
20		CONTINUE	GNPL 47
		IF(LC .EQ. 77) PC = SPC	GNPL 48
			GNPL 49
		NEGATIVE VALUES ARE NOT ALLOWED FOR LOG AXIS VARIABLES	GNPL 50
		NEGATIVE VALUES ARE SET EQUAL TO +0.0	GNPL 51
			GNPL 52
		ZERO = 1.0E-50	GNPL 53
		DO 42 I=1,N	GNPL 54
		IF((PC .GE. 2) .AND. (X(I) .LT. ZERO)) X(I) = ZERO	GNPL 55
		IF((Y(I) .LT. ZERO) .AND. ((PC .EQ. 1) .OR. (PC .EQ. 2)))	GNPL 56
		& Y(I) = ZERO	GNPL 57
42		CONTINUE	GNPL 58
		IF(LC .EQ. 77) GO TO 10	GNPL 59
		IF((XD .LT. Z) .OR. (XD .GT. 120.0)) XD = DXD	GNPL 60
		IF((YD .LT. Z) .OR. (YD .GT. 36.0)) YD = DYD	GNPL 61
		IF(XD .LT. Z) XD=DXD	GNPL 62
		IF(YD .LT. Z) YD=DYD	GNPL 63
C			GNPL 64
C		DRAW A BOX AROUND THE PLOT PERIMETER WITH A * AT EACH CORNER	GNPL 65

C

```

CALL PLOT(Z,Z,-3)
A(2) = XD
A(3) = XD
B(3) = YD
B(4) = YD
DO 1 I=1,5
CALL PLOT(A(I),B(I),2)
CALL SYMBOL(A(I),B(I),XH,ISYM(12),Z,-1)
1 CONTINUE

```

C

C

SCALE DATA

```

AXLX = XD - 2.5
AXLY = YD - 4.0
N = NPTS
CALL PLOT(2.0,3.0,-3)

```

C

C

C

C

C

C

C

C

XSCL AND YSCL FOR LOG AXIS INPUT ARE THE NUMBER OF CYCLES
IN THE PROGRAM THEY ARE CONVERTED TO THE NUMBER OF CYCLES/IN

LIMIT ON THE MAXIMUM NUMBER OF CYCLES PER INCH IS TWO

```

IF((XSCL.LT.Z).AND.(PC.LE.1)) CALL SCALE(X,AXLX,N,1)
IF((XSCL.LT.Z).AND.(PC.GE.2)) CALL SCALG(X,AXLX,N,1)
IF(PC.GE.2) XSCL = XSCL/AXLX
IF(XSCL.GT.Z) X(N+1) = XFDIV
IF(XSCL.GT.Z) X(N+2) = XSCL
IF((PC.GE.2).AND.(X(N+2).GT.2.0)) WRITE(6,24)
24 FORMAT(1H1///' PLOT BYPASSED DUE TO LOG AXIS LIMIT OF NO',
& ' MORE THAN TWO CYCLES PER INCH----CHECK INPUT DATA $$$')
IF((PC.GE.2).AND.(X(N+2).GT.2.0)) GO TO 14
IF((YSCL.LT.Z).AND.((PC.EQ.0).OR.(PC.EQ.3))) CALL SCALEGNPL
& (Y,AXLY,N,1)
IF((YSCL.LT.Z).AND.((PC.EQ.1).OR.(PC.EQ.2))) CALL SCALGGNPL
& (Y,AXLY,N,1)
IF((PC.EQ.1).OR.(PC.EQ.2)) YSCL = YSCL/AXLY
IF(YSCL.GT.Z) Y(N+1) = YFDIV
IF(YSCL.GT.Z) Y(N+2) = YSCL
IF((PC.EQ.1).OR.(PC.EQ.2)).AND.(Y(N+2).GT.2.0)
& WRITE(6,24)
IF((PC.EQ.1).OR.(PC.EQ.2)).AND.(Y(N+2).GT.2.0)
& GO TO 14
IF((PC.GE.2).AND.(X(N+1).LT.ZERO)) X(N+1) = ZERO
IF((PC.EQ.1).OR.(PC.EQ.2)).AND.(Y(N+1).LT.ZERO)
& Y(N+1) = ZERO

```

C

C

SAVE THE SCALE FACTORS FROM THE LAST PLOT

```

SPC = PC
SXF = X(N+1)
SYF = Y(N+1)
SXS = X(N+2)

```

GNPL 66
GNPL 67
GNPL 68
GNPL 69
GNPL 70
GNPL 71
GNPL 72
GNPL 73
GNPL 74
GNPL 75
GNPL 76
GNPL 77
GNPL 78
GNPL 79
GNPL 80
GNPL 81
GNPL 82
GNPL 83
GNPL 84
GNPL 85
GNPL 86
GNPL 87
GNPL 88
GNPL 89
GNPL 90
GNPL 91
GNPL 92
GNPL 93
GNPL 94
GNPL 95
GNPL 96
GNPL 97
GNPL 98
GNPL 99
GNPL100
GNPL101
GNPL102
GNPL103
GNPL104
GNPL105
GNPL106
GNPL107
GNPL108
GNPL109
GNPL110
GNPL111
GNPL112
GNPL113
GNPL114
GNPL115
GNPL116
GNPL117
GNPL118
GNPL119

```

SYS = Y(N+2)
SXD = XD
SYD = YD
NCS = NC
LCS = LC
11 IF(NPTS .EQ. 0) NPTS = N
N = NPTS
IF(LC .NE. 77) GO TO 13
X(N+1) = SXF
Y(N+1) = SYF
X(N+2) = SXS
Y(N+2) = SYS
PC = SPC
GO TO 12
13 CONTINUE

```

C
C
C
C
C
C

DRAW AXIS---COMPLETE TWO OPEN SIDES WITH LINES

IF NUMBER OF COMMENTS IS .LE. TO 0 BLANK OUT ARRAYS

```

IF(NC .GT. 0) GO TO 4
DO 5 I=1,58
COMNT(I) = BLANK
5 CONTINUE
4 CONTINUE

```

C
C
C
C
C
C

THE FIRST TWO COMMENT CARDS CONTAIN THE AXIS INFORMATION
THESE CARDS ARE LIMITED TO 20 CHARACTERS EACH

REGULAR COMMENT CARDS MAY CONTAIN UP TO 80 CHARACTERS

```

IF(PC .NE. 0) GO TO 21
CALL AXIS(Z,Z,COMNT( 1),-20,AXLX,Z,X(N+1),X(N+2))
CALL AXIS(Z,Z,COMNT( 21),+20,AXLY,90.0,Y(N+1),Y(N+2))
GO TO 30
21 IF(PC .NE. 1) GO TO 22
CALL AXIS(Z,Z,COMNT( 1),-20,AXLX,Z,X(N+1),X(N+2))
CALL LGAXS(Z,Z,COMNT( 21),+20,AXLY,90.0,Y(N+1),Y(N+2))
GO TO 30
22 IF(PC .NE. 2) GO TO 23
CALL LGAXS(Z,Z,COMNT( 1),-20,AXLX,Z,X(N+1),X(N+2))
CALL LGAXS(Z,Z,COMNT( 21),+20,AXLY,90.0,Y(N+1),Y(N+2))
GO TO 30
23 CONTINUE
CALL LGAXS(Z,Z,COMNT( 1),-20,AXLX,Z,X(N+1),X(N+2))
CALL AXIS(Z,Z,COMNT( 21),+20,AXLY,90.0,Y(N+1),Y(N+2))
30 CONTINUE
CALL PLOT(AXLX,Z,3)
CALL PLOT(AXLX,AXLY,2)
CALL PLOT(Z,AXLY,2)
12 CONTINUE

```

C
C

CHECK FOR PLOT OVERFLOW AND UNDERFLOW AFTER FIRST DATA SET

GNPL120
GNPL121
GNPL122
GNPL123
GNPL124
GNPL125
GNPL126
GNPL127
GNPL128
GNPL129
GNPL130
GNPL131
GNPL132
GNPL133
GNPL134
GNPL135
GNPL136
GNPL137
GNPL138
GNPL139
GNPL140
GNPL141
GNPL142
GNPL143
GNPL144
GNPL145
GNPL146
GNPL147
GNPL148
GNPL149
GNPL150
GNPL151
GNPL152
GNPL153
GNPL154
GNPL155
GNPL156
GNPL157
GNPL158
GNPL159
GNPL160
GNPL161
GNPL162
GNPL163
GNPL164
GNPL165
GNPL166
GNPL167
GNPL168
GNPL169
GNPL170
GNPL171
GNPL172
GNPL173

C	IF EXTENT CONDITION IS DETECTED REDEFINE DATA POINT	GNPL174
C	TO EXTREME VALUE SO THAT IT IS PLOTTED ON AN AXIS	GNPL175
C		GNPL176
	XMIN = X(N+1)	GNPL177
	YMIN = Y(N+1)	GNPL178
	XX = X(N+2)	GNPL179
	YY = Y(N+2)	GNPL180
	TEN = 10.00	GNPL181
	XMAX = AXLX*XX + XMIN	GNPL182
	IF(PC .GE. 2) XMAX = (TEN**(AXLX*XX))*(XMIN)	GNPL183
	YMAX = AXLY*YY + YMIN	GNPL184
	IF((PC .EQ. 1) .OR. (PC .EQ. 2)) YMAX = (TEN**(AXLY*YY))*(YMIN)	GNPL185
	DO 65 I=1,N	GNPL186
	PX = (X(I) - XMIN)/XX	GNPL187
	PY = (Y(I) - YMIN)/YY	GNPL188
	IF(PC .GE. 2) PX = ALOG10(X(I)/XMIN)/XX	GNPL189
	IF((PC .EQ. 1) .OR. (PC .EQ. 2)) PY = ALOG10(Y(I)/YMIN)/YY	GNPL190
	IF(PX .GT. AXLX) X(I) = XMAX	GNPL191
	IF(PY .GT. AXLY) Y(I) = YMAX	GNPL192
	IF(PX .LT. Z) X(I) = XMIN	GNPL193
	IF(PY .LT. Z) Y(I) = YMIN	GNPL194
	65 CONTINUE	GNPL195
C		GNPL196
C	PLOT DATA	GNPL197
C		GNPL198
	IF(LC .NE. 77) MM = 1	GNPL199
	IF(LC .EQ. 77) MM = MM + 1	GNPL200
	IF(MM .GT. 15) GO TO 14	GNPL201
	IF(LC .EQ. 77) LX = LCS	GNPL202
	IF((LC.EQ.77).AND.(COMNT(239).EQ.FLIP)) GO TO 345	GNPL203
	350 CONTINUE	GNPL204
	IF(LC .NE. 77) LX = LC	GNPL205
C		GNPL206
	K = 1	GNPL207
	IF(COMNT(240) .EQ. C(5)) K = - 1	GNPL208
	IF(PC .EQ. 0) CALL FLINE(X,Y,K*N,1,LX,ISYM(MM))	GNPL209
	IF(PC .GT. 0) CALL LGLIN(X,Y,N,1,LX,ISYM(MM),2-PC)	GNPL210
		GNPL211
	IF(LC .EQ. 77) GO TO 15	GNPL212
C		GNPL213
C	WRITE COMMENTS UNDER PLOT	GNPL214
C		GNPL215
	IF(XD .LT. 8) CALL FACTOR(XD/8.5)	GNPL216
	XH = 0.090	GNPL217
	IF(NC .LE. 2) GO TO 7	GNPL218
	YI = -1.5*XH	GNPL219
	YS = -1.40	GNPL220
	IF(NC .GT. 10) NC = 10	GNPL221
	DO 2 J=3,NC	GNPL222
	M=20*(J-1)	GNPL223
	CALL SYMBOL(-ONE,YS,XH,COMNT(M+1),Z,80)	GNPL224
	YS = YS + YI	GNPL225
	2 CONTINUE	GNPL226

```

7 CONTINUE
C
C
WRITE SYMBOL AND NUMBER IN UPPER RIGHT HAND CORNER OF PLOT
15 XNUM = MM
YS = FLOAT(MM-1)*(1.5*XH)
IF((COMNT(239) .EQ. FLIP) .AND. (LX .EQ. 0)) GO TO 17
CALL NUMBER(AXLX-0.7 , AXLY-0.5 -YS , XH, XNUM , Z,-1)
CALL SYMBOL(999.0, AXLY-0.5-YS,XH,'- ',Z,2)
CALL SYMBOL(999., AXLY-0.5-YS+XH/2.0, XH,ISYM(MM),Z,-1)
17 CONTINUE
IF(LC .EQ. 77) GO TO 14
C
C
WRITE DATE AND TIME ON PLOT
YS=-2.9
CALL DATE(DAT1)
CALL TIMEOD(TIME)
CALL SYMBOL(3.0,YS , XH,'DATE ',Z,6)
CALL SYMBOL(999.,YS,XH,DAT1,Z,+8)
CALL SYMBOL(999.,YS,XH,' ',Z,6)
CALL SYMBOL(999.,YS,XH,TIME,Z,8)
CALL FACTOR(1.000000)
C
C
MOVE PLOT ORIGIN
14 CONTINUE
CALL PLOT(XD,-3.0,-3)
RETURN
10 CONTINUE
PC = SPC
XD = SXD
YD = SYD
CALL PLOT(-XD,3.0,-3)
GO TO 11
C
C
USE THE SCALE FACTORS FOR THE FIRST PLOT ON AN OVERLAY
45 IF(LX.EQ.-1) GO TO 347
LX=-1
LCS=-1
GO TO 350
347 LX=0
LCS=0
GO TO 350
END

```

GNPL227
GNPL228
GNPL229
GNPL230
GNPL231
GNPL232
GNPL233
GNPL234
GNPL235
GNPL236
GNPL237
GNPL238
GNPL239
GNPL240
GNPL241
GNPL242
GNPL243
GNPL244
GNPL245
GNPL246
GNPL247
GNPL248
GNPL249
GNPL250
GNPL251
GNPL252
GNPL253
GNPL254
GNPL255
GNPL256
GNPL257
GNPL258
GNPL259
GNPL260
GNPL261
GNPL262
GNPL263
GNPL264
GNPL265
GNPL266
GNPL267
GNPL268
GNPL269
GNPL270
GNPL271
GNPL272

TABLE AP VII-1

RUN NUMBER 1
 NO. DATA POINTS 25
 NUMBER OF WAFERS 20
 POWER LEVEL RF WATTS 800.0000
 O2 FEED RATE 40.000000 CC/MINUTE
 BASELINE TRANSMITTANCE 0.8650

TIME (MINUTES)	RELATIVE TRANSMITTANCE	REACTOR PRESSURE METER (TORR)	PYROMETER METER (DEG. CELSIUS)
1.0000	0.8100	6.4000	0.0
2.0000	0.7800	6.6000	0.0
3.0000	0.7750	6.8000	114.0000
4.0000	0.7670	6.9000	120.0000
5.0000	0.7600	7.0000	128.0000
6.0000	0.7550	7.0000	141.0000
7.0000	0.7400	7.2000	150.0000
8.0000	0.7300	7.3500	160.0000
9.0000	0.7200	7.5000	167.0000
10.0000	0.7100	7.5000	174.0000
11.0000	0.7000	7.6000	190.0000
12.0000	0.7000	7.7000	194.0000
13.0000	0.7000	7.7000	198.0000
14.0000	0.7000	7.7000	200.0000
15.0000	0.6950	7.8000	204.0000
16.0000	0.6950	7.8000	206.0000
17.0000	0.6850	7.8000	208.0000
18.0000	0.6850	7.8000	210.0000
19.0000	0.6850	7.8000	212.0000
20.0000	0.6850	7.8000	214.0000
21.0000	0.6850	7.8000	215.0000
22.0000	0.6850	7.8000	216.0000
23.0000	0.6850	7.8000	217.0000
24.0000	0.6850	7.8000	218.0000
25.0000	0.6850	7.8000	219.0000

A-45a

100-100
 100-100
 100-100
 100-100
 100-100
 100-100

TABLE AP VII-2

RUN NUMBER 2
 NO. DATA POINTS 20
 NUMBER OF WAFERS 20
 POWER LEVEL RF WATTS 200.0000
 O2 FEED RATE 40.000000 CC/MINUTE
 BASELINE TRANSMITTANCE 0.8950

A-45b

TIME (MINUTES)	RELATIVE TRANSMITTANCE	REACTOR PRESSURE METER (TORR)	PYROMETER METER (DEG. CELS (US))
1.0000	0.8800	6.1000	0.0
2.0000	0.8700	6.5000	0.0
3.0000	0.8700	6.7000	0.0
4.0000	0.8700	6.8000	0.0
5.0000	0.8650	6.3500	0.0
6.0000	0.8650	6.8500	0.0
8.0000	0.8600	6.8500	0.0
10.0000	0.8550	6.8500	0.0
12.0000	0.8550	6.8500	0.0
14.0000	0.8500	6.8500	0.0
16.0000	0.8500	6.8500	0.0
18.0000	0.8470	6.8500	0.0
20.0000	0.8470	6.8500	0.0
24.0000	0.8450	6.8500	0.0
28.0000	0.8450	6.8500	0.0
32.0000	0.8420	6.8500	0.0
36.0000	0.8420	6.8500	0.0
40.0000	0.8420	6.8500	0.0
42.0000	0.8420	6.8500	0.0
44.0000	0.8420	6.8500	0.0

RUN NUMFR 3
 NO. DATA POINTS 22
 NUMBER OF WAFERS 20
 POWER LEVEL RF WATTS 400.0000
 O2 FLOW RATE 40.000000 CC/MINUTE
 BASELINE TRANSMITTANCE 0.9100

TABLE AP.VII-3

TIME (MINUTES)	RELATIVE TRANSMITTANCE	REACTOR PRESSURE METER (TORR)	PYROMETER METER (DEG. CELSIUS)
1.0000	0.8800	6.2000	0.0
2.0000	0.8700	6.6000	0.0
3.0000	0.8650	6.8000	0.0
4.0000	0.8600	6.9000	0.0
5.0000	0.8550	6.8000	0.0
6.0000	0.8500	6.9000	0.0
7.0000	0.8450	6.8000	0.0
8.0000	0.8450	6.9000	0.0
9.0000	0.8450	6.8000	0.0
10.0000	0.8400	6.9000	0.0
12.0000	0.8370	6.9000	0.0
14.0000	0.8370	6.9000	108.0000
16.0000	0.8350	6.9000	112.0000
18.0000	0.8200	6.9000	118.0000
20.0000	0.8170	6.9000	122.0000
22.0000	0.8150	6.9000	125.0000
24.0000	0.8100	7.0000	127.0000
26.0000	0.8100	7.0000	128.0000
28.0000	0.8050	7.0000	130.0000
30.0000	0.8050	7.0000	130.0000
32.0000	0.8050	7.0000	133.0000
36.0000	0.8050	7.0000	134.0000

A-45c

TABLE AP VII-4

TIME (MINUTES)	RELATIVE TRANSMITTANCE	REACTOR PRESSURE METER (TORR)	PYROMETER METER (DEG. CELSIUS)
1.0000			
2.0000	0.8850	6.7000	
3.0000	0.8700	6.8000	0.0
4.0000	0.8650	6.9000	0.0
5.0000	0.8550	7.0000	0.0
6.0000	0.8500	7.0000	0.0
7.0000	0.8450	7.0000	0.0
8.0000	0.8400	7.0000	108.0000
9.0000	0.8370	7.0000	115.0000
10.0000	0.8350	7.1000	122.0000
12.0000	0.8200	7.2000	126.0000
14.0000	0.8150	7.3000	132.0000
16.0000	0.8100	7.2000	141.0000
18.0000	0.8100	7.3000	149.0000
20.0000	0.8100	7.4000	153.0000
22.0000	0.8100	7.4000	157.0000
24.0000	0.8100	7.5000	162.0000
26.0000	0.8100	7.6000	166.0000
		7.6000	169.0000
			171.0000

A-45a

TABLE AP VII-6

RUN NUMBER 9
 NO. DATA POINTS 19
 NUMBER OF WAFERS 20
 POWER LEVEL RF WATTS 800.0000
 O2 FEED RATE 20.000000 CC/MINUTE
 BASELINE TRANSMITTANCE 0.9100

A-45f

TIME (MINUTES)	RELATIVE TRANSMITTANCE	REACTOR PRESSURE METER (TORR)	PYROMETER METER (DEG. CELSIUS)
1.0000	0.8250	4.7000	0.0
2.0000	0.7850	5.1000	0.0
3.0000	0.7800	5.5000	0.0
4.0000	0.7650	5.6000	112.0000
5.0000	0.7500	5.6000	126.0000
6.0000	0.7450	5.7000	140.0000
7.0000	0.7400	5.7000	153.0000
8.0000	0.7300	5.8000	162.0000
9.0000	0.7200	5.8000	171.0000
10.0000	0.7100	5.8000	178.0000
12.0000	0.6900	5.8000	188.0000
14.0000	0.6900	6.0000	199.0000
16.0000	0.6850	6.1000	207.0000
18.0000	0.6850	6.1000	213.0000
20.0000	0.6850	6.2000	217.0000
22.0000	0.6850	6.2000	220.0000
24.0000	0.6850	6.2000	222.0000
26.0000	0.6850	6.2000	223.0000
28.0000	0.6850	6.2000	225.0000

APPENDIX VIII

Sources of Error

During the experiments, radio frequency (rf) interference was noticed in the recording instruments. The rf problem with the thermocouple inserted directly into the plasma has been discussed. Eliminating the interference was not possible, however, the effect was minimized by use of a common mode rejection circuit. Rf interference with the mass flow controller was also experienced. This was not a significant problem because even though the rf shifted the preset flow value, the indicated flow rate always corresponded to the actual flow. For example, with rf power off the flow was preset at 20 cc/min.. When rf power (800 watts) was turned on the controller might change to 30 cc/min.. Although the rf had changed the preset value, the indicated flow, 30 cc/min., was always consistent. This supposition was verified by comparing the system pressure before and after the rf was turned on. The pressure gauges were not affected by rf.

No rf influence was detectable in the infrared pyrometer used to measure wafer temperature. However, from analyzing the data for the 800 watt runs, it appears that there might be a +5 C offset in all of the temperatures above 180 C caused by rf pickup. This pickup even if real is insignificant since it represents an error of only 3%.

VITA

Paul Saunders was born in Woburn, Massachusetts on Sept. 14, 1948 to Mr. and Mrs. Robert J. Saunders. Following public high school, he attended the University of Massachusetts at Amherst from 1966 to 1970, graduating with a Bachelor of Science degree in Chemical Engineering in June 1970. From June of 1970 to the present, he has worked on the processes and equipment for the cleaning, photolithography, diffusion, and ion implantation of silicon semiconductors at Western Electric Co., Allentown, Pennsylvania.